Fernando Moreno Lavin BSc

DEVELOPMENT OF A CONTROL CONCEPT FOR A CONTINUOUS DIRECT COMPACTION PROCESS

MASTER'S THESIS

To achieve the university degree of

Diplom-Ingenieur

Master's degree program: Chemical and Pharmaceutical Engineering

Submitted to

Graz University of Technology

Supervisor

Univ.-Prof. Dipl.-Ing. Dr.techn. Johannes Khinast

Institute of Process and Particle Technology

Dipl.-Ing. Dr.techn. Jakob Rehrl and Dipl.-Ing. Michael Martinetz

Research Center Pharmaceutical Engineering (RCPE) GmbH

Graz, January 2018

“One grain is a solid. But a lot of grains together are neither a solids, nor a liquid, no a gas…” J.M. Valverde.

STATUTORY DECLARATION

I declare that I have authored this thesis independently, that I have not used other than the declared sources/resources, and that I have explicitly indicated all material which has been quoted either literally or by content from the sources used. The text document uploaded to TUGRAZonline is identical to the present master‘s thesis dissertation.

_____ _____

Date Signature

ABSTRACT

The pharmaceutical industry is witnessing nowadays its particular challenge to improve the way drugs are being manufactured. This study attempts to implement key concepts such as Quality by Design (QbD) and Process Analytical Technology (PAT) into a continuous direct compaction pharmaceutical process to support the full adoption of continuous manufacturing. An existing published control strategy that keeps the fill level of an industrial hopper within its design space is enhanced. Ultrasonic technology is selected as PAT to measure its level continuously. The proposed model-based feedback control loop systems is designed using MATLAB Simulink and applied to various transfer function models and to a non-linear model. The models used in this study are obtained via mechanistic modeling approach (i.e. geometry data and mass balances). The ability of the control system – either with P-Only control or with PI control – to reject the unknown disturbances and to track the set-point have been analyzed. Additionally, the controller has been tuned based on IMC and SIMC principles for integrating processes to achieve the best possible performance. The validation and verification of the simulation models are eventually carried out.

Keywords: Quality by Design (QbD) · Process Analytical Technology (PAT) · Continuous Manufacturing (CM) · Model-based feedback control · P-Only Control · PI Control · IMC (Internal Model Control) · SIMC (Skogestad Internal Model Control) · Integrating processes

ACKNOWLEDGES

I would first like to thank my thesis advisors Dipl.-Ing. Michael Martinetz, Dipl.-Ing. Dr.techn. Jakob Rehrl and Dipl.-Ing. Julia Kruisz. The door to their offices was always open whenever I ran into with some troubles or had a question about my research or writing. They consistently allowed this thesis to be my own work, but steered me in the right direction whenever they though I needed it. I would like to mention that chance encounter with Michael Martinetz, before even start with the thesis, when he offered me the possibility to work with them as a Master's Student at the Research Center Pharmaceutical Engineering (RCPE) GmbH. Probably, none of these would have happen, if it wasn't for him and that little coincidence. Special thanks as well to Jakob Rehrl, for his useful advises during the calculations and simulations. He makes everything simpler than it appears to be in the first place.

Secondly, I must express my very profound gratitude to my parents and my sister that keep on pushing continuously from the distance, with non-other aim, but my success. Their support is beyond any doubt the prop of this work. Thank you. Besides, I remember in this point my entire family.

Finally I would like to thank my friends here in Graz and in Spain for being awesome and giving me the chance to disconnect from the thesis from time to time. These moments are not only priceless, but also needful to keep the motivation always up.

Table of Contents

I. INTRODUCTION

Traditionally, the productiveness and the progress of the pharmaceutical industry has been limited due to the tightly regulation the companies need to confront in order to ensure the purity and quality of their products [1][2]. Conventional pharmaceutical manufacturing has been generally accomplished using “batch processing”, which makes use of a tool known as Quality-by-Testing (QbT) to ensure product quality [3][4]. Nowadays though, the challenge of the pharmaceutical industry is mainly focused on the adoption of continuous manufacturing, which requires a better understanding of the process [5]. This enhanced process understanding can be achieved by significant advances in science and engineering approaches. Quality-by-Design (QbD), Process Analytical Technology (PAT) or model-based design are among them, and they support consequently the change from “batch” to “continuous” while improving product’s quality, process’s efficiency and flexibility [6][7].

QbD assumes that quality should be designed into the product rather than being repeatedly tested to prove whether the QTPP (Quality Target Product Profile) is met. PAT turns out to be an essential ally of QbD, since it introduces the idea of real-time process control and real-time quality assurance [8]. Similarly, model-based design is increasingly being used to solve problems and to aid in decision-making [9].

The overall goal of this thesis is therefore to put these complex concepts into practice by developing a robust control concept for a continuous rotatory tablet press. The rotation velocity of the tablet press, also known as the turret speed, is manipulated to keep the hopper fill level within its design space (i.e. control range), guaranteeing consequently the process stability.

Bearing this in mind, the chapter 3 presents the overall description of the continuous direct compaction process and the two different hopper geometries (cylindrical or conical) being used [10]. Chapter 4 establishes subsequently the main critical attributes (CAs) via process understanding and quality risk management that are more likely to threaten the correct measurement of the hopper fill level, the fundamental parameter of the control strategy.

One of the most critical steps regarding the control strategy is the correct measurement of the fill level under the given conditions of dust and uneven surfaces. The selected critical attributes together with the gained process understanding till this point shortlist the technologies that can be in charge of this duty. Five different level measuring technologies are compared in chapter 5. An ultrasonic level sensor is eventually selected as the preferred technology over others such as guided wave radar or laser to fulfil this task.

Once the technology is selected, the mathematical development of three models using ordinary differential equations (ODEs) is carried out in chapter 6. The models are obtained via mechanistic modeling approach (i.e. hopper's geometry data and mass balances). While the first model, linear in nature, represents the dynamic behavior of powder inside the cylindrical hopper, the second and the third one attempts to describe the dynamics of the same process but using the conical hopper instead. This singularity generates a non-linear system which is linearized at the operating point. The three models are compared and subsequently derived into transfer functions for control, where the integrating (non-self-regulating) behavior of the system being studied is demonstrated.

Later in chapter 6, a model-based feedback control loop system is designed using MATLAB/Simulink and applied to the three different models being studied. Several simulations area performed using either a proportional-only controller or a proportional-integral controller, and the result are compared and analyzed [11]. At the end of chapter 6, the controller is designed according to two different tuning strategies (IMC and SIMC) so that a good performance of the feedback control can be achieved for set-point tracking simulations with disturbance rejection.

In chapter 7 the validation and verification of the cylindrical hopper model are addressed by comparing the simulations performed in MATLAB/Simulink with real experiments in the pilot plant located in the Research Center of Pharmaceutical Engineering (RCPE) [12].

II. THE ECONOMIC ASPECTS OF PHARMACEUTICAL INDUSTRY'S MOVEMENT TOWARDS CONTINUOUS MANUFACTURING

The pharmaceutical industry might be defined as a group of companies engaged in researching, developing, manufacturing and marketing drugs and biologicals for human and veterinary use. These main products are substances intended for use in the diagnosis, cure, mitigation, treatment or prevention of diseases. Chemical-derived drugs are produced in forms such as pill, tablets, capsules, vials, ointments, powders, solutions and suspensions [13].

Conventional pharmaceutical manufacturing is generally accomplished using batch processing together with sample collection, which is analyzed in the laboratory to evaluate quality. This conventional approach has been successful in providing quality pharmaceuticals to the public. However, today significant opportunities based on a different way of drug manufacture exist for improving pharmaceutical development, productivity, efficiency and quality assurance through innovation in product and process development, process analysis, and process control [14][15].

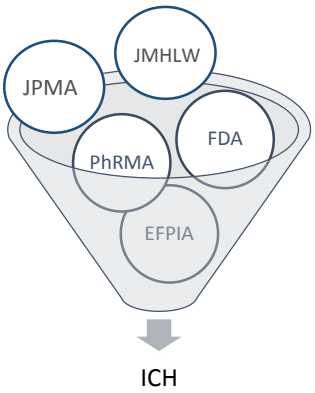

Figure 1: Co-sponsors of ICH

Pharmaceutical manufacturing operations and development have been inefficient and costly during recent years. Such low efficiency might be largely related to static manufacturing way of producing drugs, focused on testing as oppose to building the quality into the products, as quality by design (QbD) suggests. The International Conference on Harmonization (ICH), represented by regulatory bodies such as the FDA or EFPIA (see Figure 1) and the research-based industry, was launched in 1990 with the major goal of providing a forum for constructive discussion on the real world and perceived differences in technical requirements for the registration of new chemical

entities. Other goals in mind would be related with the improvement of the global drug development efficiency or with the improvement of the product quality [16].

It is widely known that the pharmaceutical industry has currently a limited ability to rapidly increase production to cover drug shortage during emergencies such as pandemics. Continuous manufacturing though, as it will be addressed along this chapter, is more agile and flexible in terms of productivity. It can potentially permit increasing production volume by for instance, removing current bottleneck related to scale-up, utilizing parallel processing lines, increasing the flow-rate through the process or operating the process for longer periods of time [17][18].

2.1 Economic Importance of the Pharmaceutical Industry

Nowadays, the pharmaceutical industry is one of the most important industrial sectors in the European Union. With its substantial investments in Research and Development (R&D), this industry represents a key asset for the European economy and a major source of growth and employment, employing directly some 700000 people and generated three to four time more employment indirectly. According to data from EFPIA, in 2015 an estimated €31,500 million was invested in R&D, representing therefore an increase of 43.33% since 2000, where the expenditure was €17,849 million. Germany and Switzerland, being the top leaders of the pharmaceutical industry in Europe, invested in 2014 € 5,813 million and € 5,446 million respectively, whereas Austria´s R&D investment was about € 650 million. As a comparison, the European industry remain still far away from the reference USA investment, located in $ 47,051 million in R&D as Figure 2 shows. [19]

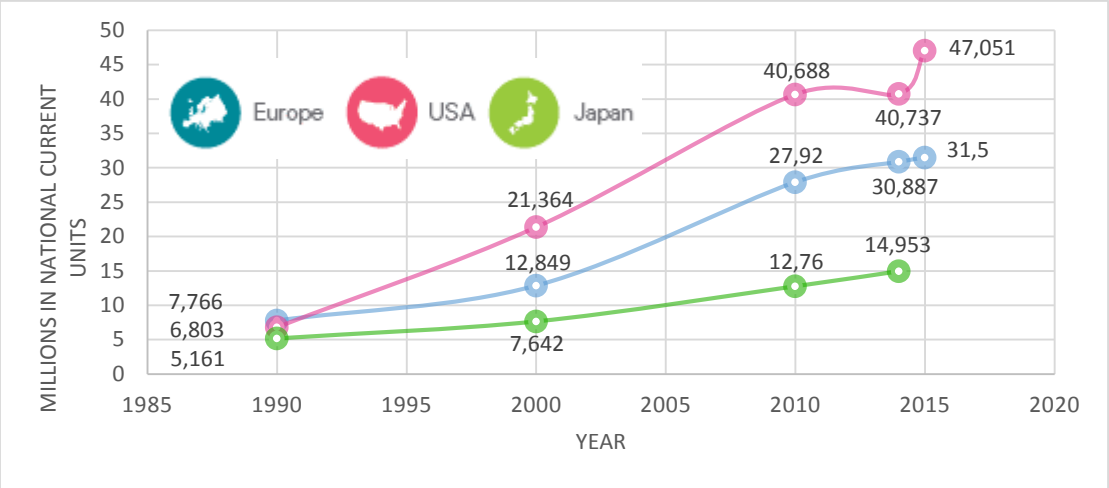

Figure 2: Pharmaceutical R&D expenditure in Europe, USA and Japan in millions of national currently units [19]

It is worth mentioning that besides the recent global crisis, the European Union represents still a major manufacturer and exporter of pharmaceutical products. So much so, that The European Union was by far the major world trader in medicinal and pharmaceutical products in 2013, with total trade amounting to € 156.9 billion. Exports made up actually about two thirds of this trade. The United States occupied the second position for trade in these products, at some distance, with trade worth € 83.9 billion. The EU is considered therefore the second global manufacturing for pharmaceuticals behind the US and ahead of Japan nowadays [20][21]. However, even though the amount invested in R&D has only just increased, as shown in Figure 2, its productivity, computed as the number of drugs introduced to the market place per year, is declining in average (see Figure 3) [22][23]. Among the most probable reasons might be found the long period of time required to approve and launch a product into the market (see Figure 4) or the lack of engineering solutions with regard to batch manufacturing.

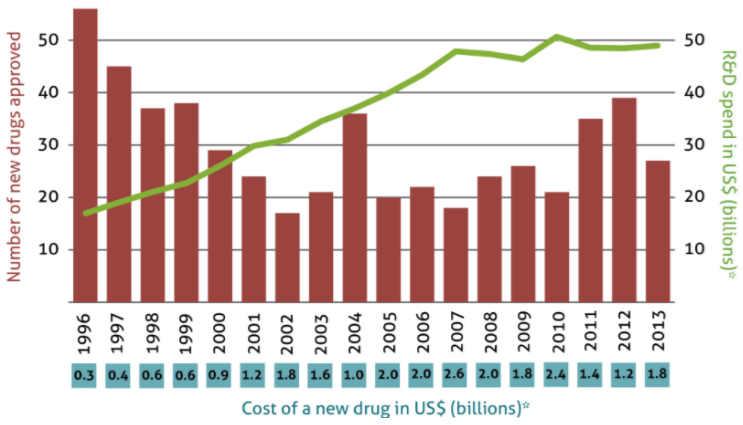

Figure 3: Number of New Drugs approved each year by the FDA (productivity) vs. the investment in R&D in the Pharmaceutical Industry. Extracted from [23]

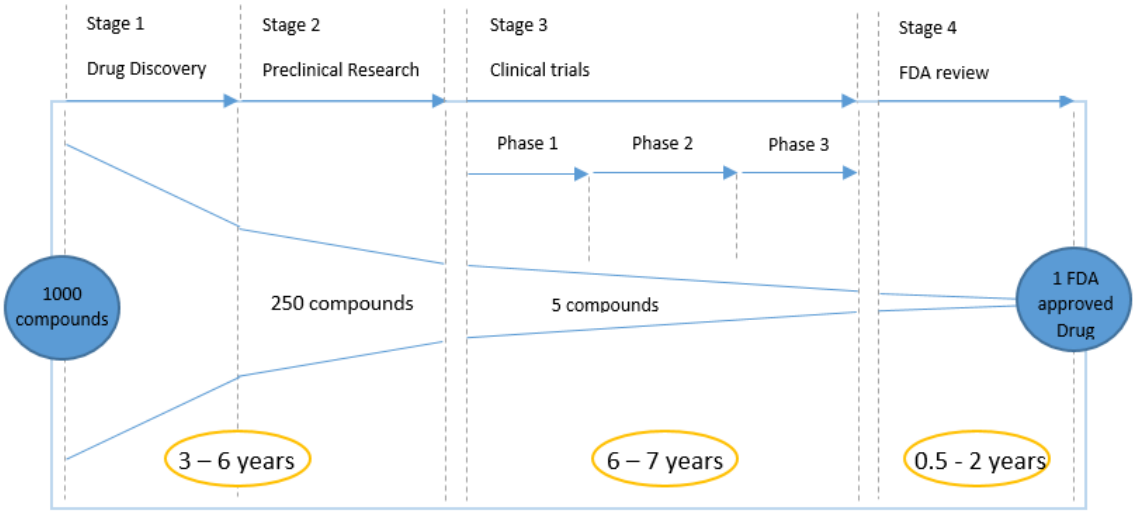

Figure 4: Drug Product Development Cycle. Adapted from [25]

The pharmaceutical sector has been always known for its high-risky nature of its business. For instance, according to data from the Tufts Center for the Study of Drug Development (CSDD), the amount of money required to launch successfully a drug into the market is about $2.6 billion [24]. These arguments, together with the fact that the competitiveness between companies for the expiration of the patents does nothing else, but increase, is somehow driving the industry to a more competitive sector, where efficiency and productivity are important terms. The industry needs to innovate the way drugs are being manufactured.

Innovation is understood to be a major stimulus to real economic growth and to improvements in society's standard of living. However, the pursuit of innovation within the pharmaceutical industry is a tough path. The pressure of public authorities together with the patent shenanigans and the long battle over dozens of patents between the generic manufacturers and the brand-name manufacturers distract the pharmaceutical companies from their real job: making new medicines (follow-on drugs) and increasing medical innovation [25][26][27]. Therefore, from an economic point of view, would be interesting to achieve a balance within the market exclusivity period (MEP) – time between the launch of a brand-name drug and the launch of its first generic compound – to provide the brand-name manufacturers with sufficient profit so that a new investment in R&D can be carried out [28][29][30][31]. Once the patent expires, 80% of the brand name sales can vanish within a year as generic competitors reach the market [32].

2.2 Shift of Paradigm: From Batch to Continuous Manufacturing

Over the last decades, pharmaceutical manufacturing processes have been largely accomplished using traditional "batch" methods, which in many cases may lack the agility, flexibility and reliability to combat failures that might affect eventually the final product quality. Besides, the way of ensuring the quality of the drug was not optimal, since it was controlled mainly by a regulatory framework based on laboratory testing of collected samples, or quality-by-testing (QbT) [1].

This practice results in very long and expensive processes that beyond any doubt might be optimized in order to satisfy the constant public demand. In fact, the pharmaceutical industry is wasting more than $50 billion a year in manufacturing costs alone. These costs could be translated into lower prices or grater research and development (R&D) - according to findings of the largest empirical study ever performed of pharmaceutical manufacturing and the FDA monitoring policies [33].

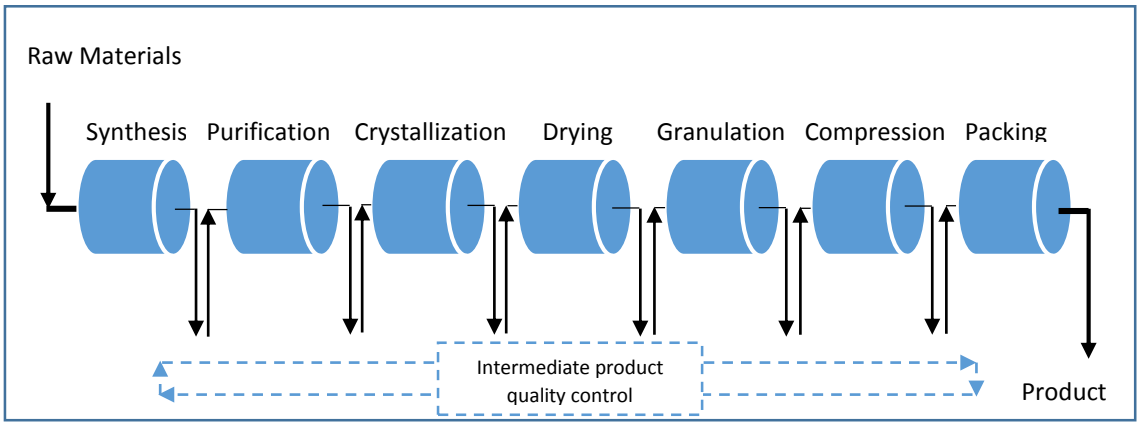

Figure 5: Pharmaceutical batch manufacturing. Adapted from [4]

The traditional way drugs have been manufactured (see Figure 5), also known as batch manufacturing, can be described as a process whereby the ultimate finished product has been achieved after many stops and starts in a series of steps. The intermediate product is therefore collected, tested offline in labs, stored in containers between each stage of production and often even shipped around the globe to the next manufacturing facility [34]. This lag-time between unit operations influences badly the production time [35]. It

is worth mentioning that according to Dr. Lawrence X. Yu, FDA´s Deputy Director, "If we used a time machine to transport a pharmaceutical scientist from the 1960s into a current pharmaceutical production plant of today, it might be surprising to learn that they would already be very familiar with most of the processes and production techniques being used" [36].

Even though there is still a long path to cover till the full adoption of continuous manufacturing within the pharmaceutical industry, over the past decade the researchers and the companies has experimented a growing interest in increasing the safety and the quality in medications while simultaneously cutting costs. There has been significant advancements in science and engineering to support the implementation of continuous manufacturing which along with the adoption of quality-by-design (QbD) and process analytical technology (PAT) enable the ultimate move from batch to continuous processing.

In contrast to batch manufacturing, continuous manufacturing (CM), (see Figure 6), is the integration of multiple manufacturing process systems (unit operations) into a single system. The idea behind is based on process system engineering that would enable continuous product flow. The process would be in fact constantly monitored and controlled by PAT analysis tools to ensure that the final product complies with the pre-defined quality target product profile (QTPP) [37][38][39].

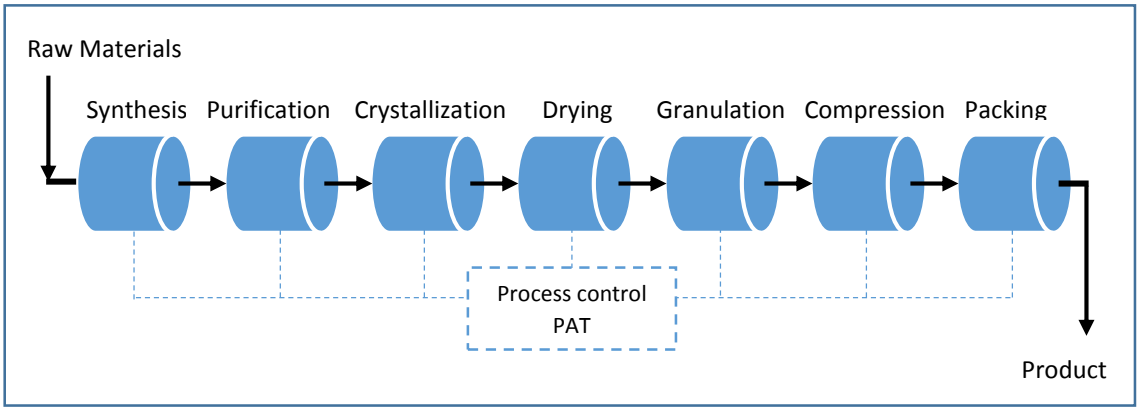

Figure 6: Pharmaceutical continuous manufacturing. Adapted from [4]

According to literature, it is expected that a continuous process uses less equipment, less labor and less utilities. Besides, it would have a smaller building footprint and it would generate less waste. Concerning the economic investment, a well-designed

continuous plant should cost about 40% less than a comparable batch plant [40]. It is worth mentioning as well, that a publication of the National Science and Technology Council says that continuous manufacturing may reduce as well manufacturing costs, which currently consume as much as 27 percent of the revenue for many pharmaceutical companies, by up to 40 to 50 percent [37][41].

2.2.1 Barriers to the adoption of continuous manufacturing. Is it possible to deal with them nowadays?

Despite the agreement that continuous manufacturing pays off according to aforementioned enforcing ideas, there is a number of technical, operational and economic challenges that have slowed down the progress towards the continuous technology, already implemented in many other industries. One of the most influencing factors concerning this slow adoption to continuous manufacturing is related, as commented previously, with the companies´ fear to any significant change in their manufacturing process. This change towards a continuous mind-set, despite the current support of the FDA, might vaguely bring regulatory delays [17]. Similarly, the existing batch infrastructure that many companies already have in place or the pervasive mind-set of the industry that pharmaceuticals should be produced via this outdated methodology simply because that is the way it has always been done, decelerate the continuous growing of this sector.

Continuous manufacturing seems to be the key for the pharmaceutical industry progress according to the previous section. Yet, not everyone is confident with the all-out transformation due to some technical issues. For instance, several unit operations commonly used in any pharmaceutical process such as blending, drying and tablet coating have been traditionally operated in batch mode and might require more development efforts to transition to continuous mode. This leads to think that there is not sufficient process understanding yet [40].

Probably, one of the most important factors that inhibits the fully acceptation of continuous manufacturing is the lack of process understanding. However, over the last decade the research regarding this issue has been strongly intensified, and there are

already mechanisms such as QbD and PAT to successfully manufacture continuously in some unit operations (i.e. continuous direct compaction process or blenders). The Figure 7 shows the balance between the factors that would support the step towards continuous processing and the ones that cast doubt on such change.

Unfortunately, it is not all about technical or operation issues. Any important innovation that could encourage this change must get adapted to the current business and economy to enjoy some recognition. Even though it is demonstrated that continuous manufacturing would increase the speed to market, the market competitiveness between for instance brand-new drug manufacturers and generic manufacturers is so conflicting that make any possible change even more challenging.

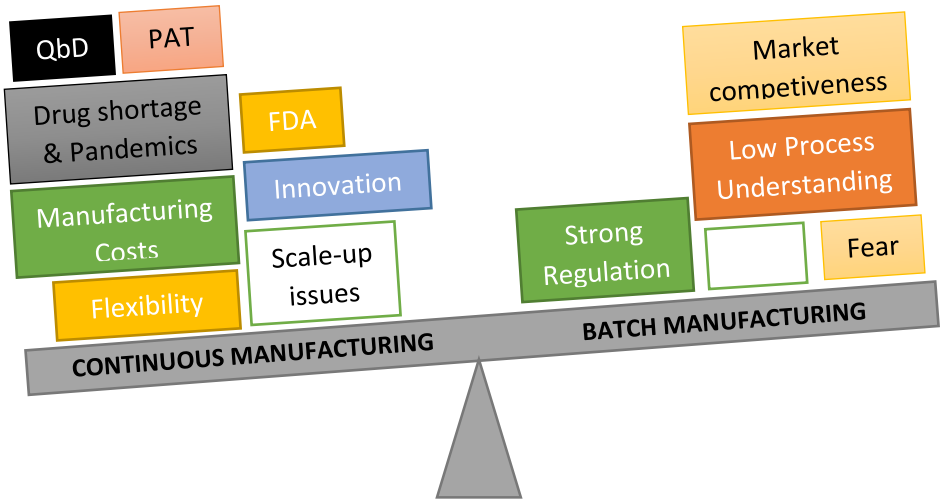

Figure 7: Balance between Continuous Manufacturing and Batch Manufacturing in the pharmaceutical industry

2.3 Process Analytical Technology (PAT) and Quality by Design (QbD) instead of Quality by Testing (QbT)

In the aforementioned introduction to batch manufacturing, it was highlighted the fact that over the last decade, the pharmaceutical industry focused the quality control mainly on Quality by Testing (QbT). Even though it might be reliable for certain processes, this testing protocol leaves significant opportunities for improvement, as it was demonstrated during years due to the large amount of recalls [42].

In contradiction with this quality-by-testing thinking, the FDA has struggled over recent years in encouraging the adoption of continuous manufacturing even though companies still show a certain rejection about it. To do so, several organization such the FDA (co-sponsor of the ICH), work in parallel with the ICH in order to implement the adoption of QbD and PAT within the pharmaceutical industry. Product and process understanding, as it will be shown along the thesis, are the key elements of QbD, and the fact of taking them as the fundamental pillar in drug manufacturing, allows the build of drug quality along the process. Within the ICH guidelines, QbD holds that quality cannot be tested into products; rather, it should be built-in as a part of the product´s fundamental design [43][44][45][46][47][48][49].

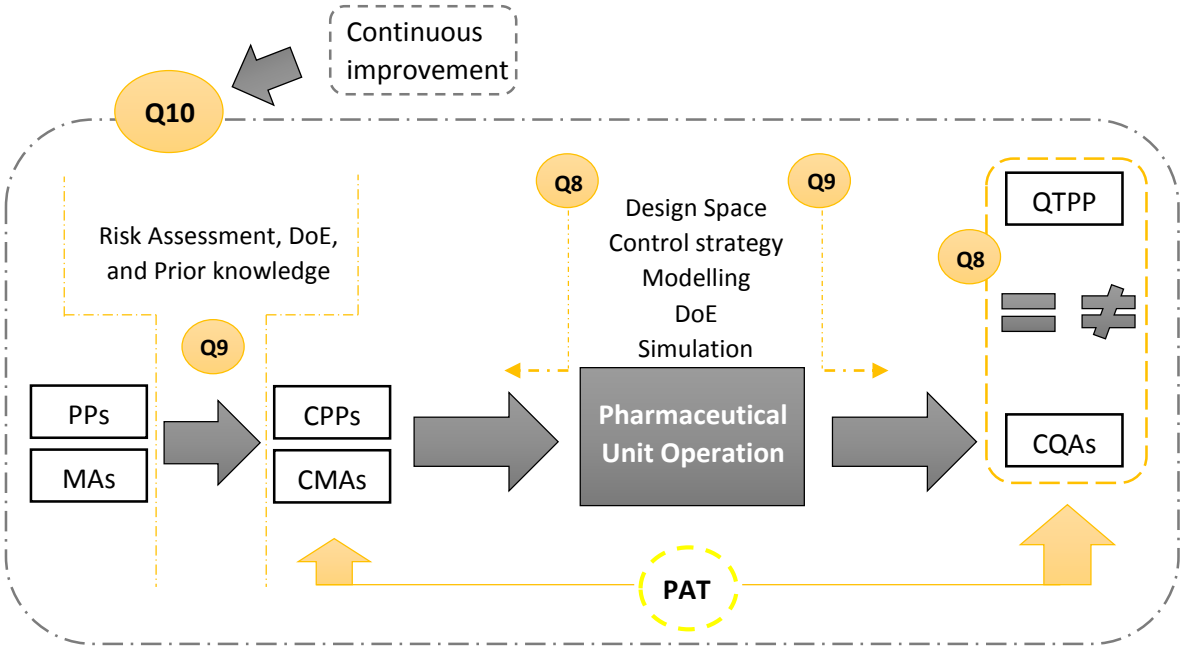

Figure 8: Relation between inputs (Critical material attributes (CMAs), Critical process parameters (CPPs)) and outputs (Critical Quality Attributes (CQAs) in a Quality by Design (QbD) sketch [6].

By the proper product and process understanding, critical parameters regarding a particular process (i.e. the hopper fill level) can be easily identified as the Figure 8 shows. However, often the influence of each individual parameter on the final drug quality is not the same, and therefore a risk assessment must be carried out in order to identify critical attributes (i.e. dust, uneven surfaces), that might potentially influence the process stability [50]. Those parameters will be accordingly monitored and controlled within their respective design spaces by the use of PAT and control strategies. Parameter´s changes within the design space are not subjected to regulatory

notification. However, deviations out of the design space would normally demand new control requirements [6][48][49][51].

It would be fair to agree that the pharma industry needs more than ever a change in its production way in order to accomplish a higher productivity while reducing the manufacturing cost. This is actually the main reason why this project has been aimed at QbD and PAT. Therefore, a proper way to sum this point up with respect to the goal of the thesis, would be the complementary use of QbD tools (ICH Q8), prior knowledge, risk assessments (ICH Q9), mechanistic models, design of experiments (DoE), data analysis, control process and process analytical technology (PAT) as well as tools to facilitate continual improvement (ICH Q10) to successfully develop the desired control strategy (see Figure 8).

2.4 Process Modeling and Simulation

Modeling and simulation are emerging as a key technologies to support manufacturing in the 21st century [9]. In fact, computer simulation is a discipline gaining popularity in both government and industry. Computer simulation and modeling can assist in the design, creation and evaluation of complex systems, before they even physically exist. Designers, program managers, analysts and engineers use computer simulation modeling to understand and evaluate “what if” scenarios from a cost-effective point of view [52][53][54]. Their predictability skills to prevent failure and their positive influence in decision-making make them over indispensable tools to remain competitive in industry [9].

In the area of process engineering, models are fundamentally mathematical in nature and they are translating our real world problem into a mathematical problem which we solve and then attempt to interpret, as the theory of modeling suggests [55]. Process modelling is one of the key activities in process systems engineering, driven by such application areas as process optimization, design and control.

Once the problem is defined and understood, the development of the mathematical method is the next step. The task of building mathematical models is the translation of

certain properties of a real system into mathematical equations. To execute this task, it is necessary to have access to information about the real system one wants to model. Even though these days most of the models developed for pharmaceutical process are black-box models, the models that will be developed in this thesis (see chapter 6) can be located within the grey-box area (see Figure 9), since they can make an analytical prediction of what is going to happen under certain conditions [56][57][58][59]. However, it is important for a model to be credible; otherwise, the results may never be used in the decision-making process, even if the model is "valid". Consequently, if a model is valid and credible, an acceptable level of confidence in the process performance might be achieved, fulfilling thus the quality requirements in regulatory bodies' eyes.

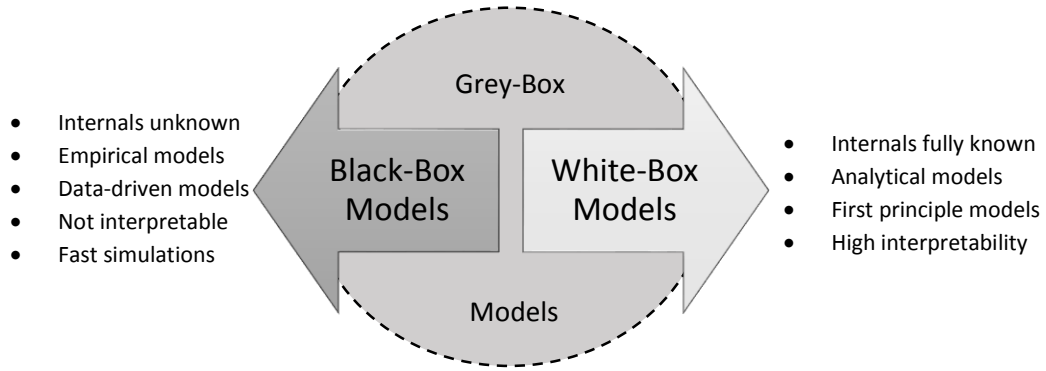

Figure 9: Black-box, White-box and Grey-box models [56]

III. DESCRIPTION OF THE CONTINUOUS DIRECT COMPACTION PHARMACEUTICAL PROCESS

The process considered for the design of a control system is a pilot plant for continuous tablet manufacturing process located in the Research Center of Pharmaceutical Engineering (RCPE) at Graz University of Technology. The process sketch of the continuous tablet manufacturing process is illustrated in the Figure 10. In the figure, it is included the two different hopper being studied, but just as a visual representation, since the process is run either with the cylindrical or with the conical. The Figure 12 illustrates in more detail the geometry of each hopper.

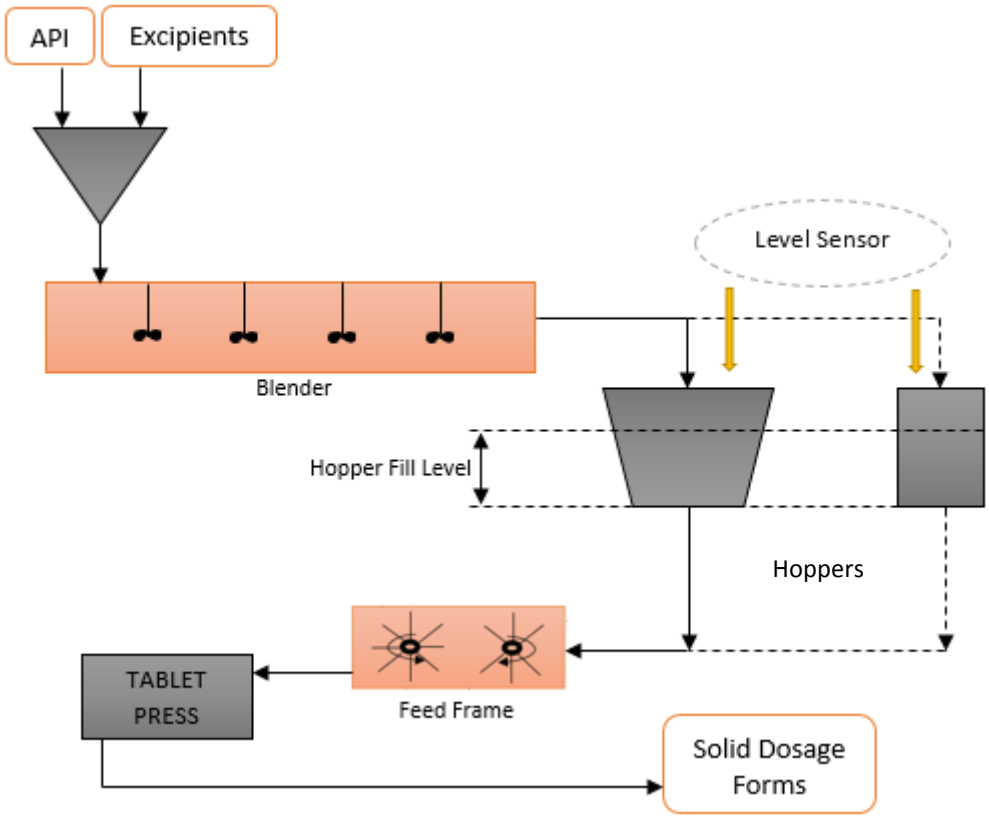

Figure 10: Continuous Direct Compaction Pharmaceutical Process. Representation of the RCPE's Pilot Plant with the two types of Hoppers being studied

The continuous tablet manufacturing process described above is equipped with a blender, one hopper, a feed frame and a tablet press. A constant mass flow of API and excipients enters the blender which produces a homogeneous mixture. The outlet from the blender feeds one of the two hoppers, depending on process specifications. Its level is

measured by an top-mounted ultrasonic device and continuously controlled by the implementation of an automated control system (see chapter 6) that adjusts the turret speed ω_{turret} of the tablet press, which is in fact linearly related with the mass flow rate that runs out of the hopper $\dot{m}_{out}$, as eq. (III – 1) shows. The main goal of the designed control system is to guarantee the stability of the process, preventing the hopper from overfilling or running empty. The outlet of the hopper is attached to a feed frame, which contains two paddles wheels that spin in opposite directions with the main purpose of keeping the motion of the powder and transfer it over to the die opening. Besides, the paddles guarantee a perfectly filled die of the tablet press under the effect of gravity and suction, so that each die contains the perfect amount of powder. The powder is continuously compressed in the rotatory tablet press that produces a continuous flow of solid dosage forms.

$$\dot{m}_{out} = \frac{n_{Die} \cdot m_{Tab}}{60} \cdot \omega_{turret} \qquad \textit{eq. (III-1)}$$

The correct performance of the system that controls the hopper fill level can be altered in two different ways: effects on the system dynamics (1) or effects on the quality of the measurement via PAT (2). Regarding the point (1) the hopper's inlet $\dot{m}_{in}$ and outlet $\dot{m}_{out}$ flow rate represent the most important variables affecting the system's dynamics. In this thesis, it is assumed that parameters such as abrasiveness, wall friction, powder attrition, particle friability or cohesive properties of the powder do not compromise the flow, and consequently, they will not be taken into account when developing the dynamic models in chapter 6. These assumptions together with the fact that the hopper's walls are sufficient steep and smooth, allow the *mass flow* behavior of the bulk solids through the hopper, as the left image of the Figure 11 attempts to illustrate. This means that the group of particles that first enter the hopper, would leave the hopper also in the first position, generating consequently narrow residence time distributions (RTD) [60]. This effect is known as *"first in / first out" or "plug flow"*. The opposite effect is called *funnel flow* (see right image of the Figure 11) and it refers to a flow pattern where only a part of the bulk solid in the silo is in motion (i.e. the region vertically above the outlet) [61].

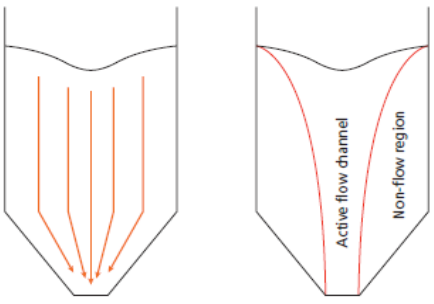

Figure 11: Illustration of mass flow (left) and funnel flow (right). Extracted from [60]

It is worth mentioning as well, with regard to the point (2) of the previous paragraph, that several process parameters such as dusty atmospheres, uneven surfaces or angle of repose might affect critically the quality of the hopper fill level measurement. Its effect will be analyzed and evaluated in the chapter 4 via risk assessments.

3.1 Hopper design

A hopper is needed in every continuous line to cope process model functions. Hoppers are commonly used in solid processing with the main purpose of holding materials and conveying them gravimetrically. In this particular case (see previous Figure 10) the hopper will bridge the upstream area with the downstream. In a well-design hopper, powder should be able to flow constantly avoiding effects such as funnel flow or arching and keeping the residence time distribution almost invariable for each particle. This particular behavior is also known as plug flow [62]. As it was previously described, the hopper used in the continuous direct compaction process can present two different geometries (see Figure 12) depending on process specifications. Regarding the conical hopper, it presents a huge hold up and hence, the tracking of the material is hard. Besides, it might not follow the *first-in first-out principle* because of slipping of material on one side (more or less sloping depending on the angle of the conical section with the vertical θ_c). The cylindrical hopper will provide, in contract with the conical one, less resistance to the movement of the powder, presenting consequently a smaller hold-up. Its geometry allows also the development of a more accurate mathematical model since the aforementioned *first-in first-out principle* can be taken into account.

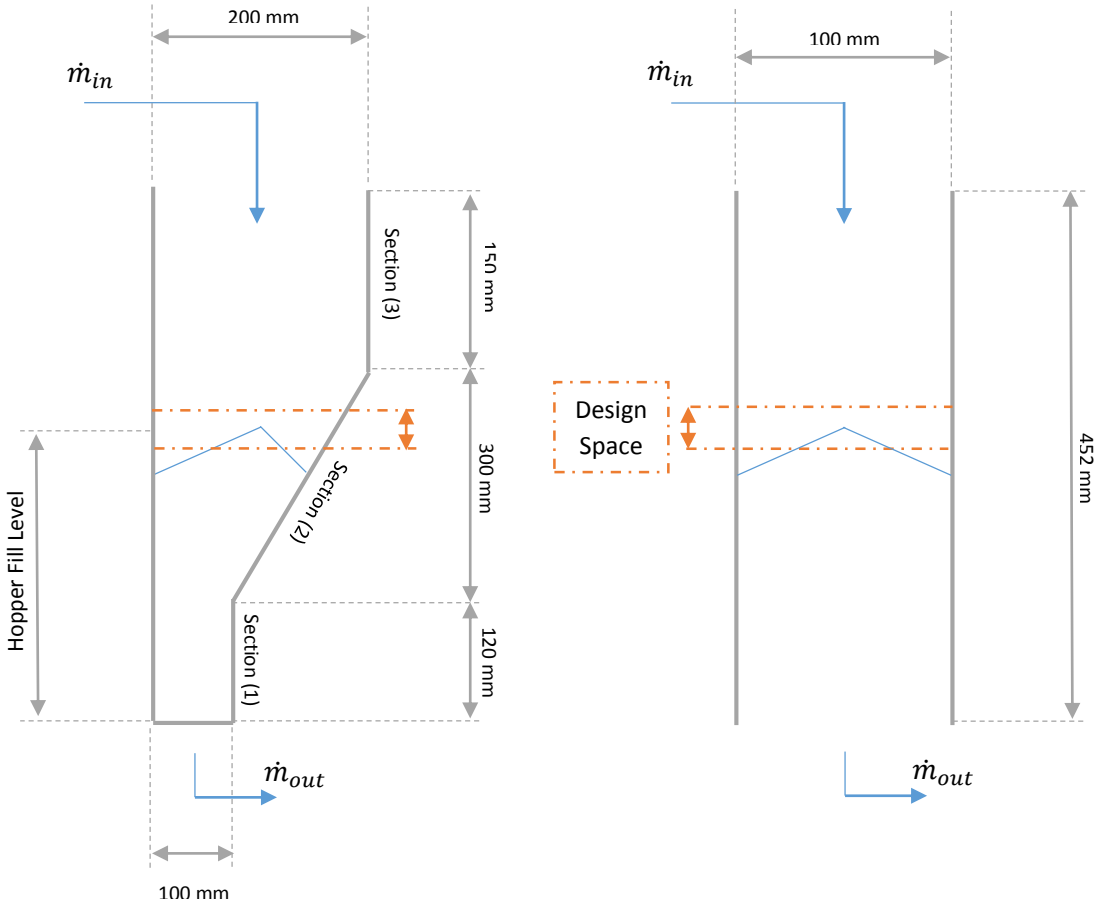

Figure 12: Hopper geometry and design: asymmetric conical geometry (left) cylindrical geometry (right)

IV. CRITICAL ATTRIBUTES AFFECTING THE STABILITY OF THE PROCESS

Among the main reasons that withhold the pharmaceutical industry from adopting continuous manufacturing, the fear to changes in the way the drugs are currently being manufactured or the lack of process understanding stand out. Tools such as quality risk management (QRM) or design of experiments (DoE) have been widely used, and recently, they are playing a major role in the pharmaceutical industry to address the lack of process understanding with regard to the dynamic behavior of powder while the manufacturing of solid dosage forms.

Solids have a very particular behavior while flowing, and unlike liquids, keeping the flow homogeneous is quite a challenge. This chapter focuses on the analysis of the parameters that more likely influence the stability of the process. As it will be demonstrated in following sections, not every parameter affects the stability of the process with the same relevance. Tools such as process understanding, DoE or risk assessments will help to identify potential sources of process variability and material attributes and process parameters likely to have the greatest impact on the process stability. The final outcome of the QbD approach (see Figure 13) would be a highly accurate design space where the control strategy will be applied to keep the CAs within the design's space limits, and hence, ensure the process performance and product quality (ICH Q10) [63]. The final goal of the thesis, as previously commented, will be the development of a robust control strategy based on the information obtained within the chapter 3, 4 and 5. In essence, an automatic control system furnishes important benefits such as meeting the final product specification (i.e. QTPPs) or maximizing overall production rate [64][65].

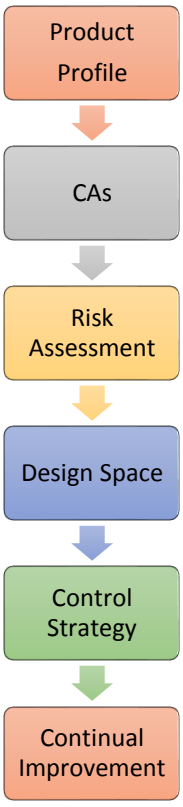

Figure 13: Example Quality by Design (QbD) Approach. Adapted from [63].

4.1 Identification of the Material Attributes (MAs), Process Parameters (PPs) and Critical Attributes (CAs) by Process Understanding and Risk Assessment

One of the most common ways to perform a risk assessment is the development of an Ishikawa diagram. The basic concept was first used in the 1920s, and is considered one of the seven basic tools of quality control [66]. In essence, the Ishikawa diagram helps to prevent quality defects both in the material and in the process, by the identification of parameters (material attributes and process parameters) that might disturb *the performance of the hopper fill level control strategy* (see Figure 14). The simultaneous execution of risk assessments and process understanding turns out to be pretty useful, so that those material and process attributes that warrant further study (i.e. CAs) can be prioritized [6]. In this section of the thesis, those parameters showing the highest probability of disturbing the correct control of the hopper fill level will be analyzed. This information will be used in the following chapter to select the most suitable level sensor.

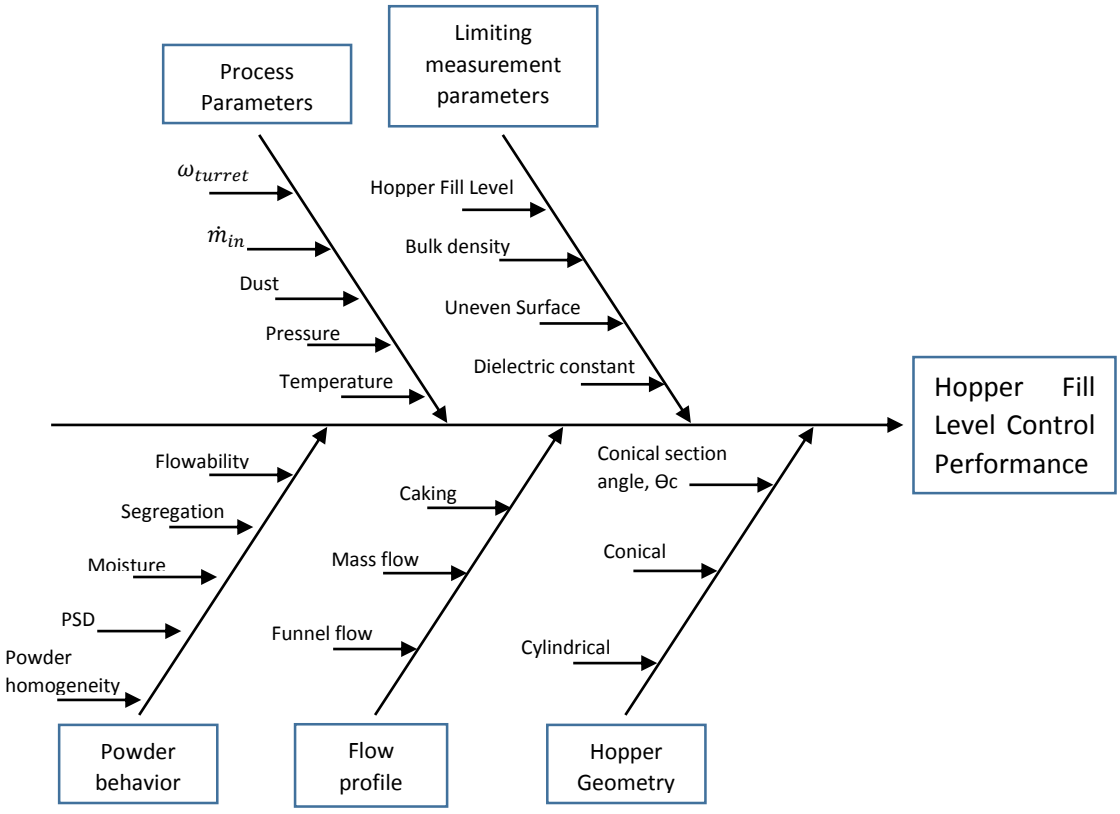

Figure 14: Ishikawa Diagram. Material Attributes (MAs) and Process Parameters (PPs) that might affect the performance of the hopper fill level control system

4.2 Interaction between the selected Critical Attributes and the Process

The box located in the far right side of the Ishikawa Diagram (see Figure 14) represents the main problem/challenge, while the other boxes and arrows might be potential factors causing an overall effect on it. As described previously, not every parameter influences in the same way the correct performance of the control system. Consequently, by process understanding, risk management and experiments in the laboratory, the Ishikawa diagram can be cut short to show the parameters that influence potentially the correct control performance (see Figure 15). For example, the effect of factors such as the pressure or the temperature will be considered negligible, since the process runs indoor and the surrounding environmental conditions are likely to be fairly stable.

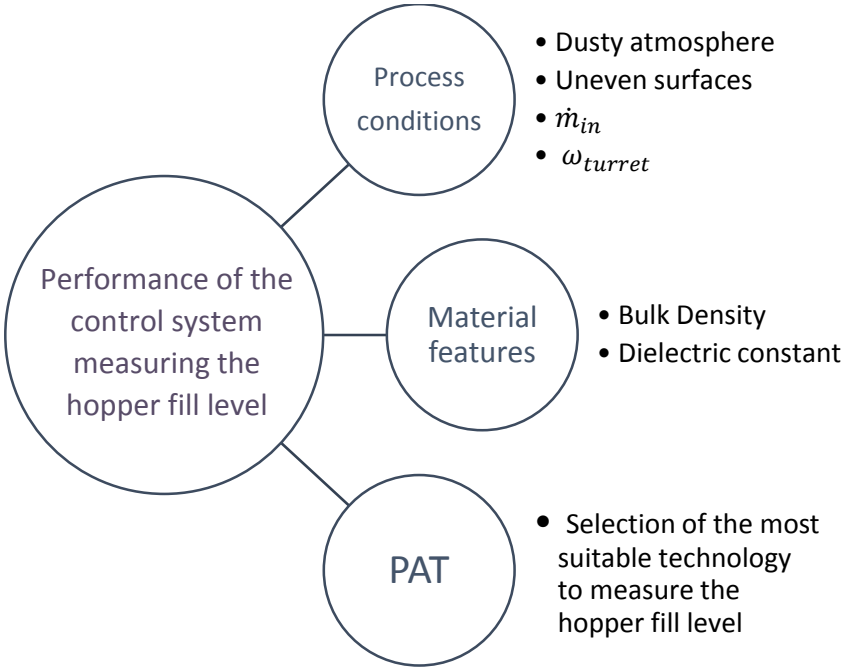

Figure 15: Critical Attributes (CAs) affecting the performance of the level measurement sensor

Dust and uneven surfaces are going to represent two of the most important challenges for the measuring device. On the one hand, the increasing concentration of dust inside the hopper when the process is running might affect critically the performance of the sensor, and consequently, it will be carefully taken into account when selecting the measurement technology. Uneven surfaces (i.e. large angle of repose or undulations, see Figure 16) on the other hand, is a classic problem encountered when measuring the level of powder or granular material from the top of a vessel or hopper, and it might lead to the dispersion of the signal waves away from the transducer [67]. Besides the bumpy surface, pharmaceutical powders are made of fine granular particles, which may also scatter the reflected wave in all directions, preventing the signal from travelling back to the transducer, and leading to wrong readings. In order to avoid as much as possible unwanted scattering, the usage of the highest possible frequency to minimize the beam's width and spot the size on the target, turns out to be really beneficial [68].

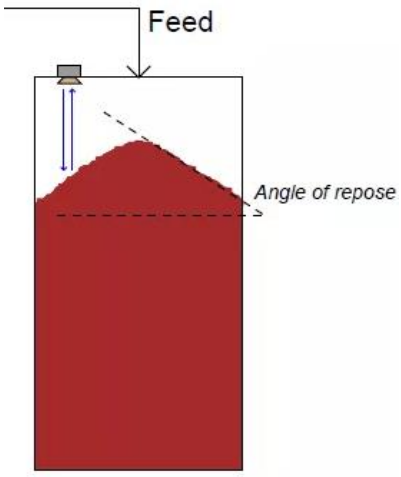

Figure 16: Angle of repose. Extracted from [67]

Regarding the flow of the bulk solids through the hopper, it is worth mentioning that its behavior depends on parameters such as the particle size distribution, particle shape, chemical composition of the particles, adhesive forces, inter-particulate interaction, moisture and temperature among others [69][70][71]. However, in this particular work, a *mass flow* or *free-flowing* behavior ($ff_c > 10$) of particles (see Figure 17) is assumed and consequently, the flowability is not considered a critical attribute. In other words, its effect on the control strategy is considered negligible due to the optimal flow of the powder.

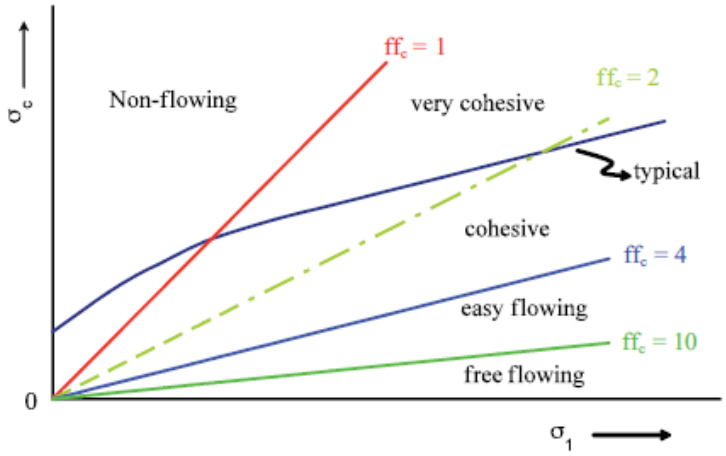

Figure 17: Flow function, Lines of constant flowability and flow ranges. Adapted from [116]

Contrary to the flowability, two material features (see Figure 16) that might influence the measuring performance of the sensor are the bulk density and the dielectric constant. On the one hand, the bulk density must be considered a critical parameter if for example, ultrasonic technology is selected (see Table 1). On the other hand, the dielectric constant of the material might influence the quality of the measurement. This parameter is a value that indicates the reflectivity of the material. A poor reflectivity would mean that the material being measured is not able to reflect enough energy back to the sensor when the waves hit the medium, leading to deficient measurements [72]. The reflectivity of a compound is actually predictable and is a function of its dielectric permittivity as the eq. (IV – 1) shows.

$$R = \frac{\left(\sqrt{\varepsilon r}-1\right)^2}{\left(\sqrt{\varepsilon r}+1\right)^2} \qquad \textit{eq. (IV-1)}$$

Where “R” is the reflection and “Ɛr” is the relative dielectric permittivity.

V. SELECTION OF SUITABLE LEVEL MEASURING TECHNOLOGY

The selection of the process analytical technology (PAT) might become an arduous task due to the presence of the aforementioned parameters (CAs). While most level measurement technology are adaptable for more than one process, there is not one single device that can work efficiently for every application. However, by sufficient process understanding and by asking the proper questions, it is possible to narrow the area of choice. This chapter is therefore focused on the research of the most suitable technology to measure the hopper fill level. To do so, an exhaustive evaluation of the advantages and disadvantages with regard to each technology will be carried out, as well as the study of the impact of the aforementioned CAs on their respective performances.

Level sensors have been a part of manufacturing processes for several decades in industries as diverse as food and beverage, semiconductors and pharmaceutical among others. However, one may be surprised at the sophistication of level sensing alternatives currently available that might satisfy our needs. To determine the best sensor for our particular application, it is important to understand the selected technology, as well as their advantages and limitations [73]. This thesis takes into consideration five different PAT that can provide real time control [74][75][76].

1. Ultrasonic technology
2. Guided wave radar technology
3. Non-contact radar technology
4. Field time control technology
5. Laser Pulse Time-of-flight distance measurement technology

Besides the different technology available nowadays in the industry for measuring distances, there is a great number of companies that offer a wide range of sensors. Their products are going to be analyzed in this point one at a time, following the previous list that enumerates the different technologies for measuring the bulk solid level.

5.1 Ultrasonic Technology

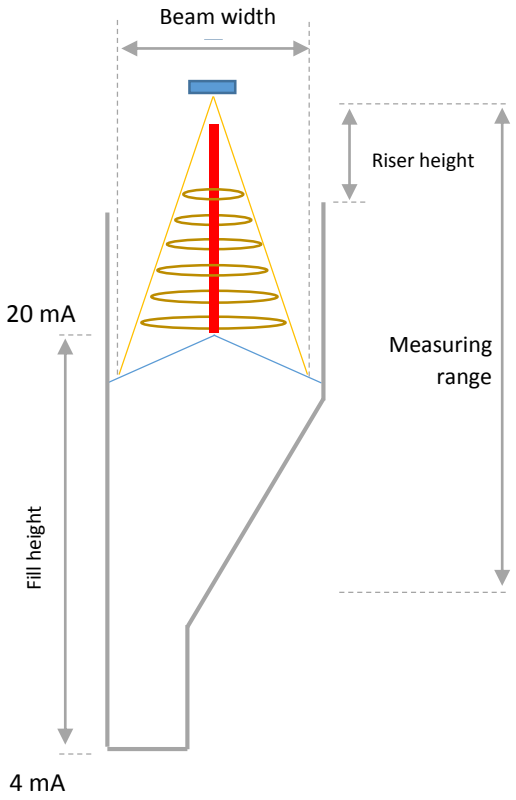

Figure 18: Ultrasonic sensor's features

Ultrasonic level measurement is the most widely used non-contact technology, mainly due to its cost-efficient features. The sensor emits a high-frequency pulse (sound waves), generally in the 20 kHz to 200 kHz range as the Figure 19 illustrates. As soon as it encounters a sudden change in material density (i.e. interface between a gas and a solid), a fracture of wave's energy, *echo*, will be reflected in the form of another wave in the opposite direction (see Figure 18) [77]. Its efficiency depends on the amount of echo reflected back to the transducer [78]. Ultrasonic level instruments, as well as radar or laser, work by the *time of flight (TOF) principle,* which is referred to the time it takes for a pulse or a wave of energy to travel from its transmitter to the target and then back to the receiver. This particular feature is an added-value for any pharmaceutical manufacturing process, due to the fact that any type of physical contact with the powder is avoided. However, precisely this benefit entails other drawbacks (see Table 1) that might affect the arrival of the signal back to the transducer such as dust, surface turbulence, uneven surface or low material densities [67].

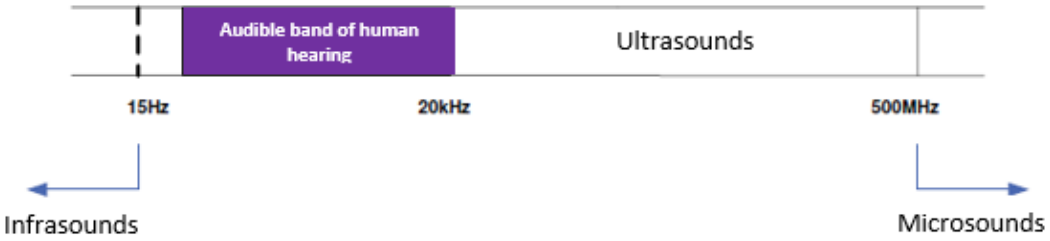

Figure 19: The frequency ranges of the sound. Extracted from [77]

The velocity "c" of the waves emitted by the sensor depends both on the density "ρ" of the medium and on the bulk modulus B, according to the following equation, eq. (V–1):

$$C = \sqrt{\frac{B}{\rho}} \qquad \text{eq. (V—1)}$$

Ambient factors such as the temperature T can influence significantly the propagation of the ultrasounds, due to its known effect on material density. The density of the air depends on the temperature which affects the propagation velocity according to the equation:

$$V_s = V_{so} \cdot \sqrt{1 + \frac{T}{273}} \qquad \text{eq. (V—2)}$$

Being V_{so} the propagation velocity of the sound wave at 0ºC, and T the absolute temperature in Kelvin.

By knowing the value of the speed of sound through a certain material with known density, its acoustic impedance Z could be calculated, as the equation eq. (V – 3) shows. This parameter holds a notable importance when measuring the level, since it is related to reflection of ultrasonic energy. The higher the difference of the acoustic impedances between two media, the more significant is the reflection of the ultrasound.

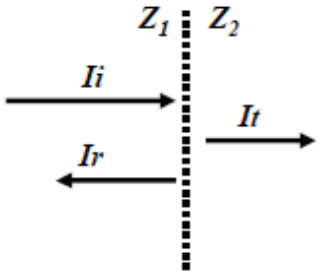

Figure 20: Reflection and transmission of an acoustic wave at normal incidence to a plane boundary. Extracted from [77]

$$Z = \rho \cdot c \qquad \text{eq. (V—3)}$$

During our level measurement, ultrasonic waves travel all along the homogeneous medium (i.e. air), till they reach the solid material, where the reflection and transmission occur. It is important to highlight that the reflection occurs only when the acoustic impedance of one media is different from the acoustic impedance of the second media at the boundary (see Figure 20). The reflection coefficient "$R_{coeff.}$" and the transmission coefficient "$T_{coeff.}$" are a function of the impedances of both mediums, as follows:

$$R_{coeff.} = \frac{Ir}{Ii} = \left[\frac{Z1-Z2}{Z1+Z2}\right]^2 \qquad \text{eq. (V—4)}$$

$$T_{coeff.} = \frac{It}{Ii} = \frac{4 \cdot Z1 \cdot Z2}{(Z1+Z2)^2} \qquad \text{eq. (V—5)}$$

$$R_{coeff.} + T_{coeff.} = 1 \qquad \text{eq. (V—6)}$$

Where "I_i" is the incident radiation Intensity, "I_r" is the reflected radiation intensity and "I_t" is the absorbed radiation intensity.

The quality of the readings depend strongly on how much energy is reflected back to the transducer after hitting the media being measured. Theoretically, and based on these previous formulas, the reflected energy should be sufficient to achieve proper measurements, since the different of densities between the bulk solid and the air is pretty wide. The bulk material being used presents a density of $\rho = 800\ \frac{Kg}{m^3}$ while the density of the air at room temperature is about $\rho_{air} = 1.20\ \frac{Kg}{m^3}$. In the following table are found the advantages and disadvantages of using an ultrasonic level sensor for measuring the fill level of an industrial hopper.

ADVANTAGES	***DISADVANTAGES***
- *Non-contact technology* - *Ultrasonic sound energy vel. (340 m/s)* - *Optimal for continuous processes* - *Top mounted* - *Easy set-up* - *Cost effective solution (1000 – 2000 $)* - *Fast response to changing level* - *Rapid response to changing level* - *PC software available to diagnose and calibrate sensor generally available* - *Time of Flight (TOF) principle* - *Normally, the dielectric constant is not a problem*	- *Interferences due to the process atmosphere* - *Might be problematic for low dielectric constants of the measured material.* - *Dust, foam, Tº, surface angles and pressure might affect the measurement, but they are better than laser devices for such conditions* - *Surface conditions (reflective surface must be flat, as much as possible)* - *Limited Pressure and Tº* - *Not flat surface might be problematic* - *These devices have a minimum sensing distance* - *Its efficiency depends on the bulk density*

Table 1: Advantages and disadvantages of the ultrasonic technology

5.2 Guide Wave Radar

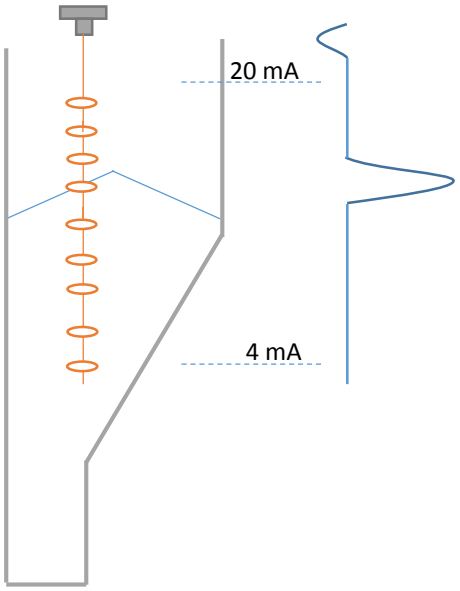

Figure 21: Guide Wave Radar installed in the hopper

Another device that should not go unnoticed is the Guide-Wave-Radar. While the ultrasonic transmitters operate by sending a sound wave generated from a piezoelectric transducer to the surface of the process material being measured, the guide wave radar (GWR) is a contacting level measurement method that uses a probe to guide high-frequency electromagnetic waves from the transmitter to the media being measured, as it is illustrated in the Figure 21. GWR is based on time domain reflectometry (TDR) that enables direct, precise and highly reliable continuous level measurement as well as point detection in almost every liquid and solid. Due to its way of measuring, physical and chemical properties of the contact media or the environmental conditions do not affect the readings, as might happen with devices based on the TOF principle, since the probe is immersed in the material being measured [79][80]. With TDR, the pulse energy is reflected up the probe to the circuitry which then calculated the fluid level from the time difference between the pulse sent and the pulse reflected [81].

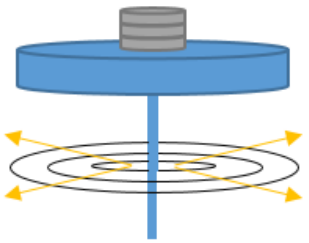

Figure 22: Sound energy pulse advances outward from the probe surface

The use of a probe to measure the bulk solid level solves one of the biggest problems when using non-contact technology, the presence of dust in the air. This characteristic together with the ones commented above (see also Table 2) might support the selection of this technology for the measurement of the hopper fill level. However, what appears to be a solution to a problem, entails occasionally a bigger trouble. In our particular case, the direct contact with the material being measured (bulk solid) must be avoided at all costs, due to possible modifications of the particle size distribution (PSD) or in a more general case, due to sanitary reasons. If a probe is

immersed in the particles as it would happen if GWR technology is selected, see Figure 21, small particles will be prone to follow downwards the motion of the probe, leading to segregation. It is important to take into account on of the most common misconceptions of the GWR. One can think that the build-up of particles around the probe might affect the quality of the measurement, but this is not true [80]. When the electromagnetic pulse comes in to contact with a mass of product on the probe, the signal is returned and analyzed to see whether it reflects the true material level or not. The GWR radar signal has a very large detection area, 360º, as the Figure 22 shows.

ADVANTAGES	***DISADVANTAGES***
- *Price comparable to Ultrasonic Tech.* - *Much more reliable solution than ultrasonic tech.* - *Suitable for both liquid and solid applications* - *Offers level measurement independent of the chemical or physical properties of the contact media* - *Changes in density, viscosity or angle of repose do not affect the measurement accuracy* - *Top mounted* - *Rapid response to changing level* - *The pulsed microwaves are guide down along the probe, making it less sensitive to disturbance*	- *Contacting level measurement tech.* - *Product built-up on the probe (not always a problems since the 360º detection area)* - *Bit more expensive than the ultrasonic technology* - *Dielectric must be > 1.6 for best accuracy* - *Probably a bit expensive comparing to the ultrasonic device*

Table 2: Advantages and disadvantages of the Guide Wave Radar (GWR)

5.3 Non-contacting Radar Technology

Figure 23: Non-contact Radar technology placed over the hopper.

Over the past 40 years, radar has been one of the preferred technologies for many industrial applications. For non-contacting radars, the microwave frequency transmitted by the device is one of the areas where more effort has been set. Traditionally, three different frequency bands have been used for the level measurement: the C-band (~6 GHz), the X-band (~10 GHz) and the K-band (~26 GHz). Frequency is a fundamental property for any radar as it has direct effects on measurement performance. Indeed, radars using different frequencies are required to solve different problems. This engineering device is based, as the GWR, on microwave technology which detects only surface that reflects energy. Microwaves are commonly defined as electromagnetic radiation with wavelengths (λ) between 300 mm and 3 mm [82]. The amount of energy reflected depends strongly on the dielectric constant, meaning that for those materials with low dielectric constant, the amount of energy reflected will be lower. Furthermore, as shown in the Figure 23, and in contract to GWR, this technology uses the TOF principle to measure distances.

First and foremost, high frequency microwave signals suffer more attenuation, which means that they are absorbed to a higher degree when propagating through a medium, resulting in weaker signal return [82]. The process being studied is expected to generate a high-dense dusty atmosphere and consequently, according to the previous affirmation, the lower the frequency the better the performance.

Furthermore, uneven solid surface (i.e. agglomeration of particles just below the entrance, see Figure 23) are common in the industrial applications and might cause problems when measuring the desired point. Instead of reflecting back upwards towards the antenna, microwaves hitting a turbulent surface may scatter and disperse. Thus, a large percentage of signal strength can be lost and give the radar problems with obtaining an accurate measure of the level. However, according to [82], “microwaves remain unaffected by surface irregularities such as turbulence if the wavelength is larger

than the ripple size". This together with other advantages and drawbacks are listed in the Table 3.

ADVANTAGES	***DISADVANTAGES***
- *Continuous level measurement* - *Non-contacting technology* - *Highly accurate and reliable direct level measurement for liquids and solids* - *Unaffected by process conditions* - *Easy installation* - *Free propagating microwaves through air* - *Frequency can be modified to achieve the desire measurement* - *Measurement is virtually unaffected by changes in Tº, pressure, dust…* - *Bulk density does not affect the measurement* - *Often large beam* - *Time of Flight (TOF) principle*	- *Still expensive comparing to ultrasonic devices (price increases with increasing accuracy), up to 4000 €* - *Measurement accuracy depends strongly on the right choice of the frequency for a particular problem.* - *Low dielectric materials are difficult to measure as there is not enough radar energy to be reflected from the product surface*

Table 3: Advantages and disadvantages of the Non-contact Radar technology

5.4 Field Time Control

FTC (Field Time Control) technology is an innovative product detection technology designed for bulk solids. An electric field is generated between the transmitting electrode and the multiple receiving electrodes. The cycle time of the FTC sensor, as shown in the Figure 24, changes as soon as the product intervenes this electric field. The amount of clock pulses is directly proportional to the measured capacitance (measured by those receiving electrodes). Even a slight capacitance change or a small level change results in a considerable increase of the amount of clock pulses. As a result the system identified which electrodes are covered by the product (i.e. powder) and determines

accurately the product level, even with a hard-to-measure product with low dielectric constant.

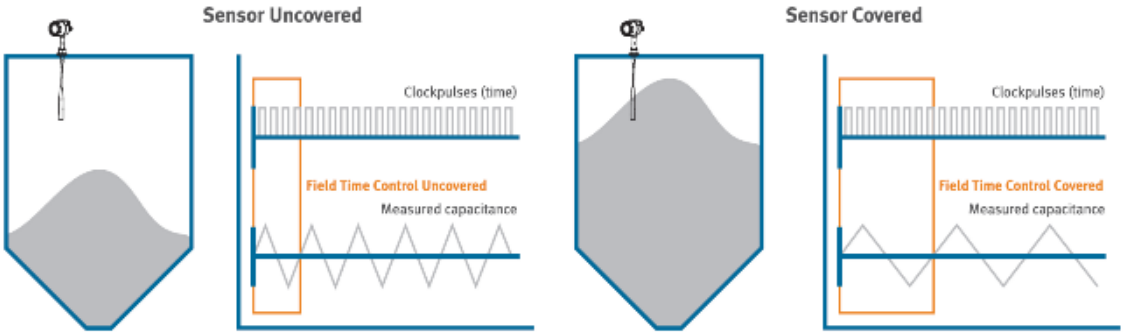

Figure 24: Level measurement by FTC technology. Extracted from [83]

Besides being an innovative way of level measurement, it provides to the costumer a reliable and cost-effective solution. The food and the pharmaceutical industry have been the first ones to prove it, and by now, even the biggest international pharmaceutical companies in USA, Switzerland and the UK are using it [83]. However, as the Table 4 shows, the use of this sensor requires a non-metallic tank. Unfortunately, the hopper being used in this work was already designed with metallic material, and this technology was not worthy it to be elected.

ADVANTAGES	***DISADVANTAGES***
- *Optimal application in bulk solids* - *Optimal accuracy with even low dielectric constants* - *Cost effective solution* - *Non-intrusive technology* - *Optimal for sensitive product like food or pharmaceuticals* - *It is mounted on the outside*	- *Non-metallic tank is a compulsory requirement* - *Vessel requirements (made of plastic or glass)* - *In order to use this technology in our process, some modifications of the hopper must be developed, since our hopper is metallic. A physical modification of the hopper might lead to several problems in its efficiency and accuracy.*

Table 4: Advantages and disadvantages of FTC technology

5.5 Laser Technology

Even though laser technology for the measurement of distance has not been on the market as long as devices such as ultrasonic or radar sensors, this technology is becoming more popular within the industry as the costs of lasers and photo-detectors are going down. A laser level sensor uses infrared light to send a focused beam towards the product surface, where is reflected and sent back towards the sensor. The distance is calculated based on the time of flight. In addition to the aforementioned devices, the laser technology comes out as a very promising technology to measure the level of any material. Unlike the technologies that use microwaves, the laser technology is not limited by the dielectric constant, and this provides a big advantage over other devices when measuring certain kind of solids. In addition, the laser beam emitted by the sensor does not diverge much, so it can target smaller areas such as the highest point of the bulk solid, formed as a consequence of homogeneous inlet flow.

However, as happens with the other non-contact devices, accumulation of dust in the atmosphere of the tank or the dirtiness of the sensor itself might produce easily the degradation of the laser beam's strength. This degradation is absolutely unwanted since as the other non-contact technologies, the laser calculates the distance of the material by measuring the time of flight of very short pulses of infrared light [84].

One of the main advantages concerning laser devices, among the other ones listed in the Table 5, is pointed out by Ivo Radanov, laser level product manager at "K.Tek": "Laser light energy is scattered from the material surface in all directions. This means that laser level measurements are independent of the angle of the material encountered by the laser beam because part of the scattered reflection will return to the sensor" [85]. In some applications, this scattering will completely defeat the measurement method. Radanov adds: "This is particularly important in solids applications where the material surface usually isn't perpendicular to the energy beam and provides an advantage over other non-contact technologies that use energy that can be reflected away from the sensor measuring the reflected energy". In other words, there is not limitation on the able of incidence for measuring solid with lasers, which simplifies installation.

ADVANTAGES	***DISADVANTAGES***
- Continuous level measurement - Infrared light (speed of light) - TOF (Time of flight) - High accuracy in bulk solids measurement - Material density does not affect the measurement - Non-reflective materials are perfectly measured. - Non-contact measurement - Time of flight lasers penetrates perfectly medium dust conditions. - Low purchase cost - No limitation on the angle of incidence - Dielectric constant does not affect the beam reflection - The laser beam does not diverge too much - Measurement not affected by the angle of repose of the material being measured	- Dirt and dust affect the performance of the device - Appropriate for applications involving distances longer than 1 meter

Table 5: Advantages and disadvantages of Laser Technology for level measurement

5.6 Comparison between the Technologies being studied

Numerous principles of operation, design variations, installation, performances at the given process conditions or the economies of operation can make the selection of the most suitable technology an arduous task. To ensure picking the right sensor for long-term durability, safety, accuracy and effectiveness, it must be considered all possible factors in the design scenario. The Table 6 evaluates the performance of different technology under these factors (i.e. critical attributes) that might affect the measurement (see Figure 15). To naked eye, Table 6 establishes the ultrasonic technology as the most suitable choice for our purpose, since any "three" or "red square" is singled out. The choice is meticulously argued in the following paragraphs.

Process Conditions	Ultrasonic	GWR	Radar	FTC	Laser
Continuous measurement	1	1	1	1	1
Bulk solids	1	1	1	1	1
Non-contact	1	3	1	2	1
Bulk Density changes	2	1	1	1	1
Low dielectric constants	1	2	2	1	1
Uneven surfaces	2	1	2	2	1
Reflection in solids	1	1	1	1	1
Angle of incidence	2	1	2	2	1
Installation easiness	1	1	1	2	1
Maintenance	1	1	1	1	1
Metallic tank	1	1	1	3	1
Measuring range	1	1	2	2	3
Cost-effective	1	2	3	1	2
Top mounted	1	1	1	2	1
Ambient temperature changes	2	1	1	1	1

Table 6: Rating of each technology based on its capability of handling each challenge

1 = Good. This condition has little or no impact on performance of this technology

2 = Moderate. This technology can handle this condition, but performance might be affected

3 = Poor. This technology does not handle the challenge properly.

The selected measuring device must be able to calculate distances fairly well, so that the automated control system keeps the bulk solid level within the design space. It is assumed that dealing with errors in the scale of millimeters will not influence the quality and efficiency of the process and hence, highly-cost technology such as laser might be rejected in the first place. It is worth mentioning that laser sensors provide some benefits over other non-contact technologies such as radar or ultrasonic. The measurement is not affected by the angle of repose of the material, since the laser light beam is narrow, and hence, it does not scatter. Yet, this technology is commonly used to measure long distances as Figure 25 suggests, where the beam is prone to disperse with higher probability.

Ultrasonic technology as well as radar (both guided wave radar and non-contact radar) are two of the most commonly used level measurement technologies in the industry despite their old fashioned characteristics. They share a common characteristic in the market, their reliability to costumers. However, according to an article published by Laura Martin [86], the price of ultrasonic devices is still a bit lower, even though the value of the radar technology in the market is dropping down currently. This different in price concerns the fact that ultrasonic, unlike radar, is subjected to interferences when it is not monitored closely [87]. However, both technologies share several features that are beneficial for our purpose such as easy set-up, top-mounted or the TOF principle.

The presence of high dense dusty atmosphere or the angle of incidence of the waves are among those factors that are going to be deciding in the selection of the technology. Usually, radar technology shows better performance as soon as foam, vapors, powder, dust or uneven surface are introduced into the equation. However, several tests that were carried out in the pilot plant with an ultrasonic level sensor proved that with the given conditions of continuous inlet flow, dust, uneven surfaces and temperature, this technology performs with enough accuracy to meet the project goal. Besides, Figure 25 justifies our inquiries about why ultrasonic technology would be the most suitable choice for low measuring ranges with intermediated dust density. Therefore, non-contact radar were rejected.

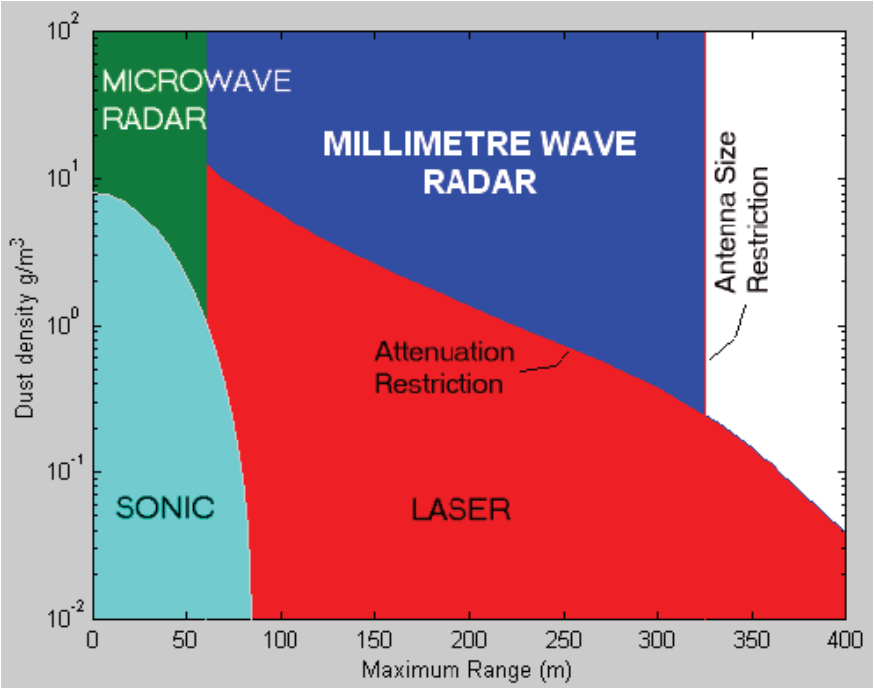

Figure 25: Cost effective sensor selection. Extracted from [68]

As happened with non-contact radar, technologies such as guided wave radar (GWR) or field time control (FTC) were rapidly rejected due to two main reasons. On the one hand, GWR is considered an invasive technology. The necessity of sanity in the process and the rejection to any disturbance in the powder properties are sufficient arguments to turn this option down. On the other hand, the FTC requires a non-metallic hopper for successful measurements as the Table 4 showed, and such investment was not worthy it at all in our particular case.

Despite the fact that ultrasonic level sensors are not currently the ultimate level technology in the market, it was proven that neither the amount of dust generated inside the hopper, nor the uneven surfaces (i.e. angle of repose) affect the measurement of the device over the time the experiments were run, about 10 to 15 minutes. Besides, the difference in densities between the air (i.e. 1,20 kg/m3 at 20ºC) and the material being measured (i.e. 800 kg/m3 at 20ºC) is enough to achieve larger reflection coefficients. The well performance of the ultrasonic device at the given conditions together with the fact that it is considered currently among the most cost-effective technologies, encouraged us to consider it as the most convenient choice for the measurement of the hopper fill level. The following section explains the features of the selected sensor together with installation guideless.

5.7 Ultrasonic Level Measurement in the Market

With the theoretical research concerning different measurement technologies, addressed along the previous chapter and to some experiments carried out in the pilot plant, the ultrasonic level sensor was the preferred technology to measure the hopper fill level. However, the market offers a wide range of possibilities with different characteristics (i.e. measuring range, price, and accuracy among others) that must be evaluated. Table 8 enumerates a list of 21 products developed by different companies that might meet the process specification. The product number of the Table 8 is linked to the list of products in Table 7.

1. U500-Da0	*12. U3M-148-3/4-18P154*
2. UNAM 12	*13. OPTISOUND 3010 C*
3. UM18-212165101	*14. EchoTouch® LU20*
4. UM18-212126111	*15. EchoSpam LU80*
5. UM30-212118	*16. UC500-30GM70-IE2R2-V15*
6. Ranger One™ LTRP-1	*17. UB500-18GM75-I-V15*
7. VEGASON 61	*18. UB400-12GM-I-V1*
8. FDU 90	*19. UB300-18GM40A-I-V1*
9. Prosonic T FMU30 1½" sensor	*20. UB300-18GM40-I-V1*
10. U3M-148 - U Series Mini	*21. LUC-M10*
11. U3M "Mini Probe"	

Table 7: List of Ultrasonic Products

ULTRASONIC PRODUCT	COMPANY	MEASURING RANGE [MM]	PRICE [$]	ACCURACY	SIGNAL OUTPUT	ENCLOSURE RATING
1	*Baumer Group*	*100…1000*	*-*	*< 0.5 mm*	*4…20 mA*	*IP67*
2	*Baumer Group*	*60…400*	*-*	*< 0.5 mm*	*< 20 mA*	*IP67*
3	*SICK*	*65… 600*	*-*	*< 0.17%/K*		*IP67*
4	*SICK*	*65… 600*	*-*	*< 0.17%/K*	*4…20 mA*	*IP67*
5	*SICK*	*65 … 350*	*-*	*± 1 %*	*4…20 mA*	*IP67*
6	*FLO-CORP*	*120…3000*	*-*	*< 0.5%*	*4…20 mA*	*IP68*
7	*VEGA*	*0… 2000*	*-*	*± 4 mm range*	*4…20 mA*	*IP66/IP67*
8	*Endress+Hauser*	*BD… 1200*	*-*		*4…20 mA*	*IP68*
9	*Endress+Hauser*	*BD… 2000*	*-*	*< 0.2% measured*	*4…20 mA*	*IP66/IP68*
10	*Madison*	*100…2740*	*470*	*± 0.25% range*	*4…20 mA*	*IP65*
11	*Madison*	*100…2740*	*451.42*	*± 0.25% range*	*4…20 mA*	*IP65*
12	*Madison*	*100…2740*	*495.68*	*± 0.25% range*	*4…20 mA*	*IP65*
13	*KROHNE GROUP*	*250…2000*	*-*	*± 0.2% range*	*4…20 mA*	*IP66/IP68*
14	*FLOWLINE ™*	*150…5400*	*950*	*± 0.25% range*	*4…20 mA*	*IP65*
15	*FLOWLINE ™*	*100…3000*	*700*	*± 0.2% range*	*4…20 mA*	*IP65*
16	*PEPPERL+FUCHS*	*45…500*	*-*	*± 0.5% range*	*4…20 mA*	*IP65*
17	*PEPPERL+FUCHS*	*30…500*	*-*	*± 0.1% range*	*4…20 mA*	*IP67*
18	*PEPPERL+FUCHS*	*30…400*	*-*	*± 0.5% range*	*4…20 mA*	*IP67*
19	*PEPPERL+FUCHS*	*35…300*	*-*	*± 0.5% range*	*4…20 mA*	*IP67*
20	*PEPPERL+FUCHS*	*35…300*	*-*	*± 0.5% range*	*4…20 mA*	*IP67*
21	*PEPPERL+FUCHS*	*250…2000*	*-*		*4…20 mA*	*IP68*

Table 8: List of the Ultrasonic Sensors with each respective characteristics

5.7.1 Detailed Technical Data of the Ultrasonic Sensor UM30-212118 from SICK

The UM30 category, developed by SICK, a world-wide leading manufacturers of sensors and sensor solutions for industrial applications, was the most suitable one for our purpose, given the process conditions [88]. At a glance, this ultrasonic sensor family provides a variety of flexible options that enables these sensors to solve nearly any application even under the most challenging conditions. Among the more distinguished features are: integrated time-of-flight technology (see Figure 26), sensing ranges up to 8,000 mm, immunity to dust and dirt, a display that enables fast and flexible sensor adjustment, as well as adjustable sensibility (see Figure 27). The latest is considered a unique functionality on the market and one of the main reasons that drove us to consider this company and similarly this sensor. Adjusting the sensor sensibility gives direct control over the sound cone's behavior and, therefore, over the sensor's detection and sensing range [89].

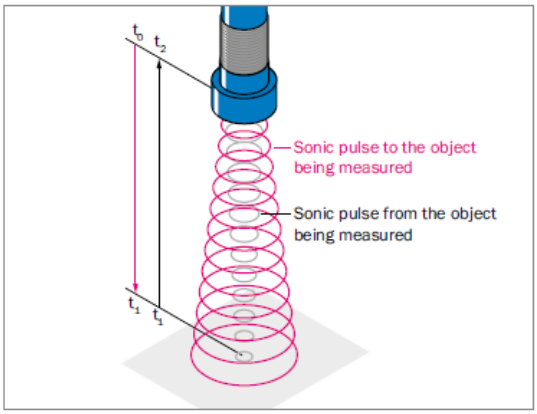

Figure 26: Sonic time-of-flight measurement. Extracted from [89]

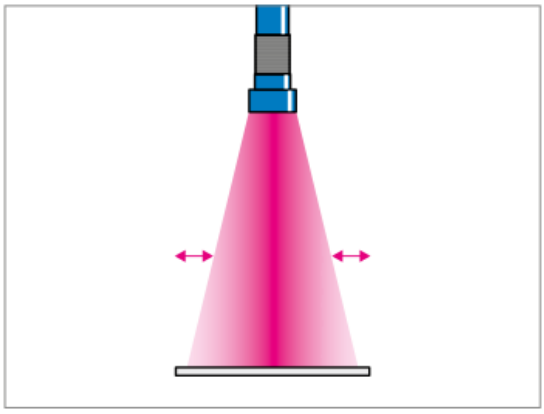

Figure 27: Sensor Sensibility's Adjustment. Extracted from [89]

The ultrasonic sensor UM30-212118 characteristics concerning performance, interfaces and mechanistic/electronic data are summarized in the Appendix. Besides, the Figure 28 illustrates the dimensional drawing. For further detailed information concerning the data sheet of this sensor can be found in the following citation ("Online Data Sheet UM30-212118") [90].

In general, the less sound the material being measured absorbs the greater the possible sensing range. This is a very particular feature of each sensor and it specifies the operating range up to which the sensor can measure under ideal conditions. Figure 29 illustrates the measuring range of the ultrasonic sensor under specific conditions. Whereas the dark blue area represents the sensor's working area if a round pipe is detected, the light blue area shows the maximum detection range which can be achieved under ideal conditions for easy detectable objects, such as an aligned plate. The area between the sensor and the material being measured should be kept free of other objects to prevent from being detected accidently.

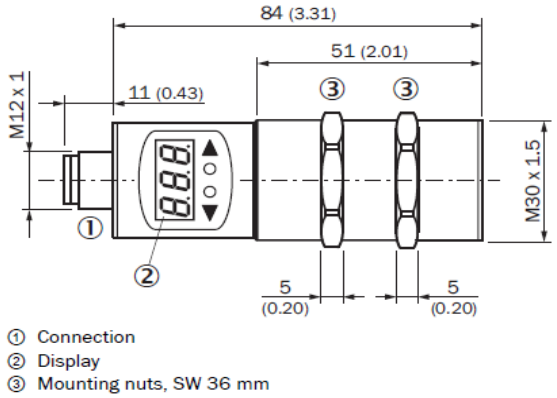

Figure 28: Um30-212118 Dimensional drawing. Extracted from [90]

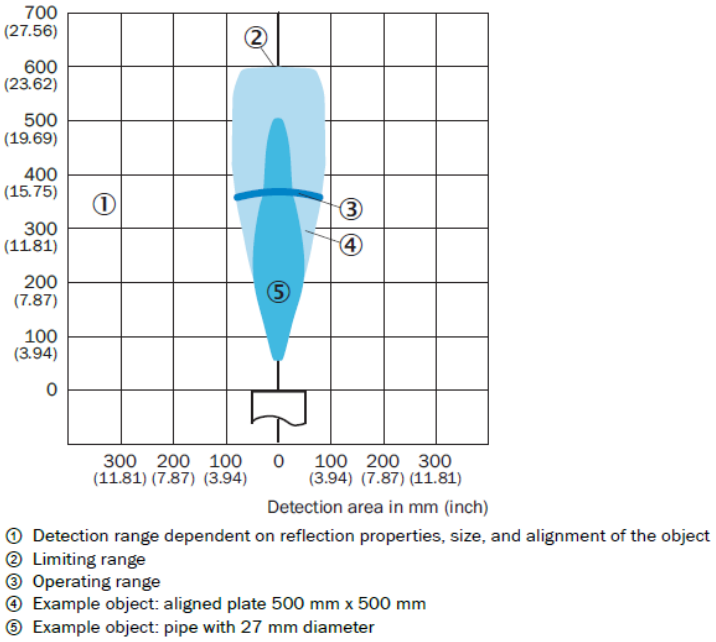

Figure 29: Um30-212118 sensing/measuring range. Extracted from [90]

VI. MODELING AND SIMULATION OF THE CONTROL SYSTEM

This new chapter presents the development of a robust control concept for a continuous compaction pharmaceutical process where the main critical process parameter, the hopper fill level, must be kept within its design space to guarantee process efficiency and process stability. The knowledge gained through the previous chapters to select the appropriated PAT will culminate now in the modeling of the process being studied and the design of the most suitable control strategy. Two models, one for each hopper, will be mathematically developed using ordinary differential equations (ODEs). Subsequently the models will be derived into transfer functions for control, where the integrating (non-self-regulating) behavior of the system being studied will be demonstrated. At the end of this chapter, after designing the controller according to two different tuning strategies, Internal Model Control (IMC) Lambda method and Skogestad Internal Model Control (SIMC), the ability of each control system to reject unknown disturbances and to the track set-point will be analyzed and compared by using MATLAB Simulink.

6.1 The Importance of Process Control and the selected Control Strategy

Continuous process monitoring in the chemical, pharmaceutical and petrochemical industries is important to ensure safety and product quality. The constant analysis of important parameters such as flow, pressure, temperature or level is required to achieve optimal processes behavior [91][92][93]. Manufacturers control the production process for several reasons: (1) Reduce variability, which has a direct impact on the end product and besides, manufacturers save money by reducing variability; (2) Increase efficiency, some processes need to be maintained at a specific point to maximize efficiency and (3) Ensure Safety, chemical processes usually handle dangerous substances that must be continuously monitored to avoid any unwanted risk [91].

This thesis addressed in the previous chapter the selection of a level measuring device that can provide real-time measurement of the hopper fill level. In general terms, the implementation of suitable PATs is indispensable for the adoption of continuous manufacturing, since any parameter would be controlled and consequently kept within its design space via the selected control strategy. In the current pharmaceutical industry predominates the absent of real-time process control in several solid-based process like powder feeding, blending, milling, tablet compaction and tablet coating [94]. This lack of engineering solution in the pharma industry has encouraged in part the development of this thesis.

Depending on the degree of automation that one wishes to apply in a pharmaceutical manufacturing process, three different degrees of control can be applied. The first one, level 1, located on the top of the pyramid illustrated in the Figure 30, represents the highest degree of automation. Input material attributes are monitored via PAT and process parameters are automatically adjusted to ensure that CQAs remain within the design. The second one, level 2, located in the middle of the pyramid, does not represent a real-time automatic control as the level one, since some end-product testing is required to keep the critical material attributes (CMAs) and the critical process parameters (CPPs) within the design space. The last one, being the base of the pyramid, is the level of control traditionally used in the pharmaceutical industry, commonly known as quality by testing (QbT), tackled in the second chapter as the opposite view of innovative quality by design (QbD) [6]. The following point addresses the full description of the hopper fill level control via the highest degree of automation, level 1.

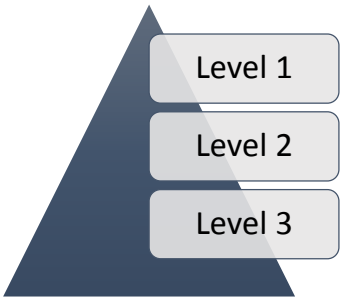

Figure 30: Level of Control Strategy. Adapted from [1] *and* [6]

6.2 Process Understanding and Operating Objectives for the Automatic Control of the Hopper Fill Level

Even though the control of the hopper fill level via PAT (i.e. ultrasonic level sensor) and standard feedback controllers just represents an example of automation or automatic

control within the pharmaceutical industry, it clearly reveals the “modus operandi” to successfully implement continuous manufacturing (CM) to other unit operations.

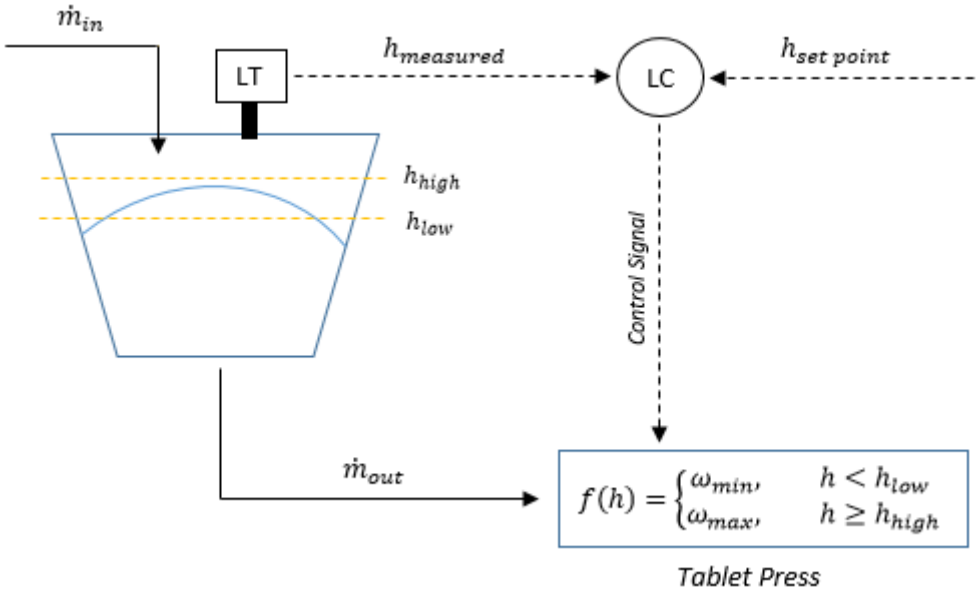

Figure 31: Hopper Fill Level Control System with control specifications in yellow lines

Well-placed PAT sensors are key elements of an efficient control strategy and besides, they enable CM and real-time release. The overall objective the system illustrated in Figure 31, is to efficiently control the hopper fill level h_{hopper} close to the defined set point value $h_{set-point}$, despite unmeasured disturbances such as the powder inlet flow, $\dot{m}_{in,hopper}$. The Figure 31 shows the desired operating range between two yellow discontinuous lines.

To achieve this control objective, a model-based feedback control loop represented in the Figure 32 is installed into the process depicted in the Figure 31. The hopper fill level is continuously measured from the upper section via ultrasonic technology, distinguished in the Figure 31 by the “LT” box. This value is compared to the defined set point. The error, the different between the measured value and the set-point, is processed and forwarded to the controller (“LC” box) that manipulates accordingly the turret speed of the tablet press. Summarizing, changes in the controller output owing to changes in the value of the error, regulate the turret speed ω_{turret}, which adjusts the mass flow rate $\dot{m}_{out,hopper}$ running out of the hopper. If the turret speed ω_{turret} is properly adjusted, the process variable will be maintained close to the set point, thus

satisfying the control objective [65]. This example, like all in process control, involves a measurement, computation and action as follows.

Measurement	*Computation*	*Action*
Hopper Fill Level	Is it higher than set point $h_{set-point} - h_{measured} < 0$?	Turret speed should increase towards its maximum value, "ω_{high}"
	Is it lower than set point $h_{set-point} - h_{measured} > 0$?	Turret speed should decrease towards its minimum value, "ω_{low}"

Table 9: Measurement, computation and control action

The centerpiece of a feedback control system is the controller structure illustrated in the Figure 32 that carries out actions on the manipulated variables based on the information provided by a continuous measurement. The hopper fill level control system of Figure 31 can be organized in the form of a traditional closed-loop feedback control block diagram as shown in the Figure 32 [95]. Most current publications suggest simple and common Proportional-Integral-Derivative (PID) control system for pharmaceutical production plant. Based on this information, the section 6.4 will present the implementation of both a P-Only controller and a PI controller in the feedback control-loop of the continuous direct compaction process being studied, with the main purpose of keeping the hopper fill level within its design space [51].

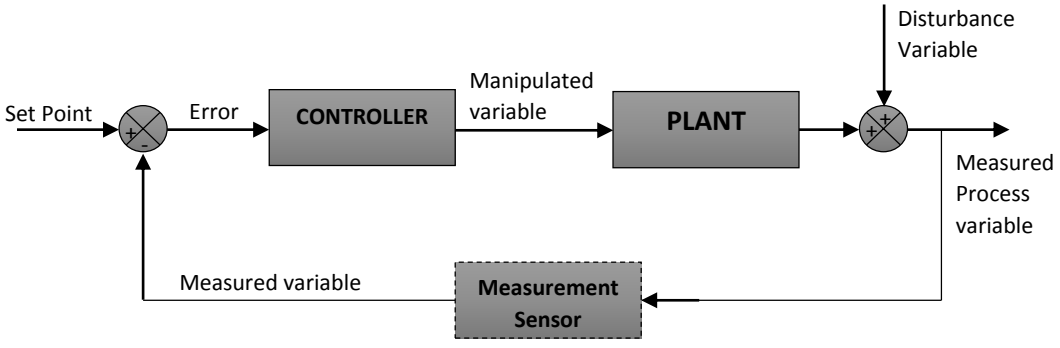

Figure 32: General Feedback Control Loop Block Diagram

6.3 Plant Model

In this section, three different models will be mathematically developed in order to express the dynamic behavior of the powder inside two different hoppers. The industrial process that this work attempts to model and control displays counter intuitive behaviors that make it surprisingly challenging to control. The beginning of the section demonstrates that the powder level inside the hopper behaves as an integrating (non-self-regulating) process, since it will not naturally settle out to a steady operating level if it is left uncontrolled [96][97][98]. For the integrating processes being studied operating at steady state, any positive step change in the inlet mass flow rate will cause the hopper level to increase linearly with time while a positive step change in the turret speed will cause the hopper level to decrease linearly. Thus, no new steady state will be attained, unless the hopper overflows or empties [99]. This integrating behavior is demonstrated in the Figure 33, by carrying out manual step changes in the turret speed (manipulated variable). The results of the Figure 33 are based on Simulink block diagrams concerning the three models being studied:

1) Model of the cylindrical hopper
2) Model of the conical hopper
3) Model of the linearized conical hopper

The behavior of the powder level inside the cylindrical hopper, represented by a red line in the Figure 33, is based on the Simulink Block diagram of the Figure 35. Similarly, the blue line and the black line represent the response of the powder level inside the conical hopper, based on the Simulink Block diagrams of the Figure 39 (non-linear model) and the Figure 41 (linearized model) respectively.

One of the first conclusions, concerns the fact that if any input variable is moved away from its steady state value, the system's output (hopper fill level) will blow up towards infinity unless some control action is carried out to compensate the disturbance's actions. This is in fact, the main characteristic of integrating processes. Besides, the Figure 33 shows instantaneous responses to disturbances, meaning that the time delay of the system would be zero ($\theta = 0$). This singularity will be taken into account in further sections when tuning the controller's parameters.

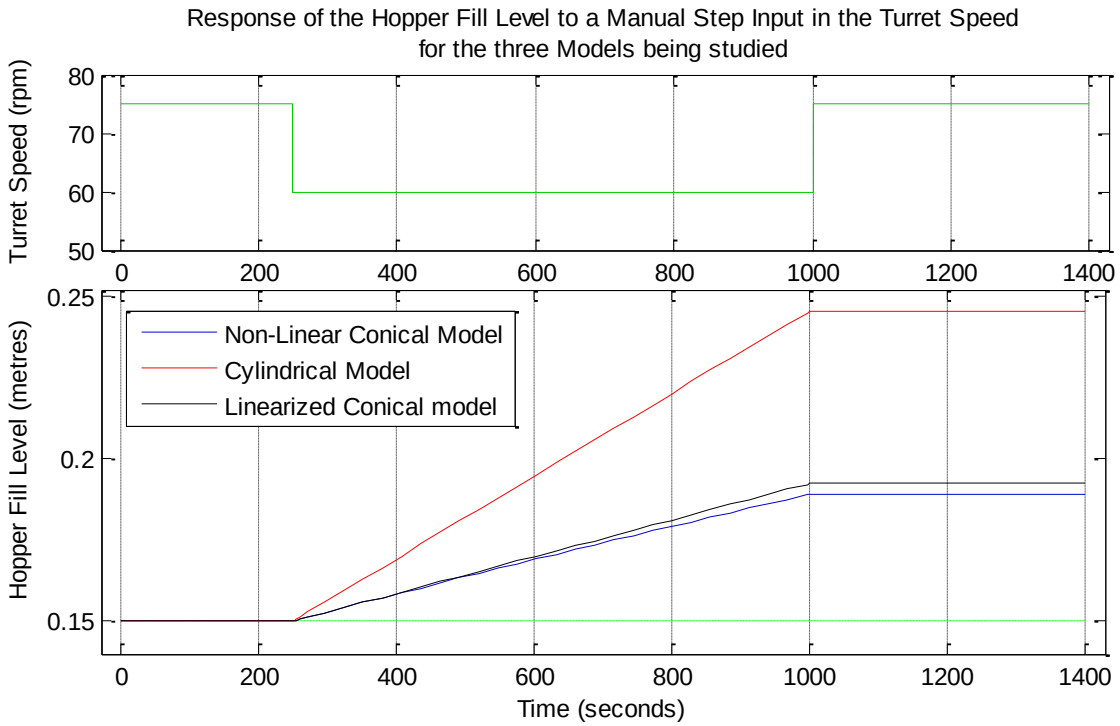

Figure 33: Integrating (Non-Self-Regulated) behavior of the three models being studied. A manual step input in the turret speed (open loop) will increase the hopper fill level towards infinity unless the controller output is stepped back up to its steady state.

This piece of work attempts to develop two models for the same unit operation (i.e. hopper) with different physical structure (see previous Figure 12) in order to express mathematically the change in the hopper fill level owing to both changes in the disturbance variable (hopper's inlet mass flow rate) and changes in the manipulated variables (turret speed of the tablet press). The models are obtained via a mechanistic modeling approach, taking into account hopper's geometry features and conservation laws. In this particular case, the conservation of mass described in the eq. (VI – 1) will be considered and used to develop the dynamic models [100].

$$\begin{Bmatrix} rate\ of\ mass \\ accumulation \end{Bmatrix} = \begin{Bmatrix} rate\ of \\ mass\ in \end{Bmatrix} - \begin{Bmatrix} rate\ of \\ mass\ out \end{Bmatrix} \qquad \textit{eq. (VI—1)}$$

To demonstrate the functionality of the proposed operating points, data from a previous project that used the software package gSolids® from Process System Enterprise (PSE) has been taken. The mass flow out of a tablet press $\dot{m}_{out}\left(\frac{Kg}{s}\right)$ is defined by the number of dies on the turret n_{Die} *(–),* the mass of a single tablet $m_{table}(Kg)$ and the turret

speed ω_{turret} (rpm). Since the pilot plant operates continuously, it is assumed that the hopper's outlet mass flow is equal to the mass flow out of the tablet press as follows:

$$\dot{m}_{out,tablet\ press} = \dot{m}_{out,hopper} = \frac{n_{Die} \cdot m_{Tab}}{60} \cdot \omega_{turret} \qquad \textit{eq. (VI—2)}$$

The goal of the modelling is to create a mathematical model for both the cylindrical hopper and the asymmetric conical hopper, which describe dependence of the hopper fill level, h_{hopper}, on the input mass flow rate, $\dot{m}_{in}$, and the turret speed, ω_{turret}. It is important to keep in mind in order to understand following simulations results, that the steady state of the hopper's inlet mass flow rate $\bar{\dot{m}}_{in}$ and the steady state of the turret speed $\bar{\omega}_{turret}$ will be defined at $0.004\ \frac{Kg}{s}$ and $75\ rpm$ respectively. This means, that if these values are held at its defined steady state, the level of the hopper will keep constant. However, if a deviation in one of these variables occurs (see previous Figure 33 or further Figure 55) the hopper fill level will be immediately affected and the risk of overfilling or running empty would increase, due to the aforementioned behavior of integrating (non-self-regulating) processes.

6.3.1 Model of the Cylindrical Hopper

Mathematical model of the cylindrical hopper

The mass balance regarding the cylindrical hopper, illustrated previously in the section 3.1 by the Figure 12, can be expressed by the eq. (VI–3), where $\dot{m}_{in}$ and the $\dot{m}_{out}$ represents respectively the inlet and outlet mass flow of the hopper.

$$\frac{\partial m}{\partial t} = \dot{m}_{in} - \dot{m}_{out} \qquad \textit{eq. (VI—3)}$$

It is assumed that the density of the powder inside the hopper remains constant as well as a constant cross-sectional area, $A_{cylindrical}$. Knowing that the powder's mass inside the hopper can be expressed as $m = \rho \cdot V$, being ρ the density of the bulk solid and V the volume of the bulk solid inside the hopper, denoted as $V = A_{cylindrical} \cdot h$, the equation eq. (VI–3) can be reorganized as follows:

$$\frac{\partial \rho \cdot V}{\partial t} = \frac{\partial \rho \cdot A_{cylindrical} \cdot h}{\partial t} = \dot{m}_{in} - \dot{m}_{out} \qquad \textit{eq. (VI—4)}$$

Substituting eq. (VI—2) into eq. (VI—4) gives a first-order linear differential equation of the dynamic system being studied: changes in the fill level of a cylindrical hopper owing to changes in the inlet mass flow rate and to changes in the turret speed.

$$\frac{\partial h}{\partial t} = \frac{\dot{m}_{in}}{\rho \cdot A_{cylindrical}} - \frac{n_{die} \cdot m_{Tab}}{60 \cdot \rho \cdot A_{cylindrical}} \cdot \omega_{turret} \qquad \textit{eq. (VI—5)}$$

Mathematical Model of the Cylindrical Hopper for Control

In order to study the behavior of a certain system (i.e. linear differential equations) for changes in its input variables, transfer functions can be derived. A transfer function is indeed an algebraic expression for the dynamic relation between a selected input and output of a process model[101].

Given the dynamic equation eq. (VI–5), the steady state $\left(\frac{\partial h}{\partial t} = 0\right)$ can be reached at any point of the hopper's height, as long as the inlet flow rate and the outlet flow rate are identical. Therefore, at steady state, the eq. (VI–5) turns:

$$\frac{\partial h}{\partial t} = 0 \quad \rightarrow \quad \overline{\dot{m}}_{in} = \frac{n_{die} \cdot m_t}{60} \cdot \overline{\omega}_{turret} \qquad \textit{eq. (VI—6)}$$

Where $\overline{\dot{m}}_{in}$ and $\overline{\omega}_{turret}$ are the hopper's inlet flow rate and the turret speed respectively at steady state.

Knowing the steady state, it is possible to develop the transfer functions which express on the one hand, how changes in the manipulated variable ω_{turret} influence the height of the powder inside the hopper and on the other hand, how changes in the disturbance variable $\dot{m}_{in}$ induce variations in the bulk's solid height.

Changes in the input variables lead to instantaneous modifications of the hopper fill level, as the Figure 33 previously demonstrated. These changes can be denoted mathematically by an apostrophe and they are known as *deviation variables*. Eq. (VI – 7), eq. (VI – 8) and eq. (VI – 9) define the deviations variables of the inlet mass flow rate, the turret speed and the hopper fill level, respectively.

$$\dot{m}'_{in} = \dot{m}_{in} - \overline{\dot{m}}_{in} \qquad \textit{eq. (VI—7)}$$

$$\omega_{turret}{}' = \omega_{turret} - \overline{\omega}_{turret} \qquad \textit{eq. (VI—8)}$$

$$h' = h - \overline{h} \qquad \textit{eq. (VI—9)}$$

If it is assumed at the first place, that just variations in the turret speed might happen, the inlet mass flow rate would remain constant at its steady state value. Therefore, substituting eq. (VI—8) and eq. (VI—9) into the eq. (VI – 5) gives:

$$\frac{\partial\,(h-\overline{h})}{\partial t} = \frac{\dot{m}_{in}}{\rho \cdot A_{cylindrical}} - \frac{n_{die} \cdot m_{Tab}}{60 \cdot \rho \cdot A_{cylindrical}} \cdot (\omega'_{turret} + \overline{\omega}_{turret}) \qquad \textit{eq. (VI—10)}$$

By taking into account eq. (VI – 6), it is obtained the following equation, that represents the changes in the hopper fill level h owing to changes in the turret speed ω_{turret} .

$$\frac{\partial\, h'}{\partial t} = -\frac{n_{die} \cdot m_{Tab}}{60 \cdot \rho \cdot A_{cylindrical}} \cdot \omega'_{turret} \qquad \textit{eq. (VI—11)}$$

Now taking Laplace transforms at both sides of eq. (VI—11) to the situation where h' is a general function of time. It is assumed in this case that at $t = 0$, the process is at its steady state; thus, $h'(0) = 0$.

$$\mathcal{L}\left(\frac{\partial\, h'}{\partial t}\right) = \mathcal{L}\left(-\frac{n_{die} \cdot m_{Tab}}{60 \cdot \rho \cdot A_{cylindrical}} \cdot \omega'_{turret}\right) \qquad \textit{eq. (VI—12)}$$

Their transforms can be expressed generally as:

$$s \cdot H_p{}'(s) = -\frac{n_{die} \cdot m_{tab}}{60 \cdot \rho \cdot A_{cylindrical}} \cdot \omega'_{turret}(s) \qquad \textit{eq. (VI—13)}$$

Rearranging, the first transfer function is obtained. $G_p(s)$ relates the deviation variable of the turret speed $\omega'_{turret}(s)$ to the deviation output $H'_p(s)$ as follows:

$$G_p(s) = \frac{Hp'(s)}{\omega'_{turret}(s)} = -\frac{n_{die} \cdot m_{tab}}{60 \cdot \rho \cdot A_{cylindrical} \cdot s} = -\frac{K_{p,\ cylindrical}}{s} \qquad \textit{eq. (VI—14)}$$

Where,

$$K_{p,\ cylindrical} = \frac{n_{die} \cdot m_{tab}}{60 \cdot \rho \cdot A_{cylindrical}} \qquad \textit{eq. (VI—15)}$$

By a similar procedure, the transfer function that represents changes in the hopper fill level owing to changes in the disturbance variable $\dot{m}_{in}$ is obtained, and it is named as $G_d(s)$.

$$G_d(s) = \frac{H'_d(s)}{\dot{m}'_{in}(s)} = \frac{1}{\rho \cdot A_{cylindrical} \cdot s} = \frac{K_{d,\ cylindrical}}{s} \qquad \textit{eq. (VI—16)}$$

Where,

$$K_{d,\ cylindrical} = \frac{1}{\rho \cdot A_{cylindrical}} \qquad \textit{eq. (VI—17)}$$

Both transfer functions $G_p(s)$ and $G_d(s)$ represent *integrating models*, characterized by the term 1/s.

Figure 34 provides a block diagram representation of the cylindrical hopper model. In the diagram, the deviation variable $H_d{}'(s)$ denotes the change in the hopper fill level owing to a change in the disturbance variable, the inlet mass flow rate $\dot{m}'_{in}(s)$ of the hopper. Similarly, $H_p{}'(s)$ is a deviation variable that denotes the change in $H'(s)$ due to a change in the manipulated variable, the turret speed $\omega'_{turret}(s)$. The effect of these changes are additive because $H'(s) = H_p{}'(s) + H_d{}'(s)$ as a direct consequence of the Superposition Principle for linear systems.

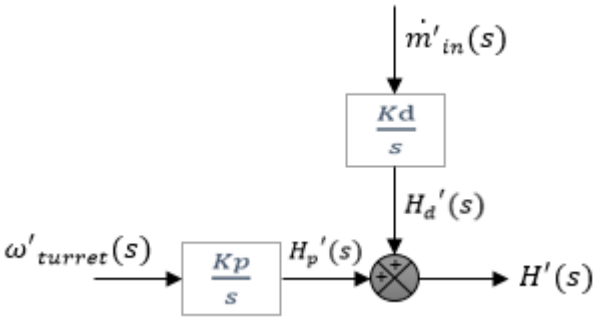

Figure 34: Block Diagram of the Cylindrical Hopper Model

This model can be built on Matlab Simulink as an open-loop system, as the Figure 35 illustrates. In the figure, two step-input blocks that affect the turret speed are included in order to check the behavior of the system for such disturbance, as it was illustrated with the red line in the Figure 33.

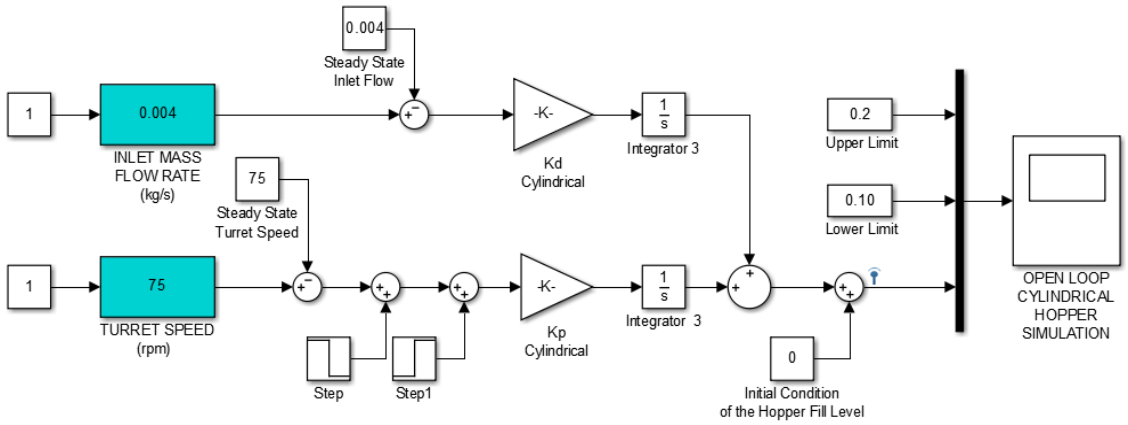

Figure 35: Simulink Block diagram of an Open-Loop System representing the Model of the Cylindrical Hopper

6.3.2 Model of the Conical Hopper

The mathematical description of the process containing a conical hopper is based as well as the previous model, on the conservation of mass, described by the eq. (VI—1). The only different between these two models is the fact that the cross-sectional area does not remain constant with the hopper's height, as it happens with a cylindrical hopper model. The eq. (VI—18) represents the general overview of this particular model:

$$\frac{\partial h}{\partial t} = \frac{\partial h}{\partial V} \cdot \frac{\partial V}{\partial t} \qquad \textit{eq. (VI—18)}$$

As it was illustrated in the section 3.1, the hopper has not a symmetrical shape, but an asymmetric conical geometry as shown in the left side of the Figure 36. The development of the mathematical model by taking into account this asymmetric shape would show some complexity and therefore some simplifications have been taken. It is expected that the impact of the real hopper's geometry (see Figure 12, left-side) on the bulk solid level is almost negligible since the angle θ_c is sufficiently small. Therefore, in order to simplify the mathematical model, the asymmetric conical shape is treated as a normal conical geometry.

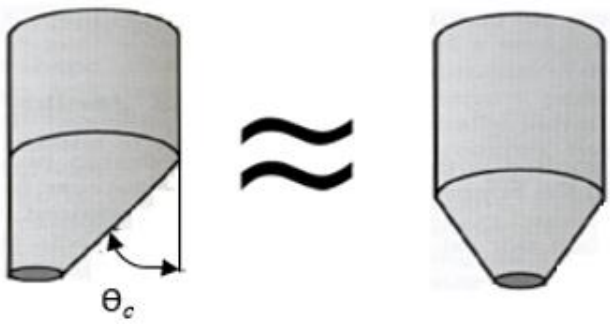

Figure 36: Simplification concerning the shape of the conical hopper

Mathematical Model of the Conical Hopper

As it was described previously in the section 3.1, the conical hopper is constituted with three different sections (see Figure 12). A cylindrical section in the bottom (1), an asymmetric conical section in the middle (2), and another cylindrical section in the top (3). For the development of the dynamic model, just the section (2) and (3) are considered, leaving the section (1) as the outlet.

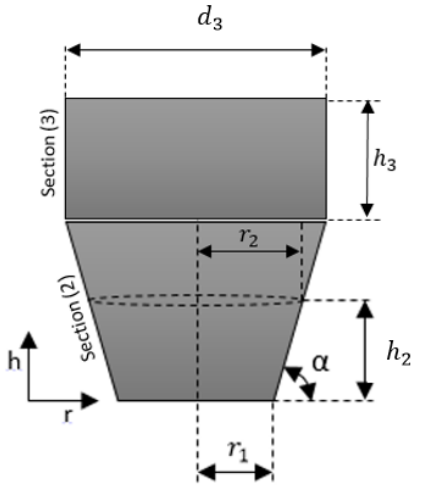

Figure 37: Graphical representation of the section (2) and section (3) of the conical hopper

In order to develop the dynamic model for the conical section, calculations are based on the eq. (VI—18). The differential equation that relates the height to the volume of bulk solid inside the conical section of the hopper must be first developed. As it is shown in the Figure 37, the cross-sectional area of the hopper increases with the height, and consequently, the radio of such cross-sectional area increases as well according to the eq. (VI—20). The eq. (VI—19) explains how the volume changes with the height for a geometrical figure as follows:

$$dV = \pi \cdot r^2 \cdot dh \qquad \textit{eq. (VI—19)}$$

Being the volume of the powder inside the hopper V, the radius of the cross-sectional area r and the hopper fill level h.

The common *linear equation* can be used to relate how the radius of the section (2) of the Figure 37 changes along the height. After rearranging:

$$r = \frac{h + r_1 \cdot tan\alpha}{tan\alpha} \qquad \textit{eq. (VI—20)}$$

Substituting the eq. (VI—20) into eq. (VI—19) leads to a non-linear ordinary differential equation (ODE), eq. (VI – 21). Figure 38, which was created by Matlab, shows clearly the non-linearity of eq. (VI—21).

$$\frac{dh}{dV} = \frac{tan^2\alpha}{\pi} \cdot \frac{1}{[h^2 + 2 \cdot h \cdot r_1 \cdot tan\alpha + {r_1}^2 \cdot tan^2\alpha]} \qquad \textit{eq. (VI—21)}$$

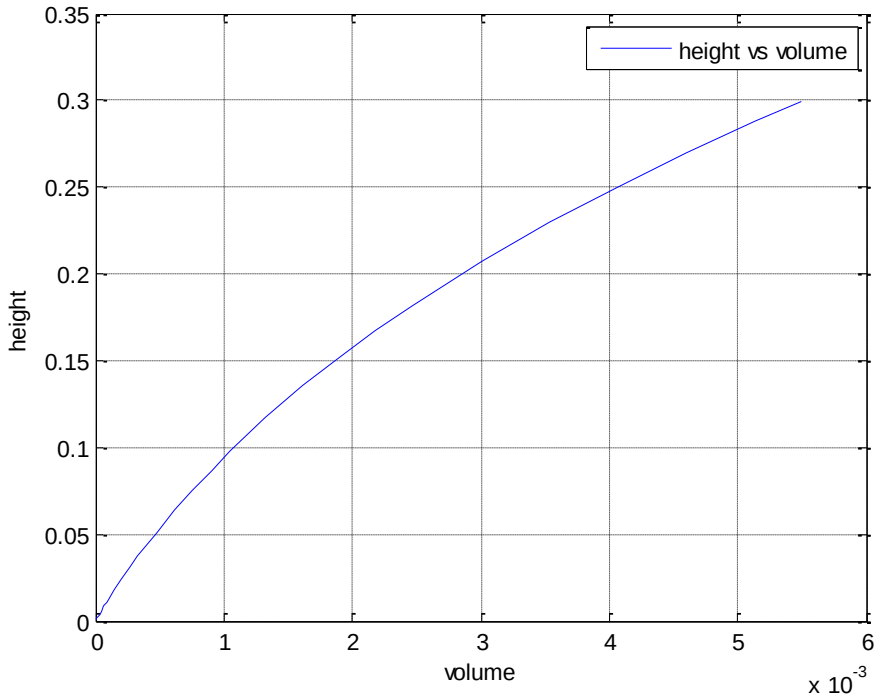

Figure 38: Non-linear ODE expressing how height increases with the volume for the section (2) the conical hopper

The second term $\frac{\partial V}{\partial t}$ of the differential equation eq. (VI—18) is fully described by the inlet and outlet flow rates. As it was already pointed out in this chapter, the hopper's outlet flow rate is governed by the turret speed, ω_{turret}.

$$\frac{\partial V}{\partial t} = \dot{q}_{in} - \dot{q}_{out} = \frac{\dot{m}_{in}}{\rho} - \frac{\dot{m}_{out}}{\rho} = \frac{\dot{m}_{in}}{\rho} - \frac{n_{die} \cdot m_{tab} \cdot \omega_{turret}}{\rho \cdot 60} \qquad \textit{eq. (VI—22)}$$

The substitution of the eq. (VI—21) and the eq. (VI—22) into the eq. (VI—18) and rearranging, results in the mathematical model, eq. (VI—23), of the hopper's conical section, section (2).

$$\frac{dh}{dt} = \frac{tan^2\alpha}{\pi \cdot \rho \cdot [h^2 + 2 \cdot r_1 \cdot h \cdot tan\alpha + {r_1}^2 \cdot tan^2\alpha]} \cdot \left[\dot{m}_{in} - \frac{n_{die} \cdot m_{tab}}{60} \cdot \omega_{turret}\right] \quad \textit{eq. (VI—23)}$$

The section (3) of the conical hopper is developed following the same procedure shown previously for the modelling of the cylindrical hopper, and its mathematical expression can be found in the eq. (VI – 24):

$$\frac{\partial h}{\partial t} = \frac{\dot{m}_{in}}{\rho \cdot A_3} - \frac{n_{Die} \cdot m_{Tab}}{60 \cdot \rho \cdot A_3} \cdot \omega_{turret} \quad \textit{eq. (VI—24)}$$

The resulted model of the whole conical hopper is then set of a one-dimensional non-linear ordinary differential equation (ODE), eq. (VI—23), and a linear ordinary differential equation, eq. (VI—24). The equation eq. (VI—25) represents, in one equation, the mathematical model of the general conical hopper (see Figure 37), represented by the conical section (2) in the range (in meters) between $0 < h_{hopper} < 0.3$, and the cylindrical section (3) in the range between $0.3 < h_{hopper} < 0.45$. A_3 is the cross-sectional area of the cylindrical hopper.

$$\frac{\partial h}{\partial t} = \begin{cases} \dfrac{tan^2\alpha \cdot \left[\dot{m}_{in} - \frac{n_{die} \cdot m_{tab}}{60} \cdot \omega_{turret}\right]}{\pi \cdot \rho \cdot \left[h^2 + 2 \cdot r_1 \cdot h \cdot tan\alpha + {r_1}^2 \cdot tan^2\alpha\right]}, & h < 0.3 \\ \dfrac{\dot{m}_{in}}{\rho \cdot A_3} - \dfrac{n_{Die} \cdot m_{Tab}}{60 \cdot \rho \cdot A_3} \cdot \omega_{turret}, & h \geq 0.3 \end{cases} \quad \textit{eq. (VI—25)}$$

In Simulink, the non-linear model of the conical hopper can be developed as a function of the two inlet parameters, the inlet flow rate and the turret speed (blue blocks in Figure 39). The mathematical model was implemented in Matlab as an "S-function" with the name of *"height_sfcn_2".* In Simulink, the model was included in a block with the same "Non-Linear Model Conical Hopper", depicted in the Figure 39. The hopper fill level response inside the conical hopper to turret speed changes was plotted in the Figure 33 with a blue line.

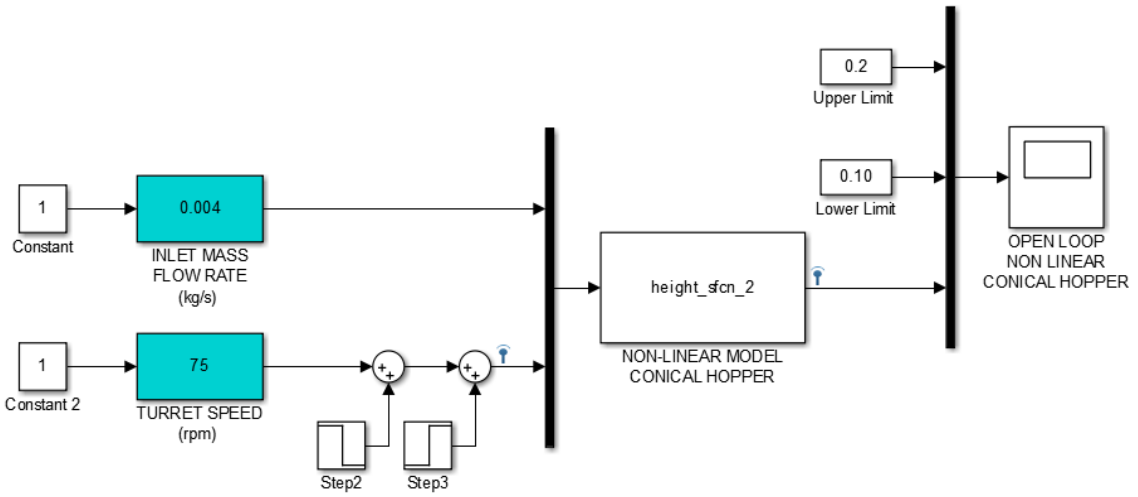

Figure 39: Simulink block diagram of an open-loop system representing the Non-Linear Model of the Conical Hopper

Mathematical Model of the Linearized Conical Hopper for Control

Unlike the mathematical model of the cylindrical hopper, developed in the section 6.3.1, which can be accurately described by linear ordinary differential equations, there is a wide variety of processes, such as this particular case concerning the conical section of the hopper illustrated in the Figure 37, for which the dynamic behavior depends on some parameters in a non-linear manner.

Even though process control theory has been developed for linear process, there are some literature available concerning the control of non-linear systems. However, non-linear system can be linearized at any point in order to show its behavior around the selected point. As shown in the Figure 40, linearization is a procedure for approximating a non-linear function with a simple linear function. The linear approximation is exact at one point, and for some systems, the behavior is also acceptable around that point. However, as the linear equation moves away from the selected linearization point, the accuracy of the approximation degrades [65].

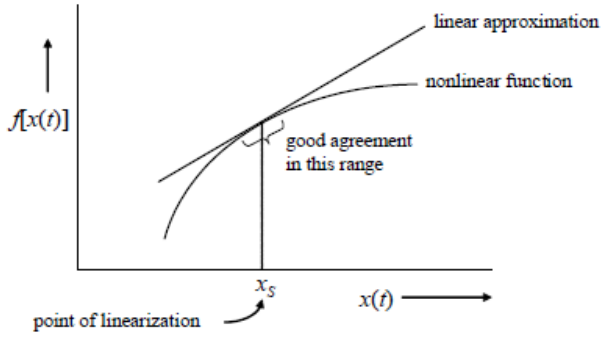

Figure 40: Linear approximation shows good performance around the operating point. Extracted from [65].

Fortunately, it is possible to select the point where the linearization is performed. Usually this point corresponds to the domain where the process spends more time, which might correspond as well to set point of the controller parameter (i.e. desired process operating point) [102]. Taylor series expansion is a common method for linearizing a non-linear differential equation, and hence is the one selected to linearized the non-linear ODE, eq. (VI—23). For this particular process, the control strategy will be developed to keep the hopper fill level at approximately 0.15 meters, which will be the reference point for linearization and the selected steady state operating point, $\overline{h}$. This point is located in the middle of the conical section of the asymmetric hopper, and as a consequence, the section (3) of the hopper can be neglected for the development of the control strategy at this particular point. In addition, the deviation variables (from the steady state) arise naturally out of the Taylor series expansion, eq. (VI—26), namely $h' = h - \overline{h}$, $\dot{m}_{in}{}' = \dot{m}_{in} - \overline{\dot{m}}_{in}$ *and* $\omega_{turret}{}' = \omega_{turret} - \overline{\omega}_{turret}$.

$$\frac{dh'}{dt} = \left.\frac{\partial f}{\partial h}\right|_s \cdot h' + \left.\frac{\partial f}{\partial \dot{m}_{in}}\right|_s \cdot \dot{m}_{in}{}' + \left.\frac{\partial f}{\partial \omega_{tur.}}\right|_s \cdot \omega_{tur.}{}' \qquad \textit{eq. (VI—26)}$$

Being $s = \overline{h}, \overline{\dot{m}}_{in}, \overline{\omega}_{turret}$, and f the eq. (VI—23).

The partial derivatives from eq. (VI—26) are as follows:

$$\left.\frac{\partial f}{\partial h}\right|_s \cdot h' = -\frac{tan^2\alpha \cdot \left[\overline{\dot{m}}_{in} - n_{die} \cdot m_{tab} \cdot \frac{1}{60} \cdot \overline{\omega}_{tur.}\right] \cdot \left[2 \cdot \overline{h} + 2 \cdot r_1 \cdot tan\alpha\right]}{\pi \cdot \rho \cdot \left[\overline{h}^2 + 2 \cdot \overline{h} \cdot r_1 \cdot tan\alpha + {r_1}^2 \cdot tan^2\alpha\right]^2} \cdot h' \qquad \textit{eq. (VI—27)}$$

$$\left.\frac{\partial f}{\partial \dot{m}_{in}}\right|_s \cdot \dot{m}_{in}{}' = \frac{tan^2\alpha}{\pi \cdot \rho \cdot \left[\overline{h}^2 + 2 \cdot \overline{h} \cdot r_1 \cdot tan\alpha + {r_1}^2 \cdot tan^2\alpha\right]} \cdot \dot{m}_{in}{}' \qquad \textit{eq. (VI—28)}$$

$$\left.\frac{\partial f}{\partial \omega_{tur.}}\right|_s \cdot \omega_{tur.}{}' = \frac{-tan^2\alpha \cdot \left[\frac{n_{die} \cdot m_{tab}}{60}\right]}{\pi \cdot \rho \cdot \left[\overline{h}^2 + 2 \cdot \overline{h} \cdot r_1 \cdot tan\alpha + {r_1}^2 \cdot tan^2\alpha\right]} \cdot \omega_{tur.}{}' \qquad \textit{eq. (VI—29)}$$

The system is going to be analyzed and linearized at the equilibrium point $\overline{h} = 0.15$ metres, since this point represents the desired operating point. Besides, it is important to take into account that the term $\left.\frac{\partial f}{\partial h}\right|_s \cdot h'$ turns to zero by keeping in mind the steady state equation eq. (VI—6). In order to solve the previous equations, geometrical data from the hopper is used; $\alpha = 80{,}54º$, $r_1 = 0.05m$, $\rho = 800\ \frac{kg}{m^3}$. Substituting:

$$\left.\frac{\partial f}{\partial h}\right|_s \cdot h' = 0 \qquad \textit{eq. (VI—30)}$$

$$\left.\frac{\partial f}{\partial \dot{m}_{in}}\right|_s \cdot h' = 7{,}074 \cdot 10^{-2} \cdot \dot{m}_{in}{}' \qquad \textit{eq. (VI—31)}$$

$$\left.\frac{\partial f}{\partial \omega_{tur.}}\right|_s \cdot \omega_{tur.}{}' = -3.77 \cdot 10^{-6} \cdot \omega_{tur.}{}' \qquad \textit{eq. (VI—32)}$$

Substituting these three partial derivatives equations into the equation eq. (VI—26) the linearized equation is obtained at the specified operating point. It is important to note that there are three variables, two input ($\dot{m}_{in}, \omega_{turret}$) and one output ($h$).

$$\frac{dh'}{dt} = 7{,}07355 \cdot 10^{-2} \cdot \dot{m}_{in}{}' - 3.77 \cdot 10^{-6} \cdot \omega_{tur.}{}' \qquad \textit{eq. (VI—33)}$$

Laplace transform is taken in both sides of the equation eq. (VI—33) with the initial state condition $h'(0) = 0.15$.

$$s \cdot H'(s) - f(0) = 7{,}074 \cdot 10^{-2} \cdot \dot{M}_{in}{}'(s) - 3.77 \cdot 10^{-6} \cdot \omega_{tur.}{}'(s) \qquad \textit{eq. (VI—34)}$$

Eventually, the input-output transfer functions that defines the linearized system of the conical hopper at the equilibrium point, $h = 0.15$, are defined in the eq. (VI—35) and eq. (VI—36) respectively. Just like the cylindrical model, these transfer functions represent an integrating system.

$$G_d(s) = \frac{H'(s)}{\dot{M}_{in}{}'(s)} = \frac{7{,}074 \cdot 10^{-2}}{s} = \frac{K_{d,\ conical}}{s} \qquad \textit{eq. (VI—35)}$$

$$G_p(s) = \frac{H'(s)}{\omega_{turret}{}'(s)} = -\frac{3.77 \cdot 10^{-6}}{s} = -\frac{K_{p,\ conical}}{s} \qquad \textit{eq. (VI—36)}$$

The two previous equations will be implemented in Simulink as gain blocks. The respective Figure 41 represents therefore the linearized model of the conical hopper at the desired operating point under open-loop conditions.

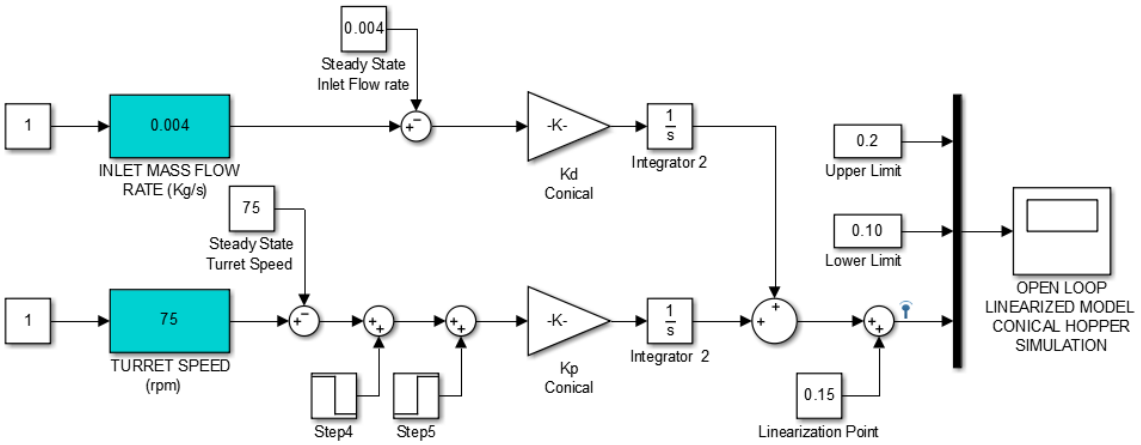

Figure 41: Simulink block diagram of an open-loop system representing the Linearized Model of the Conical Hopper

Comparison between the Non-Linear Model and the Linearized Model of the Conical Hopper

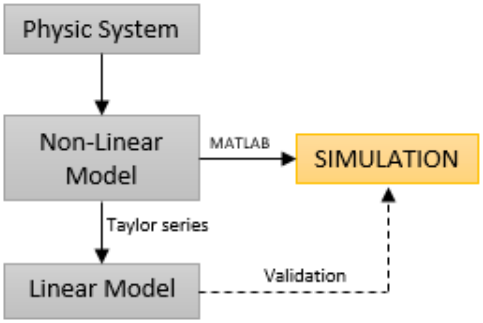

Figure 42: Work methodology

The non-linear model described in the equation eq. (VI—23) and the linearized model, represented by the two transfer functions eq. (VI—35) and eq. (VI—36) will show a similar behavior for disturbances in the input variables (turret speed and inlet mass flow) close to the operating point (i.e. linearization point, $h = 0.15\ metres$). The two mathematical models will be implemented in Simulink MATLAB® (see Figure 43) for the comparison and validation under the same atmosphere, following the work methodology illustrated in the Figure 42.

First of all, at $t = 500\ seconds$, the turret speed suffers a sudden alteration away from its steady state point ($75\ rpm$) to a lower velocity of $60\ rpm$, leading to an increase of the hopper fill level. After 600 seconds, the turret speed is turned back to its steady state point. Secondly, the inlet mass flow rate is decreased suddenly at $t = 1700\ seconds$ during 500 seconds from its current steady state point, $0.004\ \frac{kg}{s}$ to $0.00332\ \frac{kg}{s}$, leading to a decrease in the bulk solid level. The process response to perturbations in the input variables are shown in the lower plot of the Figure 44. The red line, on the one hand, represents the output variable (hopper fill level) reaction to disturbances in the input

variables for the non-linear model. The blue line, on the other hand, represents how the output variable would change as a consequences of the aforementioned disturbances for the linearized model.

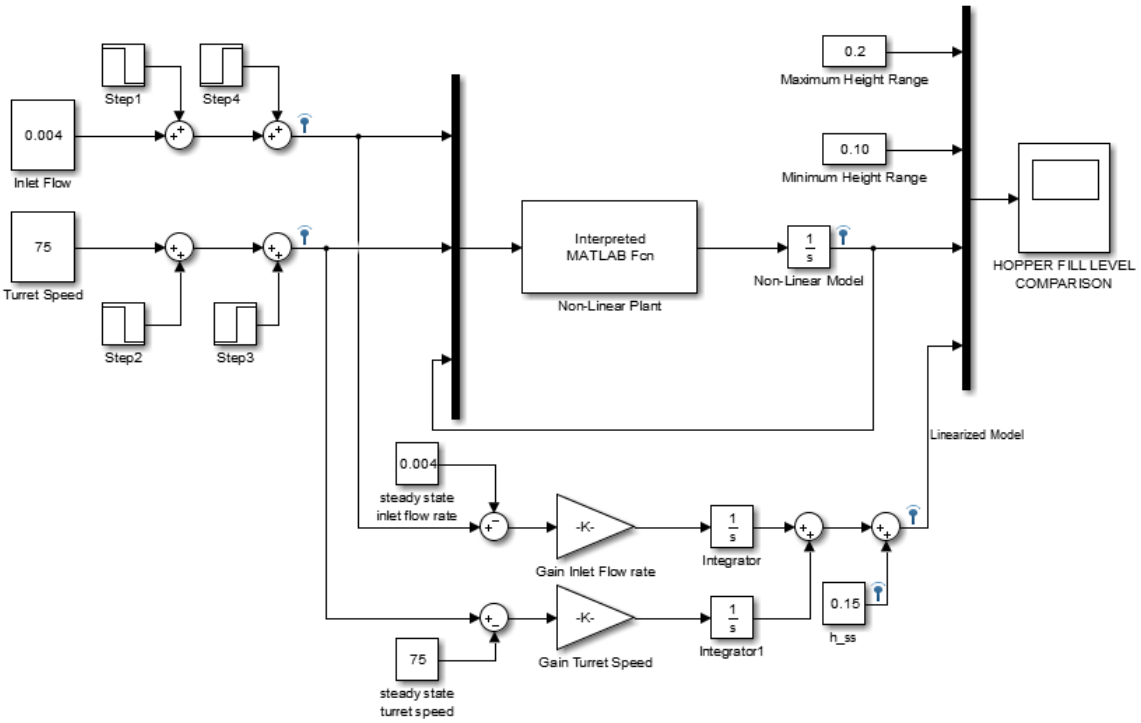

Figure 43: SIMULINK block diagram comparison between the Linear and the Non-Linear Model of the conical hopper

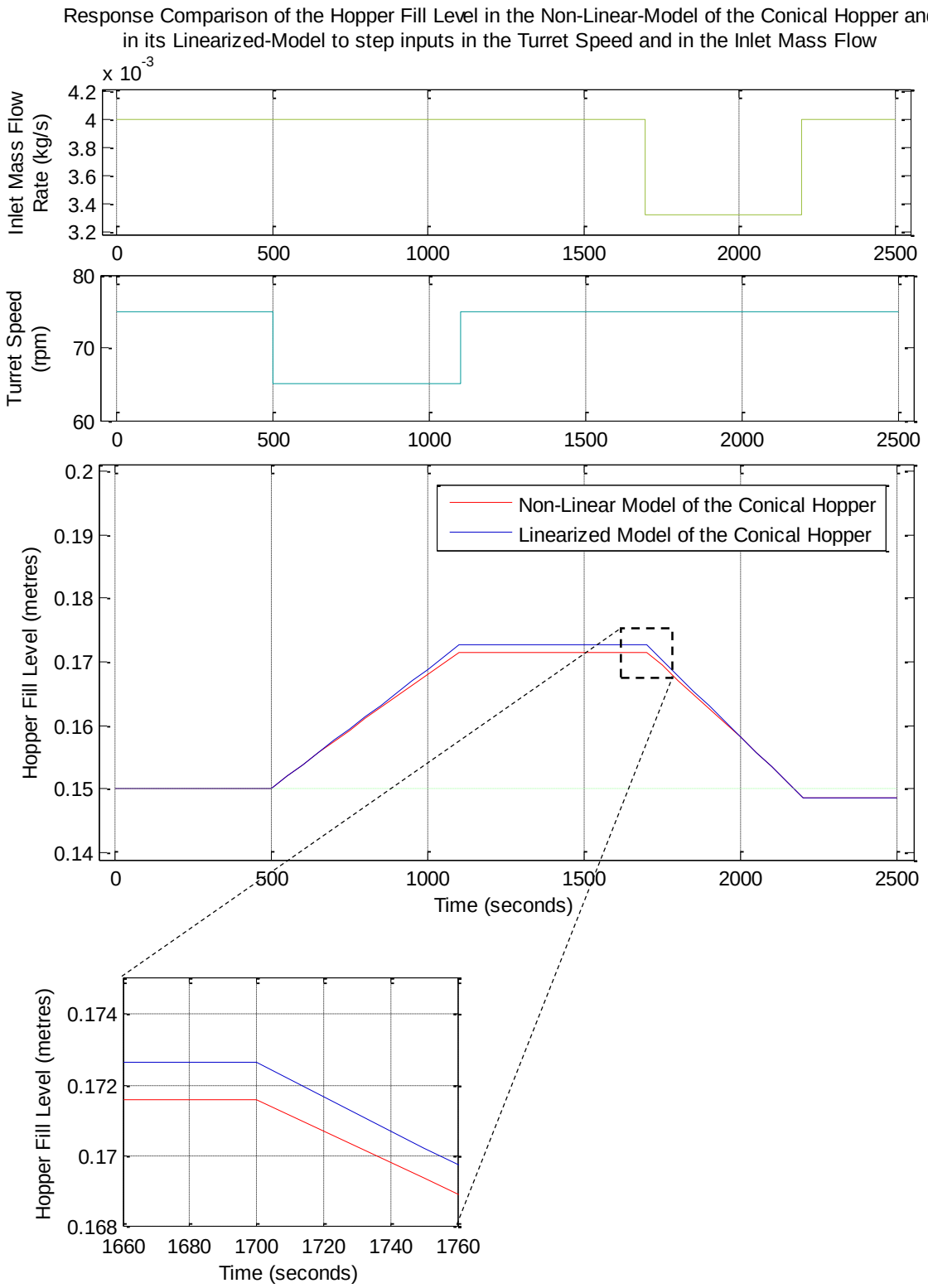

Figure 44: SIMULINK simulation results (hopper fill level) of the Linear and Non-Linear Model of the Conical Hopper after a manual disturbance in the turret speed (middle plot) at t=500 seconds and a manual disturbance in the inlet mass flow rate (upper plot) at t = 1700 seconds were carried out.

6.4 Design of the Process Control System

So far, the mathematical development of the plant model, both for the conical hopper and the cylindrical hopper, and the selection of the process analytical technology to measure the hopper fill level (ultrasonic technology) have been achieved. This new point attempts to study the behavior of the models being studied under controlled actions so that an appropriate degree of process understanding is achieved. This knowledge will be used eventually to design a controller that meets the control specifications.

Nowadays there are several control strategies (i.e. Fuzzy Controller, Model Predictive Controller) widely used in the industry to monitor and control usual processes like liquid/solid tank level. However, PID (Proportional-Integral-Derivative) is the most commonly used controller in the manufacturing industry, because of its simplicity (ease of implementation and use) and cost efficiency [2][103]. Besides, the PID controller is the most popular intermediated algorithm that allows the final control element (i.e. turret speed) to adopt intermediated positions between minimum speed and maximum speed. The basic PID algorithm is expressed as follows:

$$u(t) = u_{\text{bias}} + \underbrace{K_C\, e(t)}_{\text{proportional}} + \underbrace{\frac{K_C}{\tau_I}\int e(t)dt}_{\text{integral}} + \underbrace{K_C \tau_D \frac{de(t)}{dt}}_{\text{derivative}}$$

Figure 45: Basic PID (Proportional-Integral-Derivative) algorithm. Extracted from [102]

Where $u(t)$ is the controller output signal, u_{bias} is the null value, $e(t)$ is the controller error, K_c is the controller gain (proportional tuning parameter), τ_I is the controller reset time (integral tuning parameter) and τ_D is the controller derivative time (derivative tuning parameter).

As shown in the Figure 45, the PID controller includes a proportional term, an integral term and a derivative term. At a glance, resumed in the Figure 46, the proportional control speeds up the process response (y) and reduce the offset. The addition of integral control action, despite the fact that make the response more

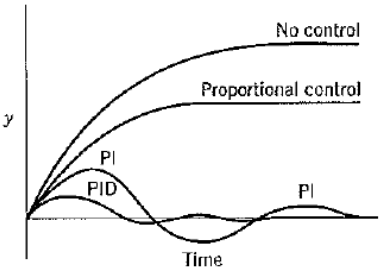

Figure 46: Typical process response with Feedback control. Extracted from [101]

oscillatory in the presented example, eliminates completely the offset, which is very important when controlling processes that required a high level of accuracy. Finally, adding derivative action would reduce both the degree of oscillation and the response time [104]. However, for processes that allows a certain degree of oscillation in the control variable, the use of the three terms is not required. Usually, and more specifically for level control, the derivative action is not normally used because the level measurements are often noisy as a result of the splashing and turbulence of the material entering the tank [101]. Therefore, in this work, the derivative action will be skipped.

In order to carry out the development of the control system, both the action of the P-Only controller and the action of the PI controller in parallel form will be integrated in the control loop in the way the Figure 47 shows. The stability of the control-loop system has to be guaranteed, and therefore stability analyses concerning the controller parameters (the proportional gain K_c and the integral time τ_I) turn out to be very convenient. This section includes stability analysis concerning each controller, as well as simulations with different controller settings for the different models being studied. At the end of the section, two different control-loop tuning strategies will be compared in order to adjust the controller setting so that the desired performance is achieved. [104] [105].

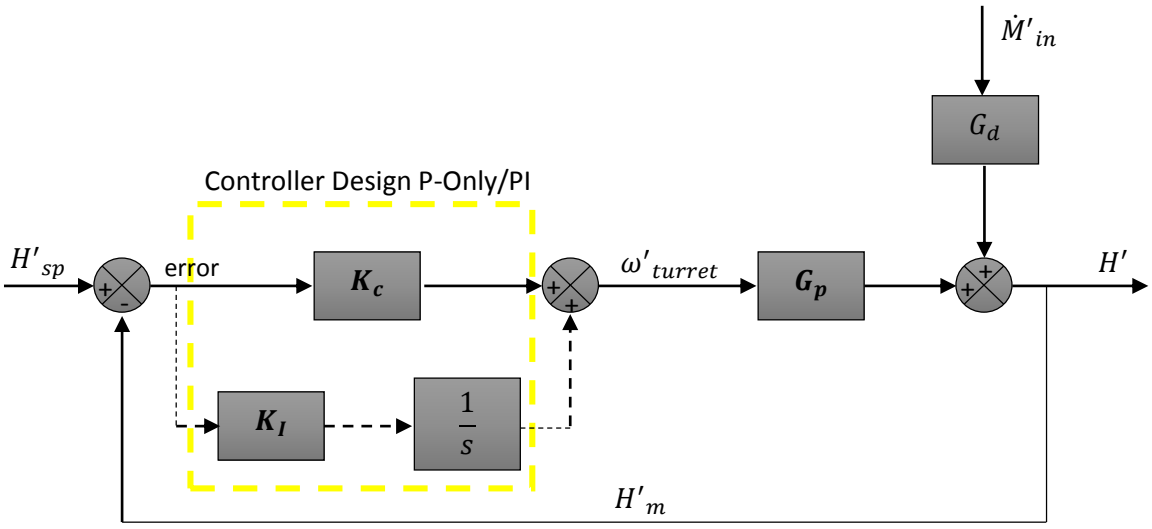

Figure 47: Block diagram of the feedback control system with P-Only control or PI control (additional discontinuous lines). Kc and Ki are the controller parameters, and represent the proportional gain and the integral gain respectively

6.4.1 Stability Analysis of the P-Only Controller

The simplest controller in the family of PID controller is called P-Only control. The error, computed in the eq. (VI—37), is the difference between the level set point $H_{sp}(t)$, and the measured level $H_m(t)$ [101].

$$e(t) = H_{sp}(t) - H_m(t) \qquad \textit{eq. (VI—37)}$$

The controller output $p(t)$ is proportional to the error as follows:

$$p(t) = \overline{p} + K_c \cdot e(t) \qquad \textit{eq. (VI—38)}$$

Being $\overline{p}$ the steady state value and K_c the controller gain.

In order to derivate the transfer function for a proportional controller, the deviation variable of the control output must be taken into account, as eq. (VI—39) shows.

$$p'(t) \triangleq p(t) - \overline{p} \qquad \textit{eq. (VI—39)}$$

Substituting eq. (VI – 39) into eq. (VI—38) and taking Laplace transforms in both side of the equations, the transfer function of the proportional controller is developed:

$$\frac{P'(s)}{E'(s)} = G_c = K_c \qquad \textit{eq. (VI—40)}$$

The feedback control system (see Figure 47) for controlling the hopper fill level must be stable as a prerequisite for satisfactory control. Consequently, knowing under what conditions the control loop becomes unstable is considered pretty important. In this case, it is important to figure out which values of the proportional controller gain K_c make the system unstable. To do so, the *characteristic equation* of the control loop system is analyzed, which is one of the most common ways to check the system stability. According to the general stability criterion, “the feedback control system would be stable if and only if all roots of the characteristic equation are negative or have negative real parts. Otherwise, the system is unstable” [101].

Applying the Superposition Principle for linear systems, it is possible to see in the eq. (VI—41) the response of the control variable (hopper fill level) to simultaneous disturbance variable and set point changes in the feedback control loop of the Figure 47.

$$H'(s) = \frac{G_c \cdot G_p}{1+G_c \cdot G_p} \cdot H'_{sp}(s) + \frac{G_d}{1+G_c \cdot G_p} \cdot M'_{in}(s) \qquad \textit{eq. (VI—41)}$$

The denominator of both terms represent the characteristic equation that must be matched to zero, in order to find the roots for stability issues.

$$1 + G_c \cdot G_p = 1 + G_{OL} = 0 \qquad \textit{eq. (VI—42)}$$

Being G_p the transfer function that related the manipulated variable $\omega'_{turret}(s)$ to the output $H_p{}'$(s), G_d the transfer function that relates the disturbance variable $\dot{m}'_{in}(s)$ to the output $H_d{}'$(s), G_c the transfer function of the proportional controller and G_{OL} the open-loop transfer function. It is clearly appreciated, that the same characteristic equation occurs for both disturbance and set point changes. Thus, if the close-loop system is stable for disturbances, it will also be stable for set-point changes. The linear system stability is fully determined by the roots of the characteristic equation, eq. (VI—42). Therefore, according to the general stability criterion, as long as the roots are negative (see Figure 48), the close-loop will be stable.

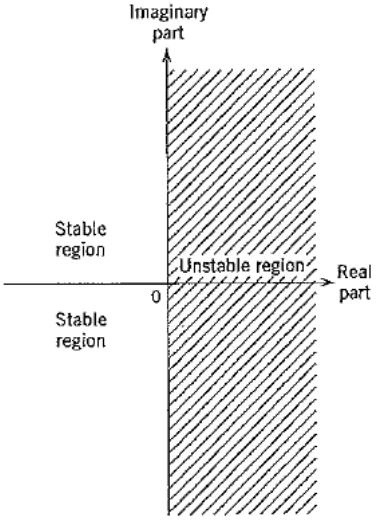

Figure 48: Stability region in the complex plane for roots of the characteristic equation. Extracted from [101]

Equalizing the characteristic equation to zero, and substituting G_p into the eq. (VI—42), the roots can be computed:

$$1 + G_c \cdot G_p = 1 + K_c \cdot \frac{-K_p}{s} = 0 \qquad \textit{eq. (VI—43)}$$

The root of the eq. (VI—43) would be $s = K_c \cdot K_p$. Therefore, the controller gain, K_c , should be kept negative in order to maintain the control-loop stable. In other words, this stability analysis has indicated that this closed-loop system will be stable for all negative values of the K_c , no matter how large.

$$K_c < 0 \qquad \textit{eq. (VI—44)}$$

6.4.2 Stability Analysis of the PI Controller

Like the P-Only controller, the Proportional-Integral (PI) controller computes an output signal $p(t)$ that influences the manipulated variable based on tuning parameters (i.e. integral time or reset time τ_I, or the controller gain K_c) and the error $e(t)$ as follows:

$$p(t) = \overline{p} + K_c \cdot \left[e(t) + \frac{1}{\tau_I} \cdot \int_0^t e(t^*) dt^* \right] \qquad \textit{eq. (VI—45)}$$

In following figures, the integral time can be also found as T_I in the legend of the plots. The eq. (VI—46) is therefore the transfer function of the PI controller that relates the output signal with the computed error, after applying Laplace at both sides of the eq. (VI—45).

$$\frac{P'(s)}{E(s)} = G_c = K_c \cdot \left(\frac{\tau_I \cdot s + 1}{\tau_I \cdot s} \right) \qquad \textit{eq. (VI—46)}$$

The main advantage of using a PI controller is the elimination of the offset that usually cannot be removed by the proportional controller. However, on other side, the corrective action of this controller depends on the duration of the deviation, which usually produce oscillations [65].

If integral control action is used in conjunction with proportional control action and implemented in the block diagram of the Figure 47, the response to simultaneous disturbances variable and set-point changes is merely the sum of the individual responses, as it was shown in the eq. (VI—41). The main different though, is the fact that in this case, G_c would be represented by the equation eq. (VI—46).

Like for P-Only controller, in order to analyze the stability of the close-loop system, the characteristic equation is taken again into account. However, for this particular control-loop that holds a PI controller, the *Routh Stability Criterion* will be used instead. Routh analysis requires, in the first place, all coefficients of the characteristic equation to be positive. And secondly, all terms in the first column of array built from the coefficients of the characteristic equation to be as well positive [106]. In order to start with the analysis, the equation eq. (VI—46) and either the eq. (VI – 14), in case of the cylindrical

hopper, or the eq. (VI—36), in case of the conical hopper are substituted into eq. (VI—42).

$$1 + K_c \cdot \left(\frac{\tau_I \cdot s + 1}{\tau_I \cdot s}\right) \cdot \frac{-K_p}{s} = 0 \qquad \textit{eq. (VI—47)}$$

Rearranging and regrouping, the characteristic equation is obtained:

$$\tau_I \cdot s^2 - K_c \cdot K_p \cdot \tau_I \cdot s - K_c \cdot K_p = 0 \qquad \textit{eq. (VI—48)}$$

On the one hand, from eq. (VI—48), and based on the first principle of the Routh method that says that all coefficients of the characteristic equation must be positive, it is possible to conclude that the integral time τ_I , must be positive. On the other hand, in order to check the values of K_c that keep the control-loop stable, the development of the Routh array is required.

1	$\boldsymbol{\tau_I}$	$\boldsymbol{-K_c \cdot K_p}$
2	$-K_c \cdot K_p \cdot \tau_I$	0
3	b1	

Table 10: Routh Array

$$b1 = \frac{-K_c \cdot K_p \cdot \tau_I \cdot (-K_c \cdot K_p)}{-K_c \cdot K_p \cdot \tau_I} \qquad \textit{eq. (VI—49)}$$

$$b1 = -K_c \cdot K_p \qquad \textit{eq. (VI—50)}$$

The term $b1$ must be positive, and to fulfil with this requirement, K_c must be therefore negative. Consequently, this stability analysis indicates that this closed-loop system will be stable for all negative values of the K_c and for positive values of the integral time.

$$\tau_I > 0 \qquad \textit{eq. (VI—51)}$$

$$K_c < 0 \qquad \textit{eq. (VI—52)}$$

6.4.3 Development of the Hopper Fill Level Control System in Simulink

So far, the operating objectives for the automatic control of the hopper fill level, the mathematical description of the three models being studied, the behavior of these models under open-loop conditions and the stability analysis of the controller parameters have been accomplished. In this section, the mathematical models will be implemented in Simulink under closed-loop conditions in order to enable the control of the hopper fill level at the desired operating point. Furthermore, the effect of adding saturation limits on the turret speed and consequently on the hopper fill level will be studied, as a first approach of the system's performance.

Under real conditions, the turret speed located in the feed frame is not able to work out of its operating limits, which are set at $59\ rpm$ and $90\ rpm$, being the lower and the upper limit respectively. Three simulations, one for each model, will be performed in this section with and without such saturation in order to compare the system performance under real and ideal conditions. The comparison has been made using the Simulation Data Inspector from Matlab [107]. The simulations will be carried out with a PI Controller and the following controller parameters (a proportional gain of $K_c = -400$ and an integral gain of $K_I = \frac{K_c}{\tau_I} = -2$). Since the system is controlled with a PI controller, an *anti-wind-up loop* will be also included in the three Simulink diagrams. Its mechanism is simple: it halts the integration of the control error when the control signal reaches either its maximum or its minimum limits. In other words, it prevents integration wind-up in PID controllers when the actuator is saturated [108].

For the following simulations, it is assumed that the disturbance variable (inlet mass flow rate) does not experiment any disturbances, remaining therefore at its steady state $0.004\ \frac{Kg}{s}$. The initial condition of the hopper fill level is set at $h_{hopper,t=0} = 0\ metres$ and the desired set point has a value of $h_{hopper,set-point} = 0.15\ metres$. The desired operating range of both the turret speed and the hopper fill level will be defined in the corresponding plots between red lines, while the set point will be highlighted with a green line.

Simulink Simulation for the Model of the Cylindrical Hopper

The transfer functions that defines the model of the cylindrical hopper were previously computed in the equation eq. (VI – 14) and eq. (VI – 16), and added into the Simulink diagram of the Figure 49. Eq. (VI – 14) denotes the change in the hopper fill level owing to a change in the manipulated variable, $G_p(s)$, while eq. (VI – 16) denotes the change in the hopper fill level owing to a change in the disturbance variable, $G_d(s)$.

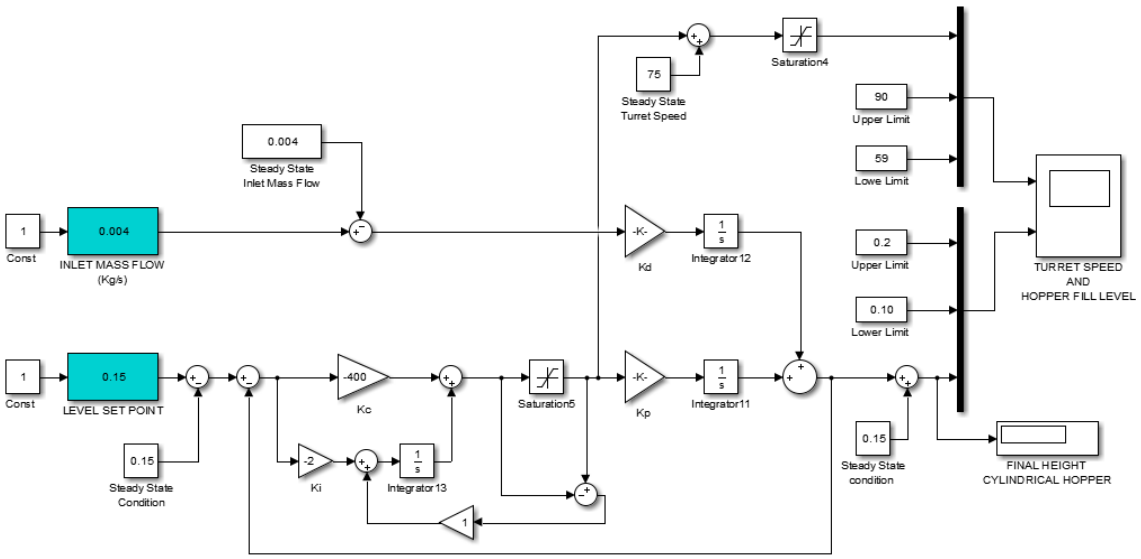

Figure 49: Simulink block diagram of the control loop of the Model of the Cylindrical Hopper

As expected, the restricted behavior of the controller output will keep the real response of the system away from its ideal (unsaturated) performance, distinguished with a blue line in the Figure 50. In the case of ideal conditions (unsaturated turret speed), the system is allowed to use a very slow turret speed at the beginning of the simulation, which results in a faster increase of the hopper fill level. The Figure 50 establishes that under ideal condition, the hopper fill level would reach the set point within the first 400 seconds, aside from oscillations caused by the selected controller settings, while under real conditions (saturated turret speed), it will take longer than 1000 seconds, since the turret speed in not allowed to perform values lower than 59 rpm. However, it is interested to point out the fact that for the same controller design, the system is stabilized at the set-point after approximately the same amount of time, 3500 seconds.

Even though the response of the controlled variable would be faster for ideal conditions, the process being studied does not require a quick response of the controller, as long as the hopper fill level increases or decreases towards a stable point, if the level is too low or too high.

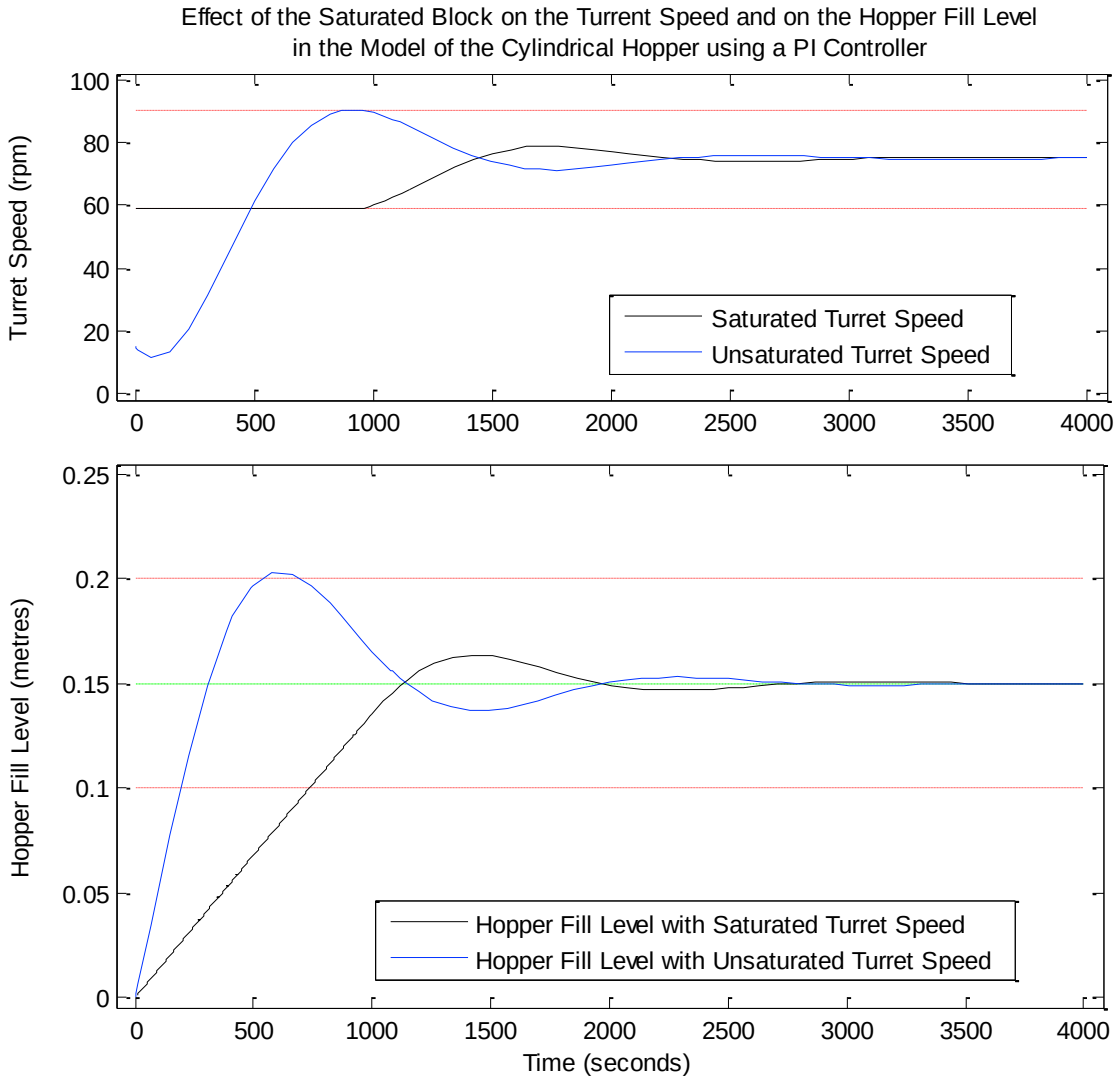

Figure 50: Effect of the saturation block on the turret speed and on the hopper fill level by using the Model of the Cylindrical Hopper with a PI Controller (Kc=-400, Ki=-2)

Simulink Simulation for the Non-Linear Model of the Conical Hopper

The respective non-linear model of the conical hopper with a feedback control loop is shown in the Figure 51. A PI Controller with an anti-wind-up loop is implemented within the model in order to control the hopper fill level at the desire set-point value, 0.15 meters. In this case, the non-linear differential equation, eq. (VI – 23), is included directly in the Simulink block diagram as an *S-function Block.* The system has two input; the inlet flow rate and the turret speed, which is adjusted by the controller output (turret speed deviation variable) to fulfil the process requirements.

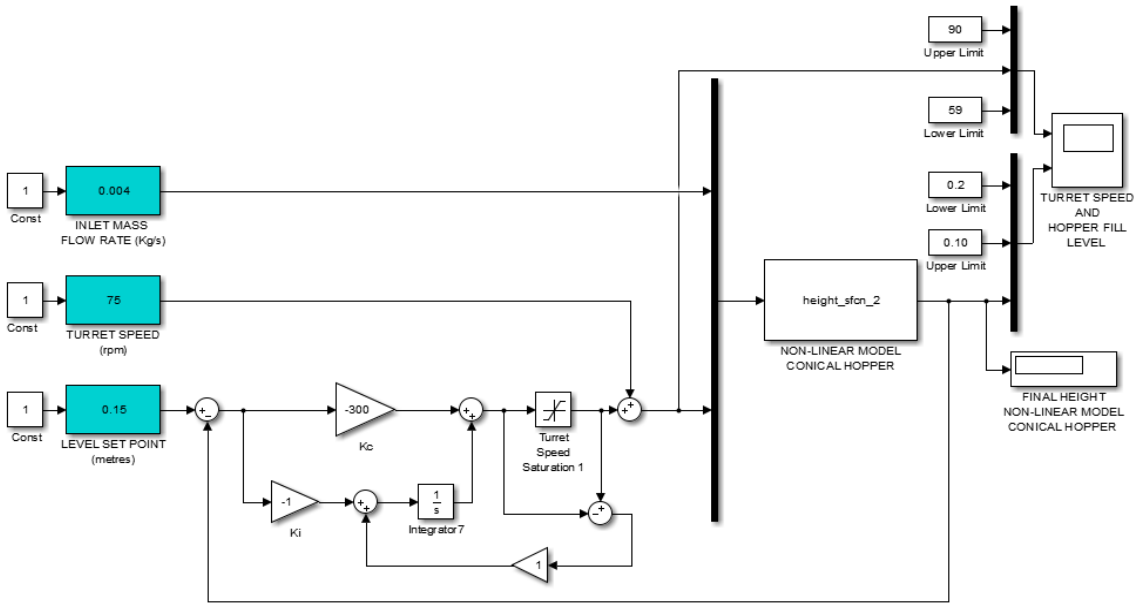

Figure 51: Simulink block diagram of the control loop of the Non-Linear Model of the Conical Hopper

The results of the simulations are very similar to the ones obtained from the Simulink model of the cylindrical hopper. In resume, if the system could work under fictitious conditions, where the turret speed could be able to perform any value, the response of the controlled variable would be steeper and more oscillatory for the same controller design, as the hopper fill level plot of the Figure 52 shows. In this case, under ideal conditions, the process variable (hopper fill level) takes about 400 seconds to cross over its set point, while under real conditions (saturated turret speed), the set point is reached after 1500 seconds. Again, as it happened with the previous case, both the real simulation and the ideal simulation settle down at the set-point approximately at the same time, 7500 seconds, according to the Figure 52.

It is worth mentioning as well, that the comparison between the current Figure 52 and the previous Figure 50 demonstrates that the hopper fill level takes longer to stabilize at the selected set point for the conical hopper. This is actually an expected outcome, due to the differences in geometry between the two hoppers being studied. The cylindrical hopper shows a smaller average in diameter along its height when it is compared to the conical hopper.

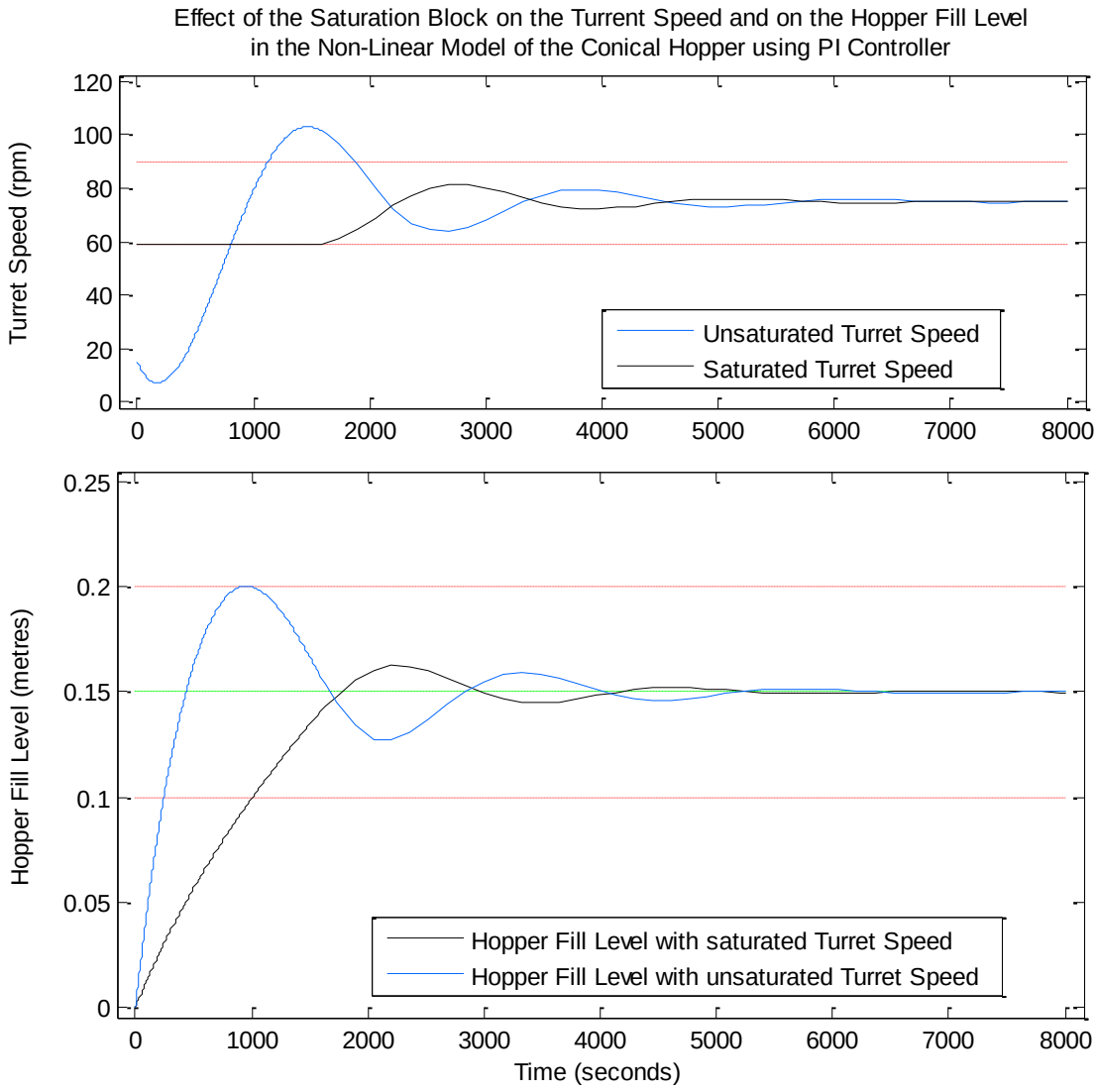

Figure 52: Effect of the saturation block on the turret speed and on the hopper fill level by using the Non-Linear Model of the Conical Hopper with a PI Controller (Kc=-400, Ki=-2)

Simulink Simulation for the Linearized Model of the Conical Hopper

The transfer functions that defines the linearized model of the conical hopper were previously computed in the equation eq. (VI – 35) and eq. (VI – 36), and added into the Simulink diagram of the Figure 53. Eq. (VI – 35) denotes the change in the hopper fill level owing to a change in the disturbance variable, $G_d(s)$, while eq. (VI – 36) denotes the change in the hopper fill level owing to a change in the manipulated variable, $G_p(s)$. This model is suitable only for simulations that are performed close to the linearization point, 0.15 meters, and therefore, it is added just before the feed-back control loop and just after it. For this particular simulation, the initial condition is set at 0.15 meters, and the set point at 0.19 meters. A PI Controller with $K_c = -400$ and $K_I = -2$ is included in the control-loop. Additionally, an anti-wind-up loop is added.

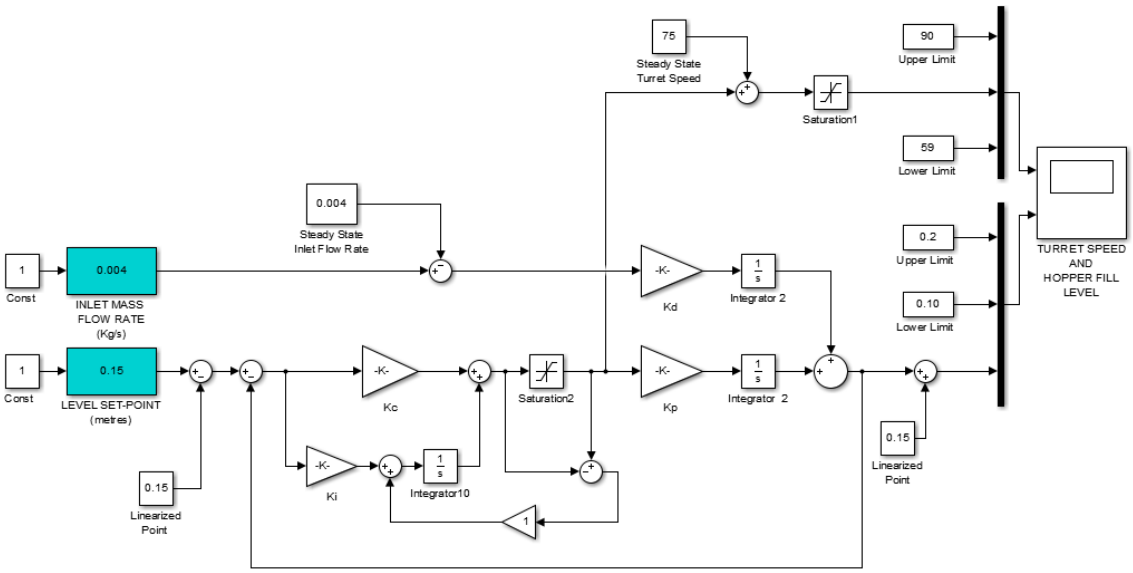

Figure 53: Simulink block diagram of the control loop of the Linearized Model of the Conical Hopper

The results of the simulation of the Simulink block diagram of the Figure 53 are found in the Figure 54. Again, if the turret speed would be able to perform any value (ideal conditions), the response of the hopper fill level would be faster as expected. For the selected parameters of the controller, some oscillation occurs both in the turret speed (see upper plot of the Figure 54) and in the hopper fill level (lower plot of the Figure 54). Usually, in the control process industry, this oscillations are unwanted for several reasons related with, for example, variability. Fortunately, as it will be shown in further

sections, such oscillations can be reduced or avoided by adjusting the controller parameters properly.

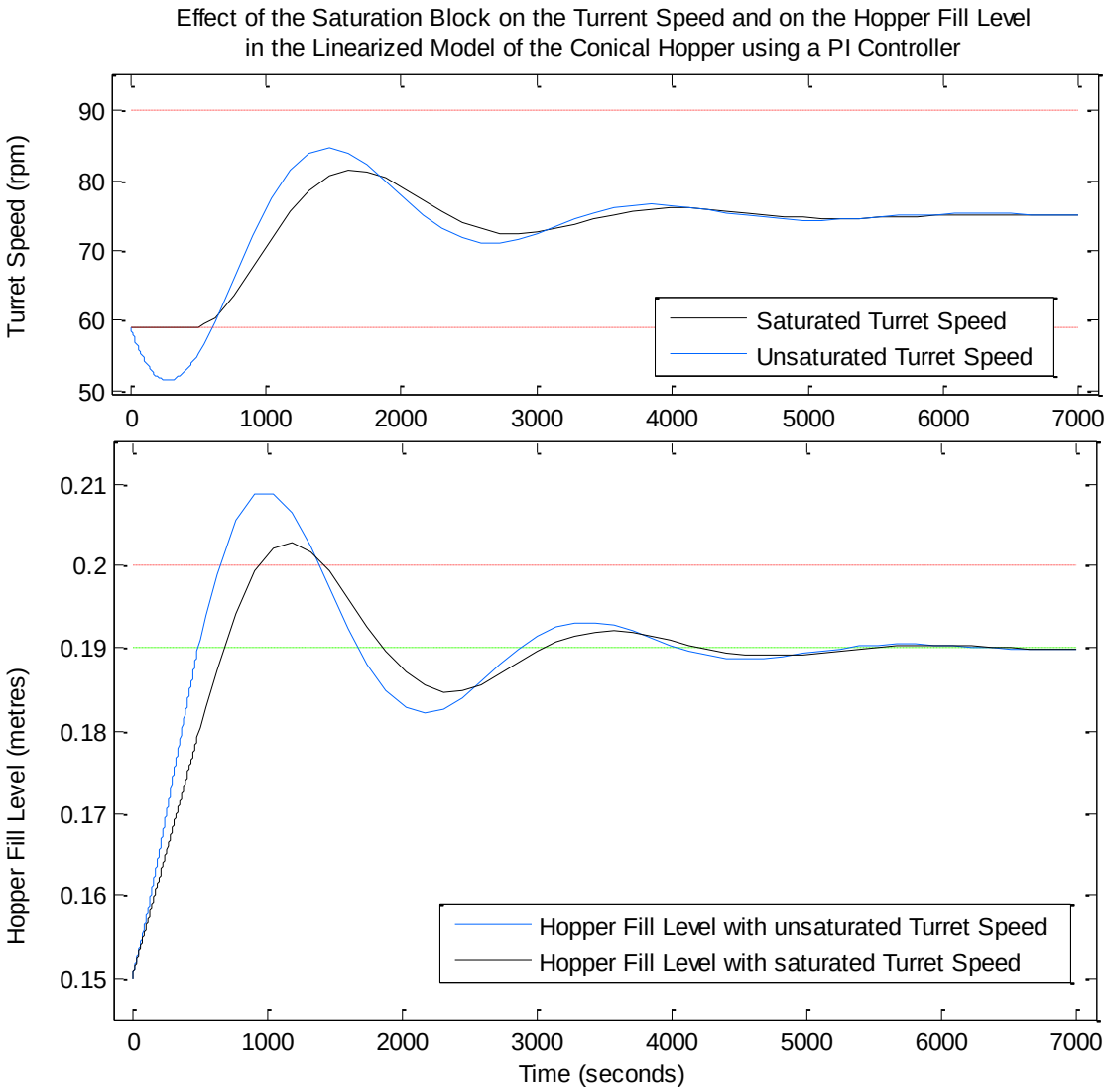

Figure 54: Effect of the saturation block on the turret speed and on the hopper fill level by using the Linearized Model of the Conical Hopper with a PI Controller (Kc=-400, Ki=-2)

6.4.4 Implementation of an Effective Control-Loop Tuning Strategy

Before developing the control strategy for tuning and setting the controller parameters, the operation objectives must be properly defined so that the control action could be adapted to the required process specifications. In this case, as it was previously explained in the section 6.2, the hopper fill level must be controlled continuously within a maximum and minimum bound, to satisfy the process operating performance.

Two of the main features that characterize a good control system are *performance* and *robustness.* "A control system exhibits a high degree of performances if it provides rapid and smooth responses to set-point and disturbance changes with little oscillation"[101]. Robustness, on the other hand, is achieved when the control system responses successfully under a wide range of process conditions. Therefore, in order to provide a controller for the aforementioned integrating process with these two characteristics, two different techniques will be used to define its settings (controller tuning). In the first place, *lambda tuning* is used. Lambda tuning is a form of internal model control (IMC) that endows a proportional-integral (PI) controller with the ability to generate smooth and non-oscillatory control efforts when responding to changes in the set-point and disturbance [109][110]. To guarantee the correct tune of the controller, several simulation will be done in Simulink both with the open-loop and closed-loop feedback control, following defined steps [111]. In order to check the reliability of the lambda tuning technic, a second method will be used, and both results will be compared for the different models being studied. This second strategy, refereed as *Skogestad's PID tuning method,* is a model-based tuning method where the controller parameters are expressed as functions of the process model parameters [108].

Integrating processes are indeed challenging to control and as a consequence, precise understanding of the system dynamics is required to achieve acceptable control performance [112]. The execution of step inputs both in disturbance variables (i.e. inlet flow rate) and in the manipulated variables (i.e. turret speed) together with a well-establish control specification (i.e. keeping the powder level within certain limits) turn out to be extremely useful to obtain information regarding the process dynamics. The

better the understanding of the process dynamics, the easier to achieve the optimal controller [113][114].

Previously, the Figure 33 proved the integrating behavior of the powder level inside the hopper for each of the models operated in open-loop, as well as the immediate response of the level to changes in the outlet flow rate. Now, the Figure 55 attempts to show the response of the three models being studied to disturbances in the inlet flow rate under closed-loop conditions. A PI controller with a proportional gain of $K_c = -300$ and a random integral gain of $K_I = -1$ was selected for the simulation.

The simulation of the model of the cylindrical hopper, the non-linear model of the conical hopper and the linearized model of the conical hopper has been performed using the Simulink Block diagram of the Figure 49, 51 and 53 respectively. The two only required modifications of these three Simulink diagrams to perform this tasks are, on the one side, the fact that the initial condition was changed to $0.15\ metres$ for the three models, and in the other side, the addition of a step input in the inlet flow rate with a value of $0.0006\ \frac{Kg}{s}$ at the time $t = 500\ seconds$.

It is worth mentioning firstly, that according to the Figure 55, and as happened in the step input simulation of the Figure 33, the response to disturbance changes in the inlet flow rate is as well instantaneous, giving therefore a time delay of zero.

Secondly, this simulation has a huge value for the validation of the linearized model of the conical hopper around the operation point. The Figure 55 clearly shows that the non-linear model of the conical hopper and its linearized one have a very similar behavior when the last one operates close to the linearization point.

Lastly, it is as well appreciated that, as demonstrated before in the Figures 50, 52 and 54, the hopper fill level response to disturbances is steeper when a cylindrical model is used. Besides, and with reference to the following figure, the hopper fill level stabilizes faster for the cylindrical hopper when using the same controller design.

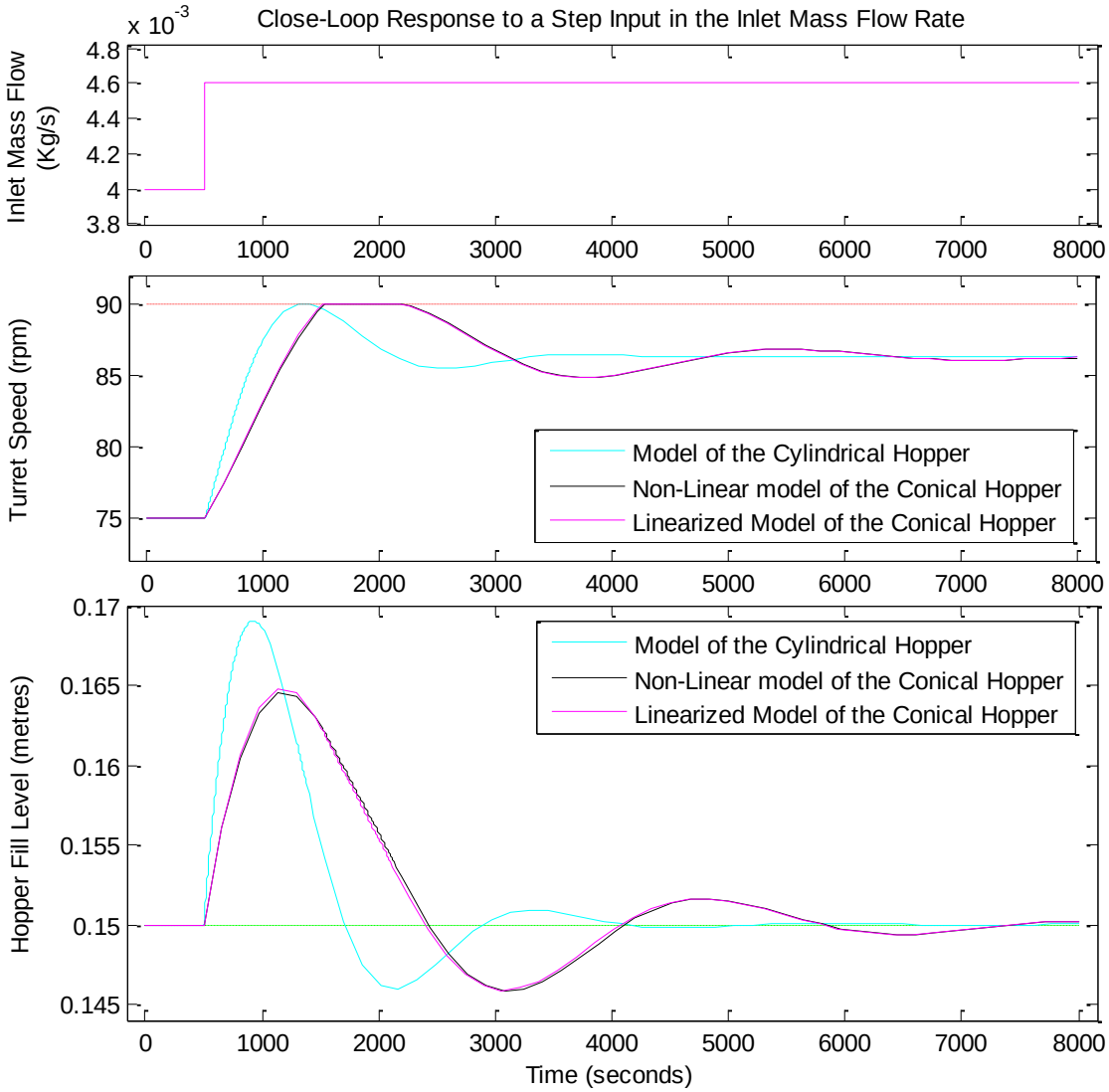

Figure 55: Control loop response using a PI Controller (Kc = -300 and Ki = -1) to an inlet mass flow rate step input (upper plot) for the three different Models being studied: (1) Model of the Cylindrical Hopper – light blue line, (2) Non-Linear Model of the Conical Hopper – black line and (3) Linearized Model of the Conical Hopper – pink line

It is pretty clear the fact that the process variable response depends on the controller's parameters. For instance, in the lower plot of the Figure 55, the response of the powder level inside the cylindrical hopper after inlet flow rate disturbances follows the blue line till stabilization. This is actually a particular response for a given PI controller design and it could be modified by adjusting the controller parameters.

The Figure 56 would represent additionally several hopper fill level responses for different designs of the PI Controller. The simulation was performed using the Simulink Block diagram of the Figure 49, corresponding to the model of the cylindrical hopper. A step input in the inlet flow rate of $0.0007\ \frac{Kg}{s}$ was added into the diagram to carry out

the simulation. In essence, the three models being studied represent integrating (non-self-regulating) processes, so just the model of the cylindrical hopper is going to be used to study the influence of the controller settings on the controlled variable under the described conditions.

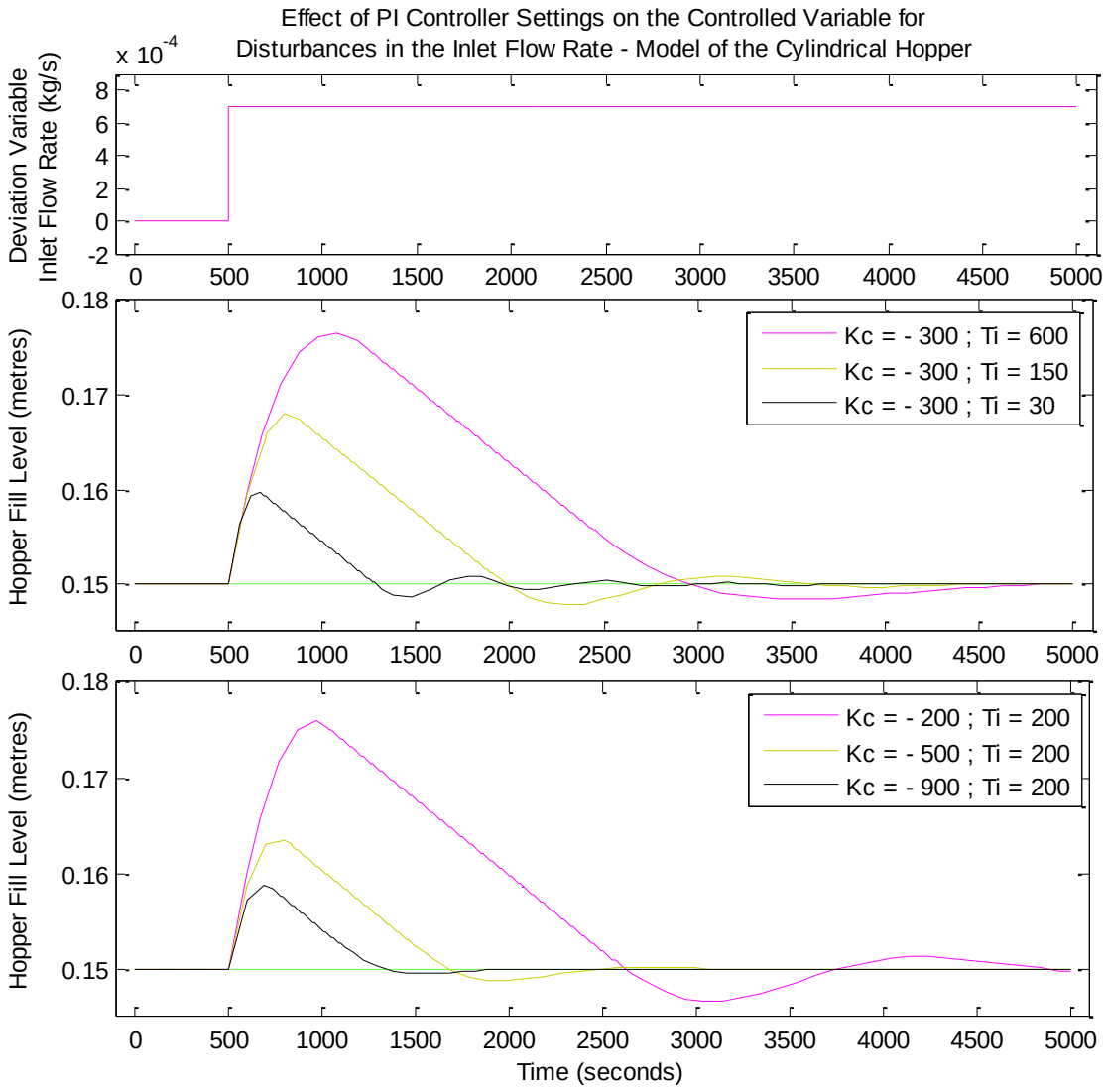

Figure 56: Effects of PI Controller settings on disturbance responses for the Model of the Cylindrical Hopper (being Kc = Proportional Gain and Ti = Reset or Integral Time)

Figure 56 points out that, on the one hand, if the proportional gain K_c is held constant, low values of the integral time T_I would produce a faster response but unfortunately more oscillatory. On the other hand, if instead, the integral time T_I is held constant, larger negative values of the proportional gain K_c tend to make the closed-loop

responses less oscillatory and faster. The result of the lower plot of the Figure 56 can be summarized as follows:

Value of K_c	**Closed-Loop Responses**
small	oscillatory
moderate	not too oscillatory
large	stable

Table 11: Closed-Loop Responses for Disturbances Changes when the Integral Time Ti is held constant while the value of the Proportional Gain Kc is modified

6.4.4.1 Set-Point Tracking Simulations of the Models being studied with different Designs of the P-Only Controller and PI Controller

The response of a control system to set-point or disturbance changes depends strongly on the controller parameters as it was previously noted. The study to identify the influence of different controller designs (proportional gain K_c and the integral gain K_I) on set-point tracking simulations can be done with Simulink, by using the "PID Tuner" tool. This tool allows to choose the desired response time as well as its transient behavior, when using a PI Controller, and it automatically computes the corresponding value of the proportional and the integral gain that will define the controller performance.

Generally, for P-Only control, decreases in the response time leads to a more negative value of the proportional gain and hence, as it will be shown in the corresponding plots, faster responses are achieved with unfortunately, pronounced oscillations in the manipulated variable. If an integral action is added to the controller, the PID Tuner allows to define simultaneously the transient behavior between 0 and 1; being 0 a very aggressive response of the control-loop and 1, in contrast, a very robust response. On the one hand, a very aggressive behavior would allow the system to reach the set point faster, but with higher oscillation and larger overshoot. If, on the other hand, oscillations are unwanted and the overshoot cannot be higher than a certain value, the transient behavior should be adjusted close to the unity.

In this section, two simulations, one using a P-Only Controller and another using a PI Controller, will be carried out for both the model of the cylindrical hopper and the model of the non-linear conical hopper following the next annotation:

- If a P-Only Controller is used, the proportional gain K_c will be progressively increased so that different responses are obtained for each model.
- If a PI Controller is used, the simulation will be designed differently for each of the models, since the dynamic behavior of the models is similar as it was shown for instance, in the Figure 55. Their responses differed mainly in time, and therefore, the system's responses for different controller settings can be extrapolated from one model to the other, to explain its effects. In the case of the cylindrical hopper, the proportional gain K_c will be held constant while the integral time T_I , also found as τ_I , is progressively modified. In the other case, when performing the simulation with the non-linear model of the conical hopper, the working procedure will be the opposite. The integral time will be held constant while modifying progressively the proportional gain.

The simulations are performed using the Simulink Block diagrams of the Figure 57 (representation of the control loop both with a P-Only Controller and a PI Controller concerning the model of the cylindrical hopper) and Figure 58 (representation of the control loop both with a P-Only Controller and a PI Controller concerning the non-linear model of the conical hopper). The operating limits are located in the right side of both figures; 59 rpm and 90 rpm defines respectively the lower limit and the upper limit of the turret speed; 0.1 meters and 0.2 meters defines the range where the hopper fill level must be controlled. For both simulations, the inlet flow rate operates at steady state and the initial conditions of the hopper fill level are set to zero. The set-point is defined at 0.15 meters.

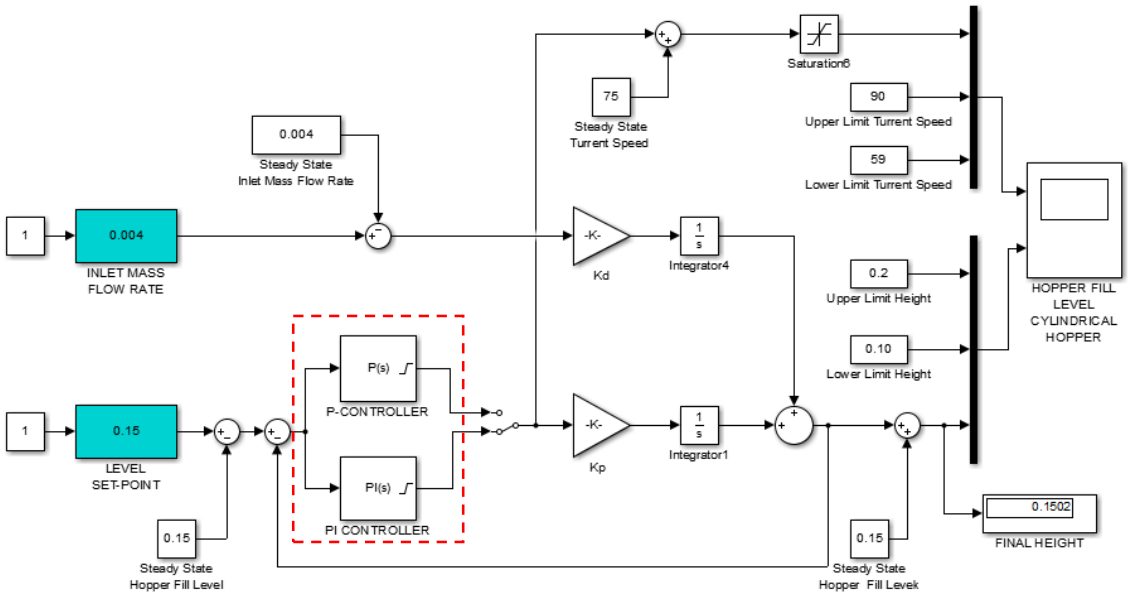

Figure 57: Simulink block diagram with regard to the control loop of the Model of the Cylindrical Hopper with a P-Only Controller/PI Controller

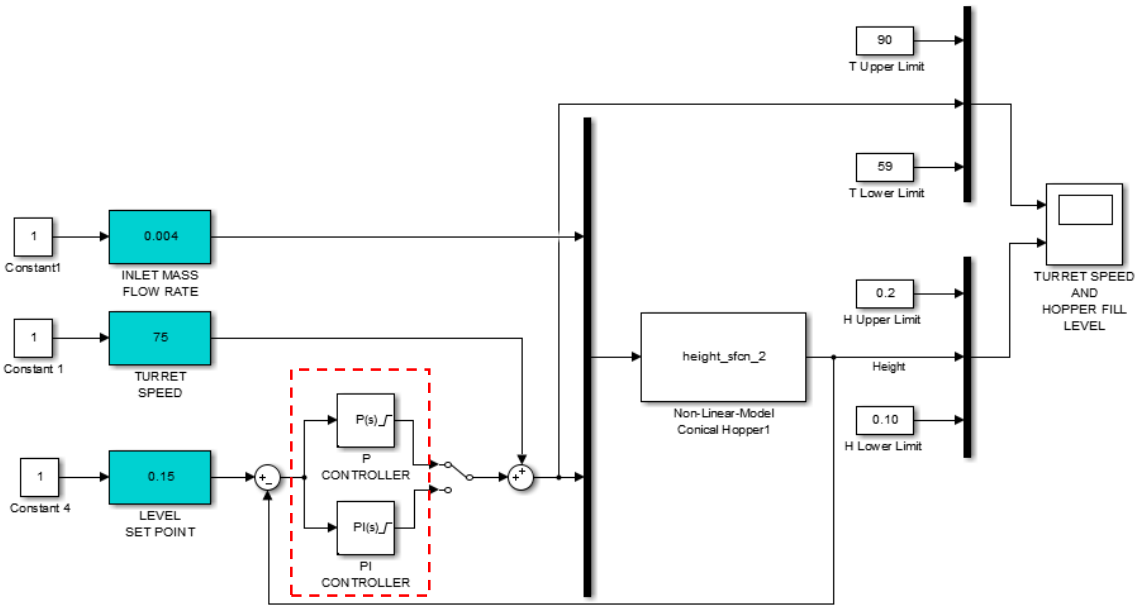

Figure 58: Simulink Block Diagram with regard to the control loop of the Non-Linear Model of the Conical Hopper with a P-Only Controller/PI Controller

Model of the Cylindrical Hopper with a P-Only Controller

The controller response to the aforementioned set-point tracking simulation together with the hopper fill level simulation towards the defined set-point is plotted in the Figure 59. The results are based on the Simulink Block diagram of the Figure 57. The P-Only

controller was selected, and four simulations with different values of the proportional gain K_c were performed as follows:

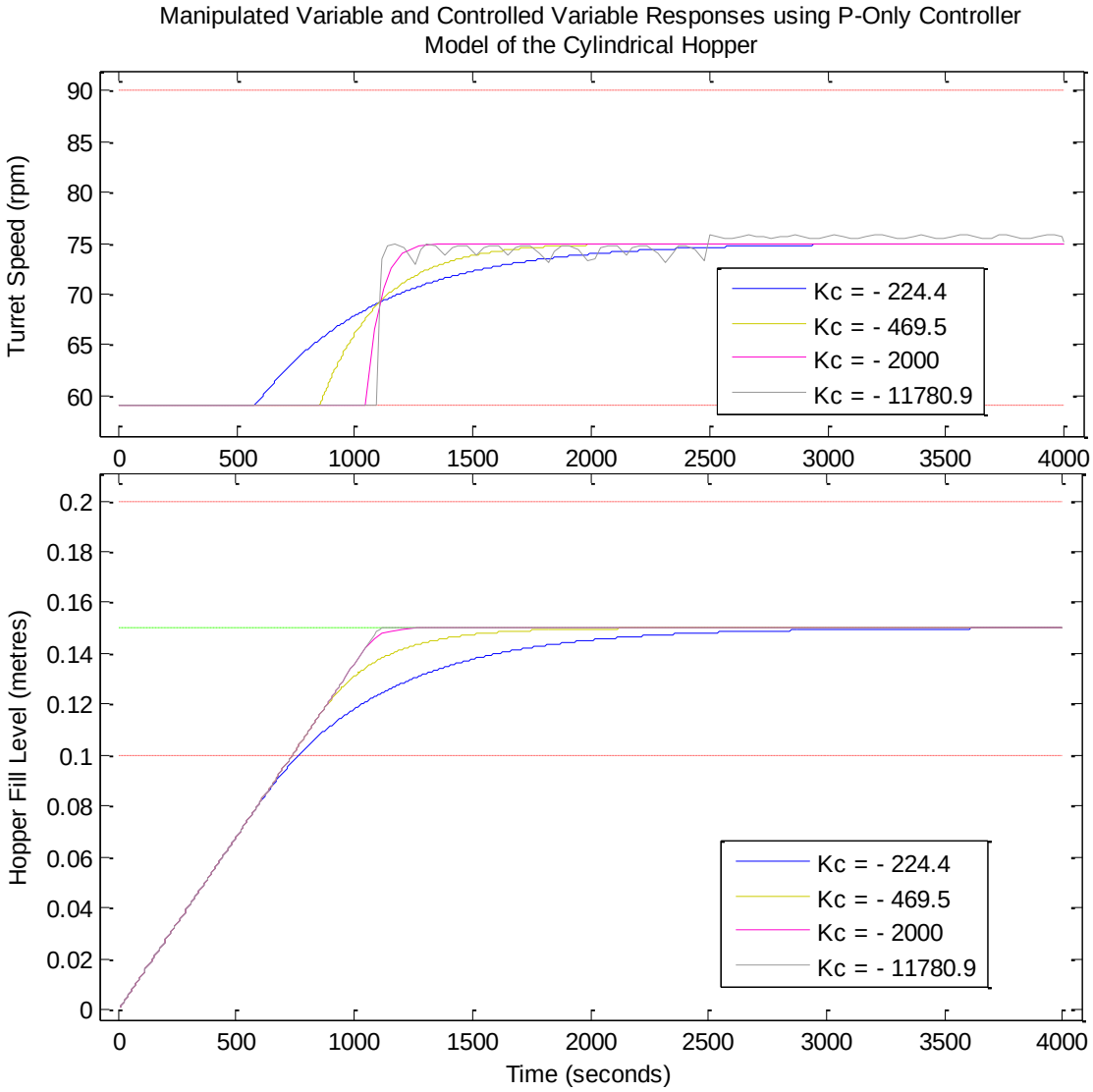

Figure 59: Responses of the turret speed (manipulated variable) and the hopper fill level (controlled variable) for a Set-Point Tracking Simulation using a P-Only Controller with different parameters of the proportional gain (Kc) for the Model of the Cylindrical Hopper

Model of the Cylindrical Hopper with a PI Controller

This second simulation is carried out with the same Simulink Block diagram as the one before (see Figure 57), but in this case, a PI Controller is used. The manipulated and the controlled variable are plotted in the Figure 60. Similarly, four simulations are

performed. As it was previously described, for this particular case, the proportional gain K_c will be held constant while the integral time T_I or τ_I is progressively modified.

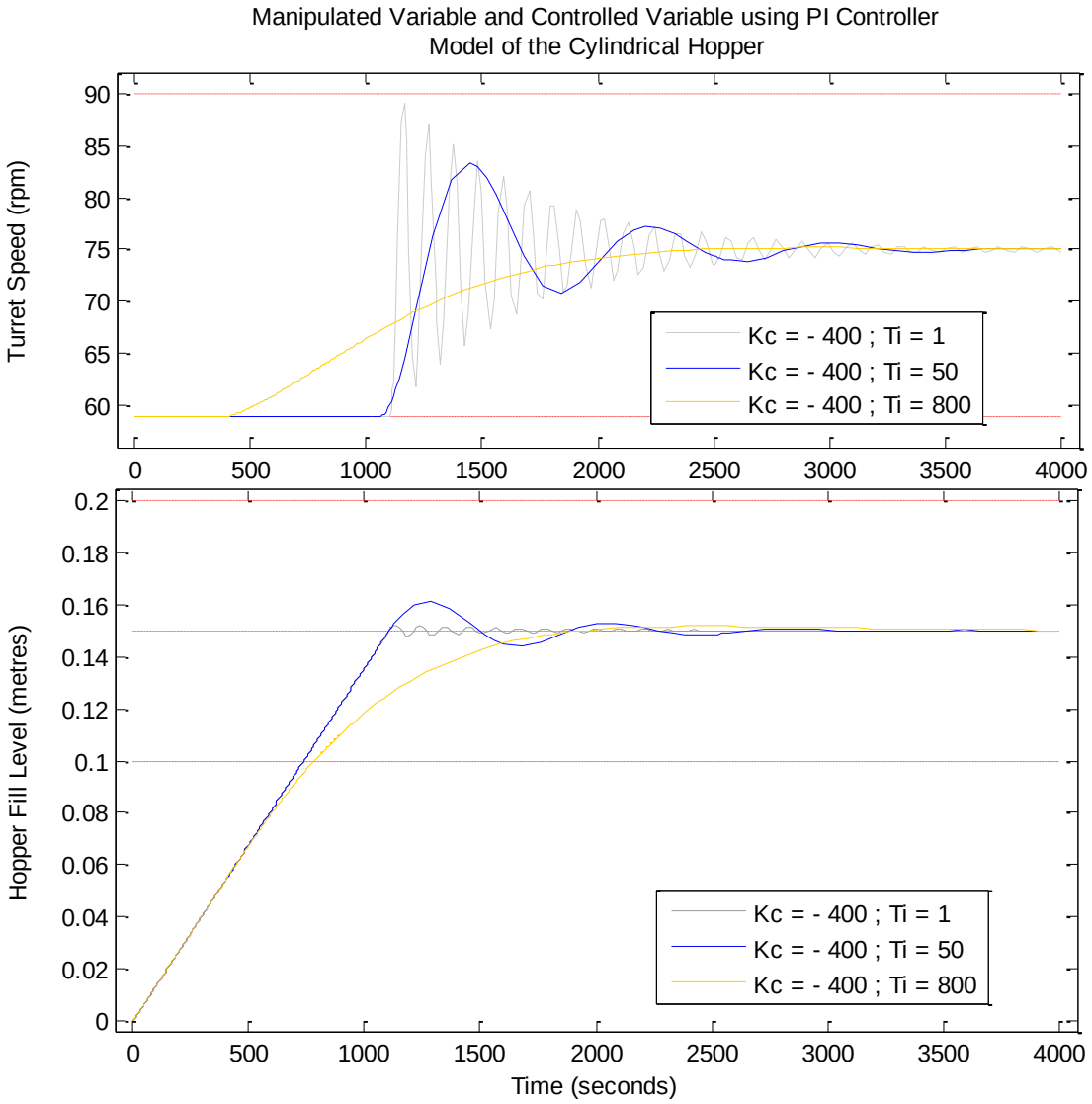

Figure 60: Responses of the turret speed (manipulated variable) and the hopper fill level (controlled variable) for a Set-Point Tracking Simulation using a PI Controller with different parameters of the proportional gain (Kc) and the integral time (Ti) for the Model of the Cylindrical Hopper

Non-Linear Model of the Conical Hopper with a P-Only Controller

The same procedure as in the case of the model of the cylindrical hopper with a P-Only controlled is followed now. The controller response to the set-point tracking simulation together with the hopper fill level response are plotted in the Figure 61. The results are based on the Simulink Block diagram of the Figure 58. The P-Only controller was

selected, and four simulations with different values of the proportional gain K_c were performed as follows:

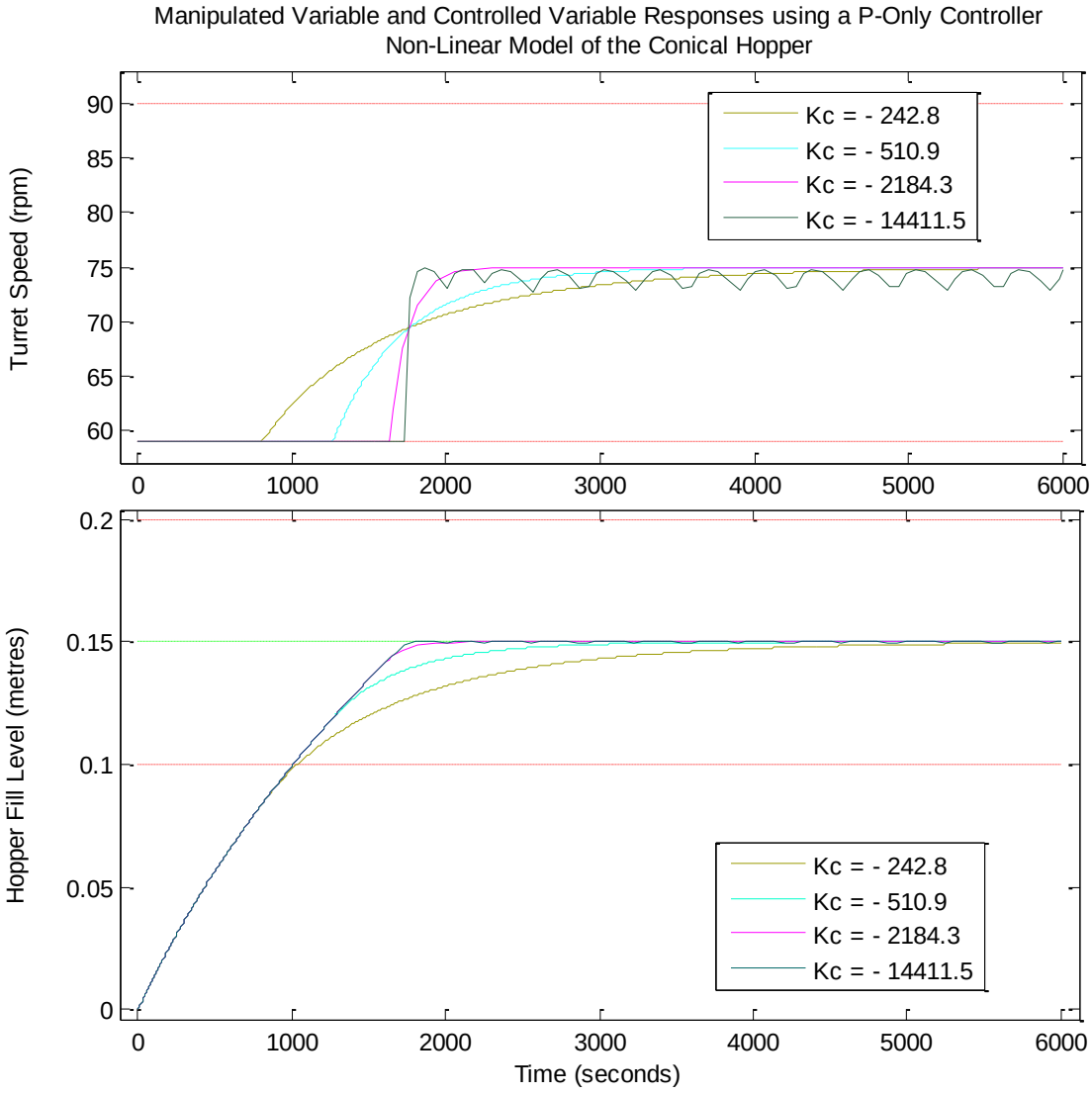

Figure 61: Response of the turret speed (manipulated variable) and the hopper fill level (controlled variable) for a Set-Point Tracking Simulation using a P-Only Controller with different parameters of the proportional gain (Kc) for the Non-Linear Model of the Conical Hopper

Non-Linear Model of the Conical Hopper with a PI Controller

The last simulation regarding this set-point tracking experiment is carried out with the non-linear model of the conical hopper, represented in Simulink as the Figure 58 showed. The responses of the turret speed and the hopper fill level are plotted in the Figure 62. The PI Controller is selected, and in this case, the integral time T_I is held

constant with a value of 400 seconds while the proportional gain K_c is progressively increased as follows:

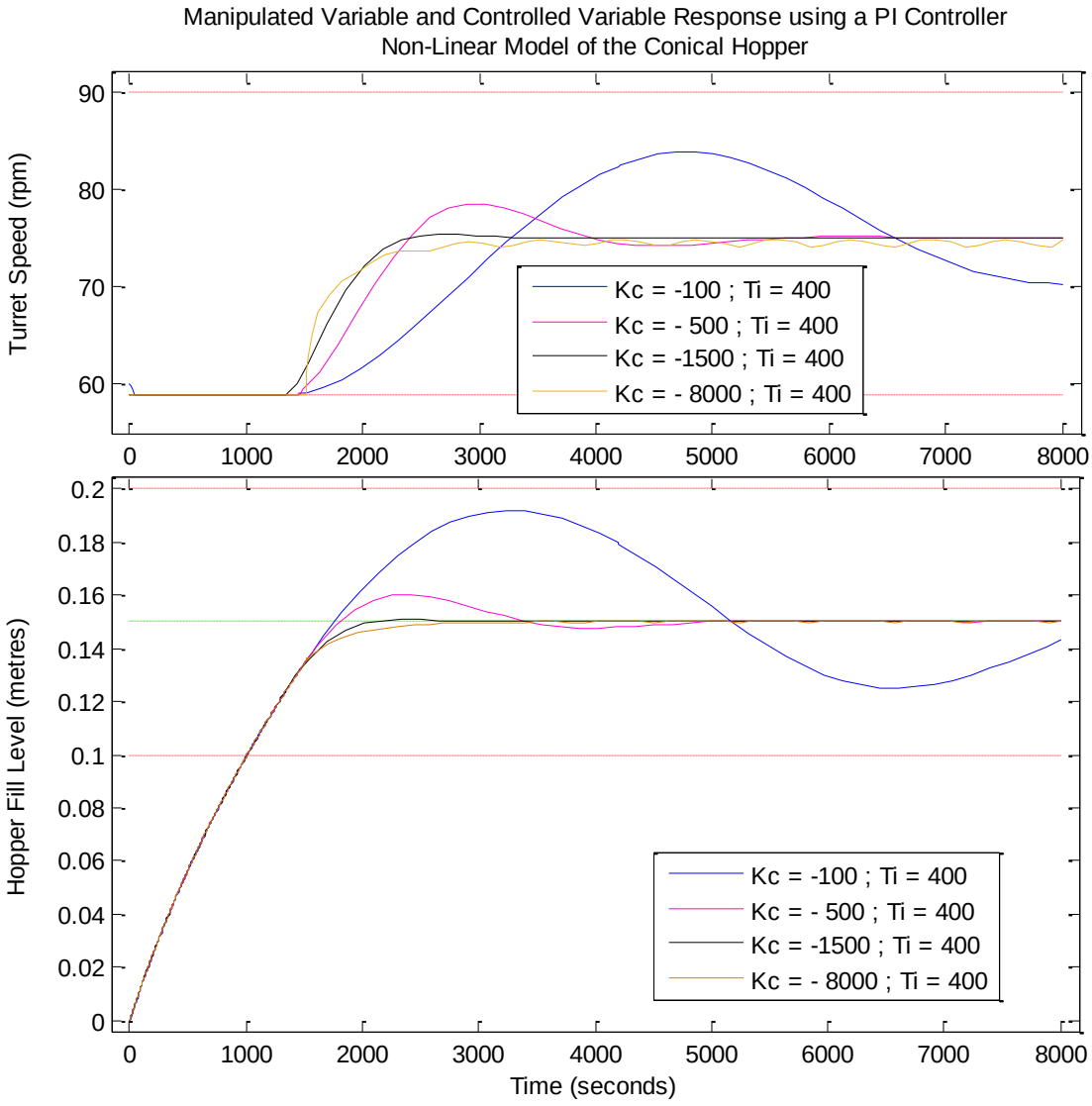

Figure 62: Response of the turret speed (manipulated variable) and the hopper fill level (controlled variable) for a Set-Point Tracking Simulation using a PI Controller with different settings of the proportional gain (Kc) and the integral time (Ti) for the Non-Linear Model of the Conical Hopper

At first glance, and before even checking any result, the first impulse would be the selection of the larger possible negative proportional gain to achieve a fast response, together with an additional robust performance, if an integral action is included in the controller. However, according to the Figures 59 and 61, large negative values of the proportional gain causes huge oscillations in the turret speed regardless of the defined robustness, when P-Only controller is used. Small negative values of the proportional

gain however, lead to slower responses. This direct conclusions concerning the previous P-Only controller simulations can be summarized as follows:

Value of K_c	**Closed-Loop Responses**
small	Non-oscillatory but slow responses
large	Fast but oscillatory responses (mainly in the manipulated variable)

Table 12: Closed-Loop response conclusions for different values of the Proportional Gain (Kc) when using a P-Only Controller

If an integral action is added in the controller, the results are slightly different. The Figure 60 and 62, representing in both cases integrating (non-self-regulating) processes, suggested the following; on the one hand, if the proportional gain of the controller is held constant, the progressive increase of the integral time will reduce efficiently the degree of oscillation both in the manipulated and in the controlled variable. For instance, in reference to the lower plot of the Figure 60, for a constant value of the proportional gain ($K_c = -400$) an integral time of $T_I = 800\ seconds$ would produce a pretty stable response where the oscillations might be almost negligible. However, for $T_I \gg 800$, the responses of the hopper fill level would be too slow, and hence, unwanted. On the other hand, according to the Figure 62, if instead, the integral time is held constant at 400 seconds, the increase of the negative value of the proportional gain leads to smaller oscillations in both plotted variables. It is important to realize that, as happened in the other case, the selection of too large values of the proportional gain would produce an oscillatory response of the manipulated variable, as the upper plot of the Figure 62 illustrated.

6.4.4.2 Set-Point Tracking Simulation with Disturbances in the Inlet Flow Rate for the model of the Cylindrical Hopper

It is worth mentioning as well, that in reference to the previous simulations, both the P-Only Controller and the PI Controller can provide pretty similar response to set-point tracking simulation, if the controller is accordingly adjusted. However, what would happen if disturbances in the inlet flow rate occur meanwhile a set-point tracking simulation is running? Which would be the performances of the P-Only Controller and

the PI Controller in such situation? The Figure 63 answers this question clearly. This new simulation is performed in Simulink using again the block diagram of the Figure 57. A step input of 0.0007 $\frac{Kg}{s}$ in the inlet flow rate was at $t = 4500\ seconds$ was included in the Simulink diagram. The controller is going to be designed by using information from previous simulations, with the only purpose of showing clearly the difference between using P-Only and PI controller when disturbances occur simultaneously with set-point changes. Therefore, the P-Only controller is set with a proportional gain of $K_c = -400$ while the PI controller shows a proportional gain of $K_c = -400$ and an integral time of $T_I = -400\ seconds$. The initial condition of the hopper fill level is set to zero, $h_{initial} = 0\ metres$ and the set-point is kept constant at $0.15\ metres$.

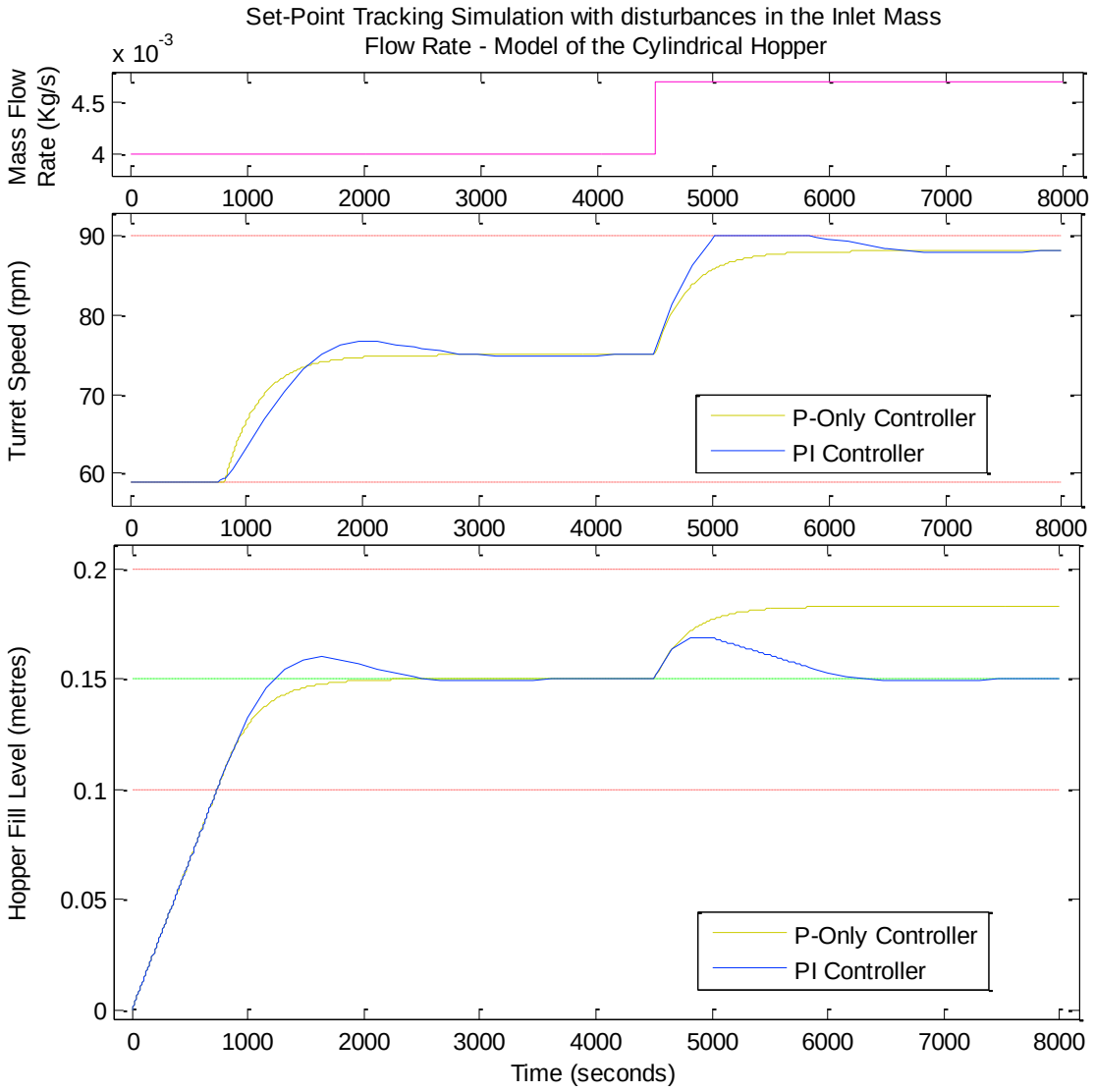

Figure 63: Set-Point tracking simulation with a disturbance in the inlet mass flow rate using either a P-Only Controller (Kc = -400) or a PI Controller (Kc = -400; Ti = 400) for the Model of the Cylindrical Hopper

For the selected parameters of the controller, no matter which one is used, the process variable is able to track the set-point (green line) with no offset as long as just perturbations in the set point occur, as shown in the Figure 63 till $4500\ seconds$. This behavior, typical for integrating processes, might be quite confusing, since it does not fit the expected behavior of the more-common self-regulating processes.

However, a relevant difference in the controller performance for integrating processes arises when perturbations in the disturbance variable (see Figure 63) occur together with a previous set-point change. The positive step input in the inlet mass flow rate at $t = 4500\ seconds$ supposes an increase in the hopper fill level. In order to compensate this new deviation from the set-point, the controller regulates accordingly the turret speed, which will reach a higher steady state value. If, on the one side, the action is monitored by a P-Only controller, a *steady state error* or *offset* (difference between the yellow line and the green line at t=8000 seconds) develops, (see lower plot of the Figure 63). This happens because "integrating processes have a natural accumulating character (and is, in fact, why "integrating process" is used as a descriptor for non-self-regulating processes). Since the process integrates, it appears that the controller does not need to" [113]. Simulations demonstrate though, that the offset might be reduced by increasing the negative value of the proportional gain K_c . On the other side, the addition of integral action in the controller would eliminate the offset completely for the step change in the disturbance variable, as the blue of the lower plot of the Figure 63 demonstrated. This is clearly the main advantage of using PI Controller over P-Only Controller.

The following two points present two different controller design and tuning procedures for the integrating (non-self-regulating) process being studied. Firstly, the controller will be design according to IMC (lambda) tuning strategy. Secondly, the same controller will be tuned according to SIMC (Skogestad) strategy. Finally, both methods will be compared in the last point of this section.

6.4.4.3 IMC (Lambda) Tuning Method for PI Controller

Lambda tuning method refers to all tuning method in which the control loop speed of response can be selected as a tuning parameter [114]. It is therefore related to the known tuning strategy called Internal Model Control (IMC), which is based on a process model that leads to analytical expression for the controller settings. The math behind it uses pole-zero cancellations to achieve the desired closed-loop response.

The main advantage of this Lambda PID tuning method, is the fact that it allows to select the *desired lambda* λ, or also known in this particular case as the *desired closed-loop time constant* τ_c *or* T_c *(in the legend of the plots),* to meet the control strategy performance with the control objective. This parameter is therefore the tuning key. The selection of the desired closed-loop time constant will make the controller more aggressive (small T_c) or less aggressive (large T_c) [101].

As it was proved in the Figure 33, the models being studied in this thesis show an integrating (non-self-regulating) response to disturbances in the inlet parameters. The following equations (see Table 13) present the PI controller tuning relations according to IMC-Based PID Controller Settings for $G_c(s)$ (Chien and Fruehauf, 1990), for integrating models:

	$\boldsymbol{K_c}$	$\boldsymbol{\tau_I}$	$\boldsymbol{\tau_D}$
PI Controller	$\dfrac{2 \cdot \tau_c + \theta}{K_p \cdot (\tau_c + \theta)^2}$	$2 \cdot \tau_c + \theta$	-

Table 13: IMC (Lambda) Tuning correlations for PI Controllers for Integrating Processes

Being K_p the gain of the transfer function that denotes the change in the hopper fill level owing to a change in the turret speed, and θ the process time delay, which in this particular case is zero (see Figures 33 and 55). Besides, since the controller is designed in parallel, the integral gain is computed as follows:

$$K_I = \frac{K_c}{\tau_I} \qquad \textit{eq. (VI—53)}$$

In general, and as it is demonstrated in the two following simulations (one for the model of the cylindrical hopper and the other one for the linearized model of the conical

hopper), increasing τ_c produces a more conservative controller because K_c decreases while τ_I increases.

The Table 14 shows the different controller parameters depending on the selected closed-loop time constant that are going to be used to perform the simulations of the Figure 64 and Figure 65. The values are calculated according to the equations located in the Table 13 and to the eq. (VI – 53).

$\boldsymbol{\tau_c}$	25	100	250	500
$\boldsymbol{K_c}$	-9424.77	-2356.19	-942.48	-471.24
$\boldsymbol{\tau_I}$	50	200	500	1000
$\boldsymbol{K_I}$	-188.5	-11.781	-1.885	-0.47

Table 14: Proportional Controller Gain (Kc), Integral time (Ti) and Integral Gain (Ki) for different values of the desired closed-loop time constant (Tc). Data used for the Model of the Cylindrical Hopper

In order to compare the performance of the different controller designs (see Table 14), a simulation is arranged by using the Simulink diagram of the Figure 49, and the data is collected in the Figure 64. First of all, a manual step input ($0.0007\ \frac{Kg}{s}$) in the inlet mass flow rate takes place at $t = 500\ seconds$. Subsequently, another manual change is generated at $t = 5500\ seconds$. In this case, the hopper fill level set point changes from a value of $0.15\ metres$ to a value of $0.19\ metres$.

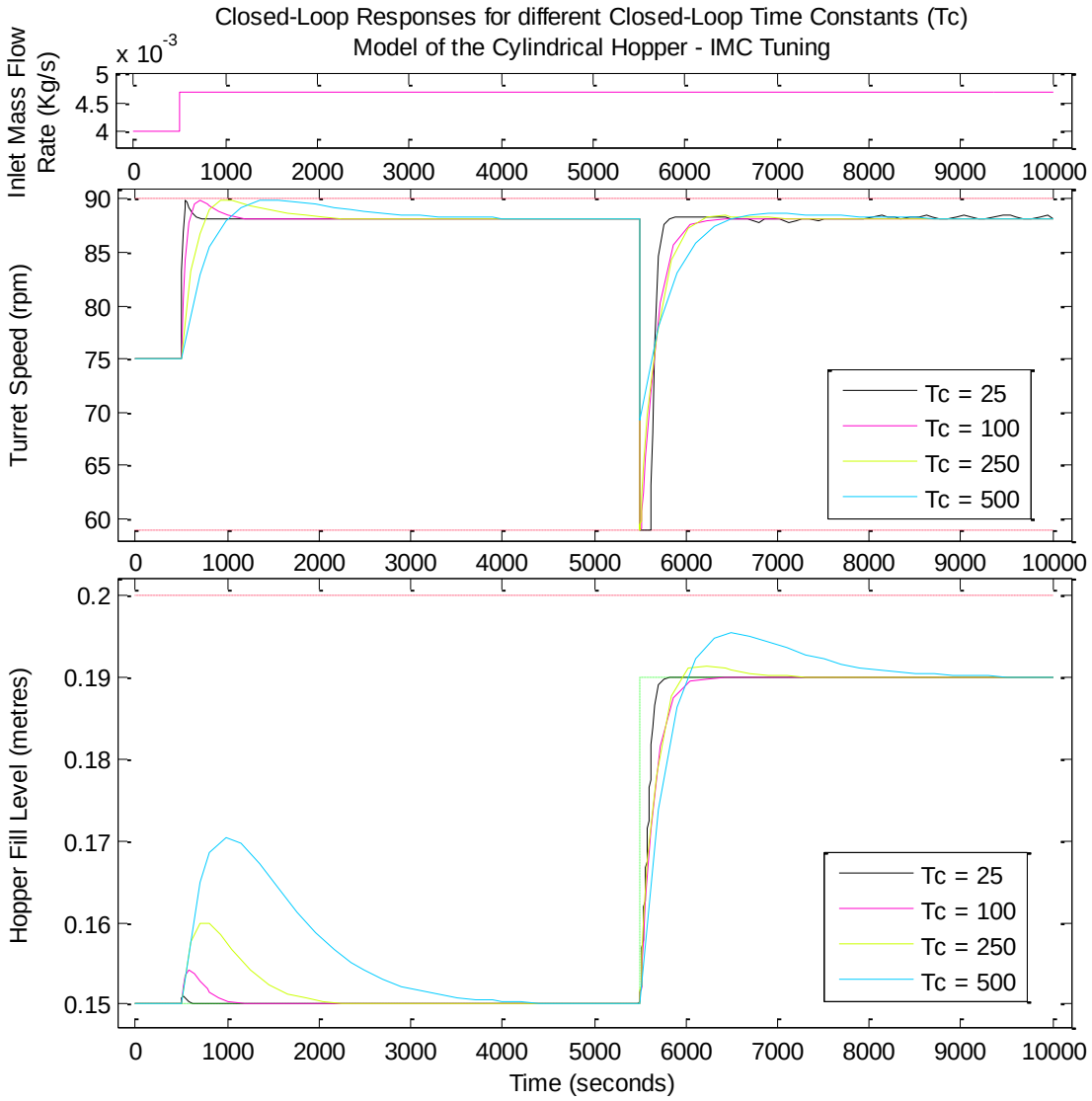

Figure 64: Simulation results for different desired closed-loop time constant (Tc) - (IMC – Lambda - Tuning) using the Model of the Cylindrical Hopper while a manual step input occurs both in the disturbance variable and in the hopper fill level set-point

As expected, Figure 64 proves that, on the one hand, larger τ_c (see the blue line in the lower plot) generates more sluggish and overshot responses to disturbances and set-point tracking. For instance, for a closed-loop time constant of 500 seconds the system needs more than 4000 seconds to settle the hopper fill level back at its set-point. On the other hand, a closed-loop time constant with a small value of $\tau_c = 25\ seconds$ (see black line) results in quite fast responses of the hopper fill level to disturbances. However, if the turret speed response is analyzed (see middle plot of the Figure 64), some oscillations are observed. Therefore, even though a really fast response might be accomplished as the closed-loop time constant is decreased, some unwanted oscillations start happening in the manipulated variable. But not only this, besides, in

order to fulfil such quick response, the manipulated variable is required to change from high values to its minimum saturation limit (59 rpm) instantaneously (see black line of the turret speed plot in Figure 64), which in reality might take some more time. This analysis lead to think that, according to these simulations, a suitable design for the controller might comprehend values of the τ_c between 25 and 100 to generate the faster possible response with the minimum possible oscillation.

The Figure 65 represents the same experiment, but in this case, using the Simulink diagram of the Figure 53, which corresponds to the linearized model of the conical hopper. This model, as it was before mentioned, gives around the linearized point $h_{linearization} = 0.15$ a very similar response when it is compared to its non-linear model, as the Figure 55 corroborated previously. The simulation is designed in the following way: a step input in the inlet flow rate of $0.0006\ \frac{Kg}{s}$ occurs at $t = 500\ seconds$, and the set-point of the hopper fill level is changed to $0.18\ metres$ after $t = 6000\ seconds$ so that different controller's performances can be compared under the cited conditions.

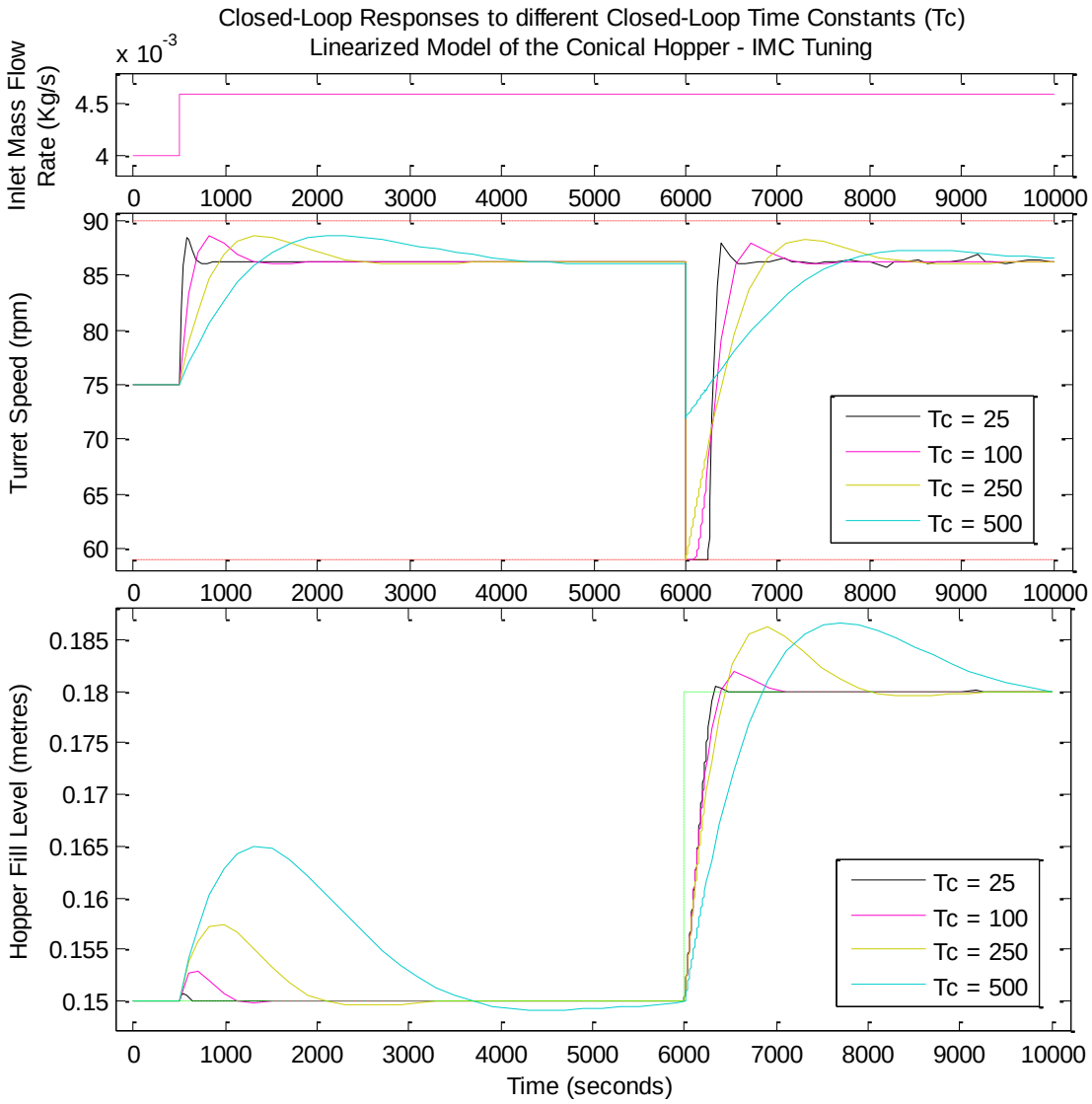

Figure 65: Simulation Results for different desired closed-loop time constant (IMC Tuning) using the Linearized Model of the Conical Hopper while a manual step input occurs both in the disturbance variable and in the hopper fill level set-point

Regarding the conical hopper, decreases in the desired closed-loop time constant not only leads to a faster response as shown in the Figure 65, but also reduces the over-damping effect when the process variable turns back to the set-point after disturbances owed to inlet flow rate deviations. Comparing the Figure 64 and 65 for the same $\tau_c = 100\ seconds$, some overshoot is appreciated in the case of the conical hopper after set-point changes ($t = 6000\ seconds$). A lower value of the closed-loop time constant is therefore selected $\tau_c = 25\ seconds$ in order to study the behavior of the system for a very aggressive controller. As expected, the overshoot is reduced (see black line of the lower plot of the Figure 65), but the required turret speed to achieve such response

becomes oscillatory (black line of the middle plot of the Figure 65), as the Figure 62 predicted previously for too large values of the proportional gain K_c.

In resume, and according to the IMC tuning method for the PI Controller, a closed-loop time constant τ_c with a value between $15\ and\ 100\ seconds$ would present a reasonable performance of the controller for the model of the cylindrical hopper. If, otherwise, the conical hopper is used in the process, a closed-loop time constant between 25 and 100 should be selected. It is important to take into account though, that a τ_c close to 25 seconds would lead to oscillatory responses in the turret speed, while values around 100 seconds would produce some overshoot in the process variable for disturbances in the set-point. The best tuning design of the controller according to this method is summarized in the Table 15.

Unit Operation	$\boldsymbol{\tau_c}$
Cylindrical Hopper	$25 < \tau_c < 100$
Conical Hopper	$25 < \tau_c < 100$

Table 15: Controller's best performance according to the IMC (Lambda) Tuning Method for the PI Controller

6.4.4.4 SIMC (Skogestad IMC) Tuning Method for PI Controller

The idea behind the Skogestad Internal Model Control (SIMC) is pretty similar to the one before commented. This method presents as well a single tuning parameter (τ_c) that gives a good balance between the PID parameters, and which can be adjusted to get a desired trade-off between performance ("tight" control) and robustness ("smooth" control) [115].

Skogestad proposed that the desired closed-loop time constant τ_c should be equal to the process time delay, $\tau_c = \theta$ [101]. However, as proved in the Figure 33, the time delay of the process being studied is zero and this would lead to an infinite controller gain, which is clearly not realistic. Therefore, as suggested in [108], if the process has no *time delay,* τ_c must be specified to some reasonable value larger than zero.

In resume, the closed-loop time constant should be located within a defined domain in order to fulfil the process requirements. Too low τ_c might lead to oscillatory behavior while too large τ_c , makes the response too sluggish. Stogestad's tuning formulas for integrating process are extracted from [115]:

	K_c	τ_I	τ_D
PI Controller	$\frac{1}{K_p} \cdot \frac{1}{(\tau_c + \theta)}$	$4 \cdot (\tau_c + \theta)$	-

Table 16: SIMC (Skogestad) Tuning correlations for PI Controllers for Integrating Processes

Being K_p the gain of the transfer function that denotes the change in the hopper fill level owing to a change in the manipulated variable (turret speed). The relation between the controller gain and the integral time is given in the eq. (VI – 53).

The Table 17 shows different PI controller designs according to the SIMC tuning strategy equations commented above. Two simulation, one with the Simulink model of the cylindrical hopper and the other one with the Simulink linearized model of the conical hopper will be performed using the data from the Table 17. Both simulations follow the same procedure as the one performed for the IMC tuning strategy.

τ_c	25	100	250	500
K_c	-4713.39	-1178.1	-471.24	-235.62
τ_I	100	400	1000	2000
K_I	-47.124	-2.945	-0.471	-0.118

Table 17: Proportional Controller Gain (Kc), Integral time (Ti) and Integral Gain (Ki) for different values of the Desired Closed-Loop Time Constant. Data used for the Linearized Model of the Conical Hopper

Figure 66 suggests that a really aggressive controller ($\tau_c = 25$) would generate a rapid response in the hopper fill level. Unfortunately, it would require a tiny oscillatory behavior in the turret speed when the set-point tracking simulation is carried out at 5500 seconds. It is worth mentioning, that for the same τ_c , the oscillatory behavior of the turret speed is more pronounced when designing the controller according to IMC than to SIMC. Designing on the other hand a more conservative controller ($\tau_c = 500$), slower responses will be obtained. By following the blue line in the lower plot of the Figure 66, one realizes that the controller is not capable of settling back the hopper fill level to $0.15\ metres$ after the step input of $0.0007\ \frac{Kg}{s}$ in the inlet flow rate happens.

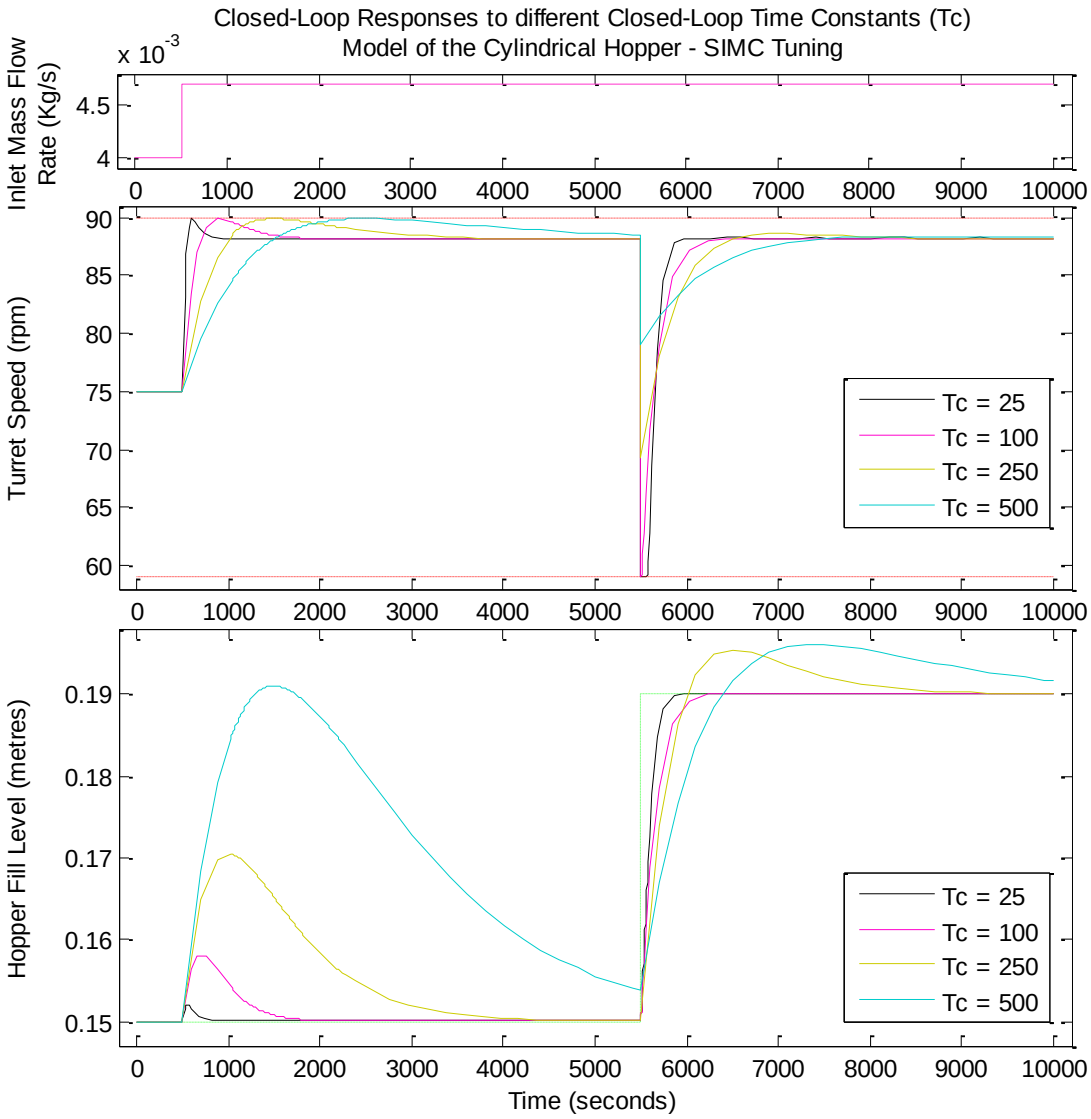

Figure 66: Simulation results for different desired closed-loop time constant (SIMC Tuning) using the Model of the Cylindrical Hopper while a manual step input occurs both in the disturbance variable and in the hopper fill level set-point

Again, for the simulation with the linearized model of the conical hopper, the Figure 67 suggests an aggressive controller for keeping the powder level within its desired design space. It is appreciable in this particular case, and in contrast to the previous ones, that the turret speed does not experience any kind of oscillations when the closed-loop time constant is defined at 25 seconds. However, both for τ_c equal to 25 and 100, the turret speed needs to accelerate and decelerate extremely fast to fulfil the rapid response of the hopper fill level, as shown in the Figure 67. In reality, such performance might be unreachable. Nevertheless, according to the performed simulations, a reasonable value of the closed-loop time constant wouldn´t be larger than $100\ seconds$ due to slow responses, but neither smaller than 25 seconds.

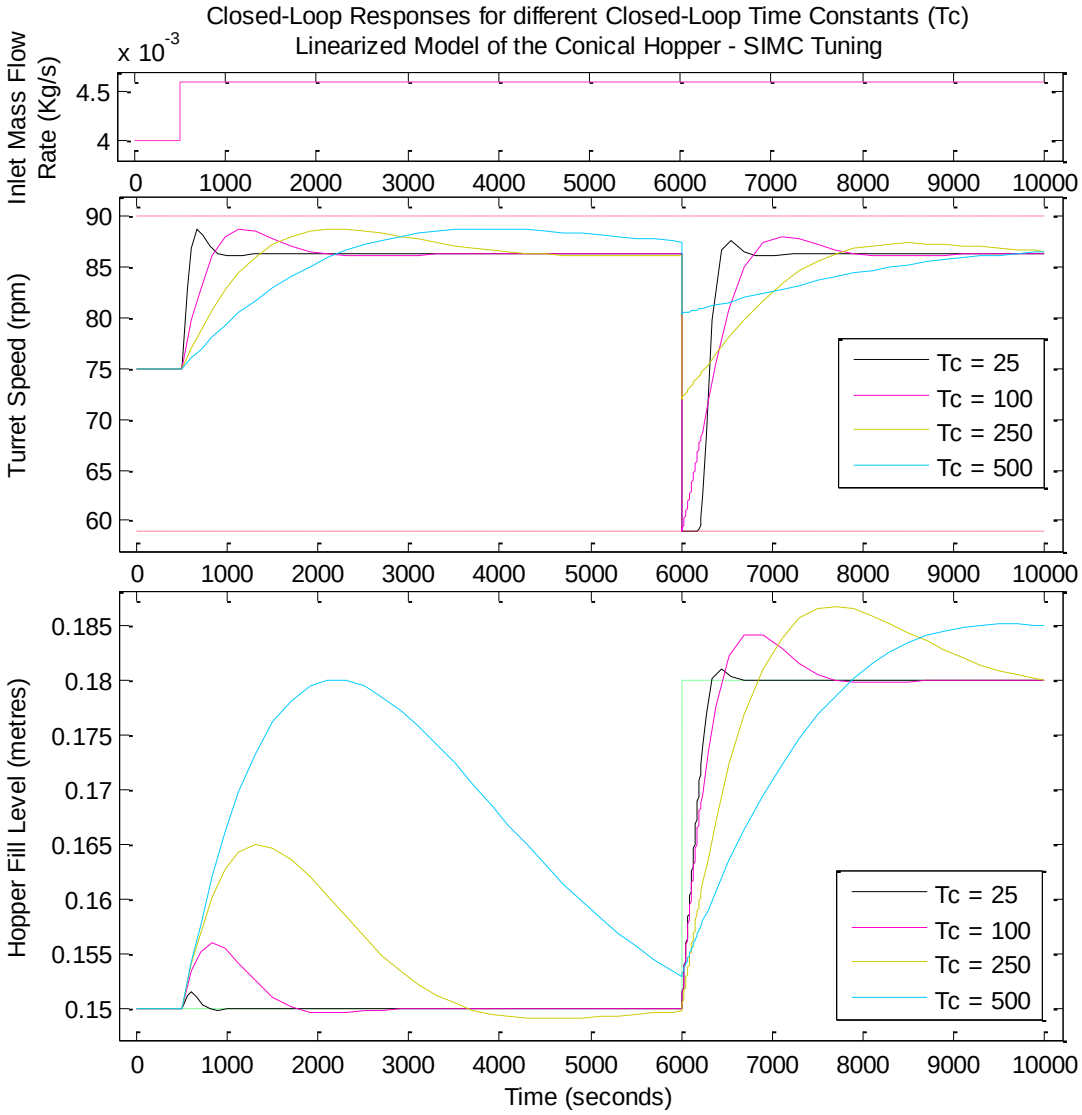

Figure 67: Simulation Results for different desired closed-loop time constant (SIMC Tuning) using the Linearized Model of the Conical Hopper while a step input occurs in the disturbance variable and in the desired set-point

The best tuning design of the controller according to the SIMC method is summarized in the Table 18.

Unit Operation	$\boldsymbol{\tau_c}$
Cylindrical Hopper	$25 < \tau_c < 100$
Conical Hopper	$25 < \tau_c < 100$

Table 18: Controller's best performance according to the SIMC (Skogestad) Tuning Method for the PI Controller

The Table 19 summarizes, according to previous simulations using IMC and SIMC tuning strategies, the main effects regarding the design of the closed-loop time constant τ_c on the manipulated variable, ω_{turret} and on the controlled variable, h_{hopper} .

Closed-Loop Time Constant τ_c	Hopper Fill Level h_{hopper}	Turret Speed ω_{turret}
Small (τ_c < 200)	*Fast response*	*Extreme acceleration/deceleration*
Large (τ_c > 200)	*Slow response*	*Slight acceleration/deceleration*

Table 19: Summarized Effects of the Closed-Loop Time Constant both on the Hopper Fill Level and on the Turret Speed

6.4.5 Set-Point Tracking Simulations with Disturbance Rejections for the designed P-Only Controller and PI Controller

By taking advance of the Simulink block diagrams of the Figure 49 and 53, several set-point tracking simulations with disturbance rejections will be performed using the cylindrical hopper and the conical hopper respectively around the operating point $h_{powder} = 0.15\ metres$. The simulations are run using either P-Only controller or PI controller. While the P-Only controller is designed based on the simulation results obtained in the Figures 59 and 61, the PI Controller is tuned according to the IMC and SIMC tuning methods previously described in the section 6.4.4.3 and section 6.4.4.4 respectively. The different controller designs are summarized in the following Table 20:

	Cylindrical Hopper			Conical Hopper		
P – Only Controller	$K_c = -2300$			$K_c = -2100$		
PI – Controller	$\tau_c = 60$	IMC	SIMC	$\tau_c = 60$	IMC	SIMC
		$K_c = -3926.99$ $\tau_I = 120$	$K_c = -1963.5$ $\tau_I = 240$		$K_c = -3926.99$ $\tau_I = 120$	$K_c = -1963.5$ $\tau_I = 240$

Table 20: Controller Design for the Set-Point tracking simulations with disturbance rejection for the Cylindrical Hopper and the Conical Hopper

The Figures 69 and 71 show the results of the set-point tracking simulation for the cylindrical hopper and for the conical hopper respectively, using different configurations of the controller. Figures 68 and 70 show the respective performed inlet mass flow rate disturbances.

Firstly, the P-Only control of an integrating process, see Figure 69 (light purple line) and Figure 71 (dark yellow line), can provide a rapid set-point response with no overshoot until a disturbance changes the balance point of the process. Under this circumstances,

the PI controller turns out to be more beneficial, since it can reject the upset and return the process variable to its set-point. This is because the constant summing of integral action continue to move the controller output until the controller error is driven to zero [113]. Thus, as shown in the lower plot of both Figures (69 and 71), PI control requires accepting some overshoot during set-point tracking in exchange for the ability to reject disturbances.

Secondly, both PI controller strategies show outstanding performances for the same closed-loop time constant $\tau_c = 60\ seconds$. However, the IMC tuning method provides a controller's design capable to response faster to set-point changes than the SIMC, as the blue line in the lower plot of both figures show. Besides, IMC method gives the controller the required characteristics to settle the hopper fill level back in the desired set-point faster and with smaller oscillations when disturbances in the inlet flow occur.

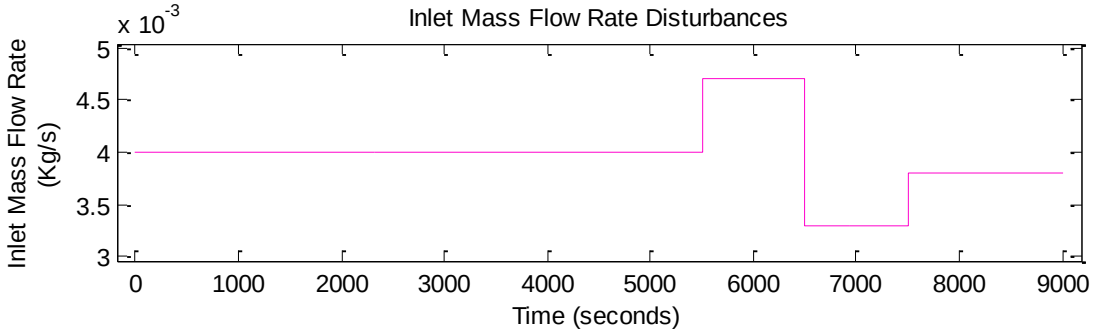

Figure 68: Inlet mass flow rate disturbances for the set point tracking simulation of the Model of the Cylindrical Hopper

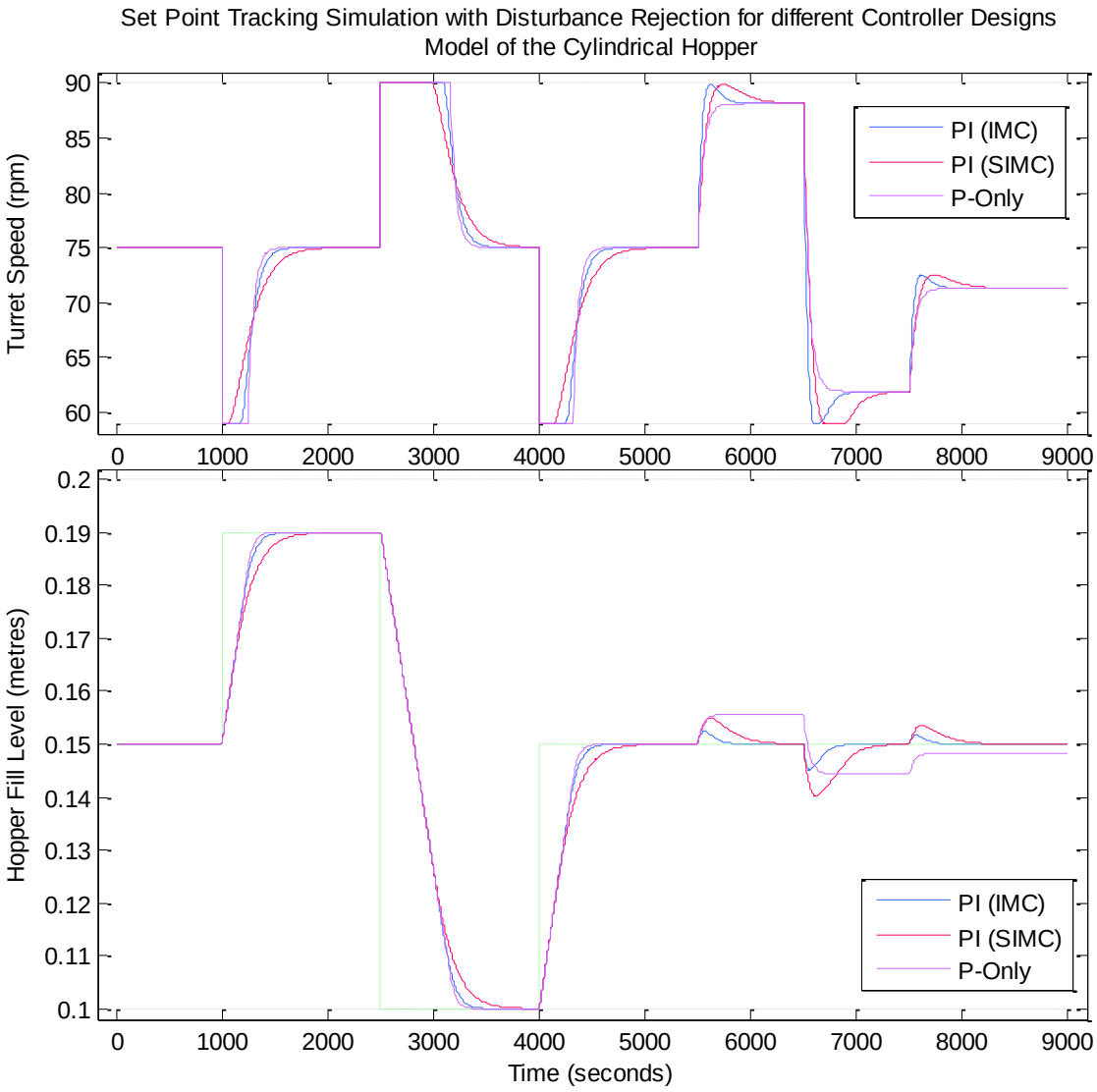

Figure 69: Set-Point Tracking and Disturbance Rejection for different Controller Designs: PI Controller based on IMC Tuning (blue), PI Controller based on SIMC Tuning (red) and P-Only Controller (light purple). Simulation performed using the Model of the Cylindrical Hopper

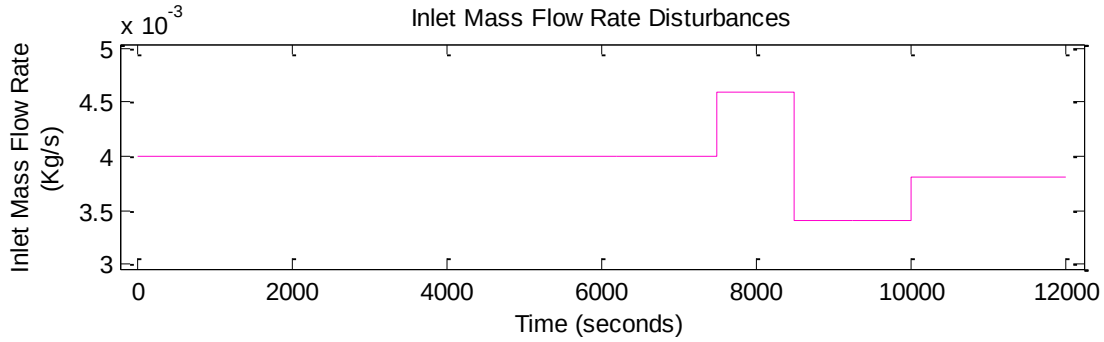

Figure 70: Inlet mass flow rate disturbances for the Set Point Tracking Simulation of the Linearized Model of the Conical Hopper

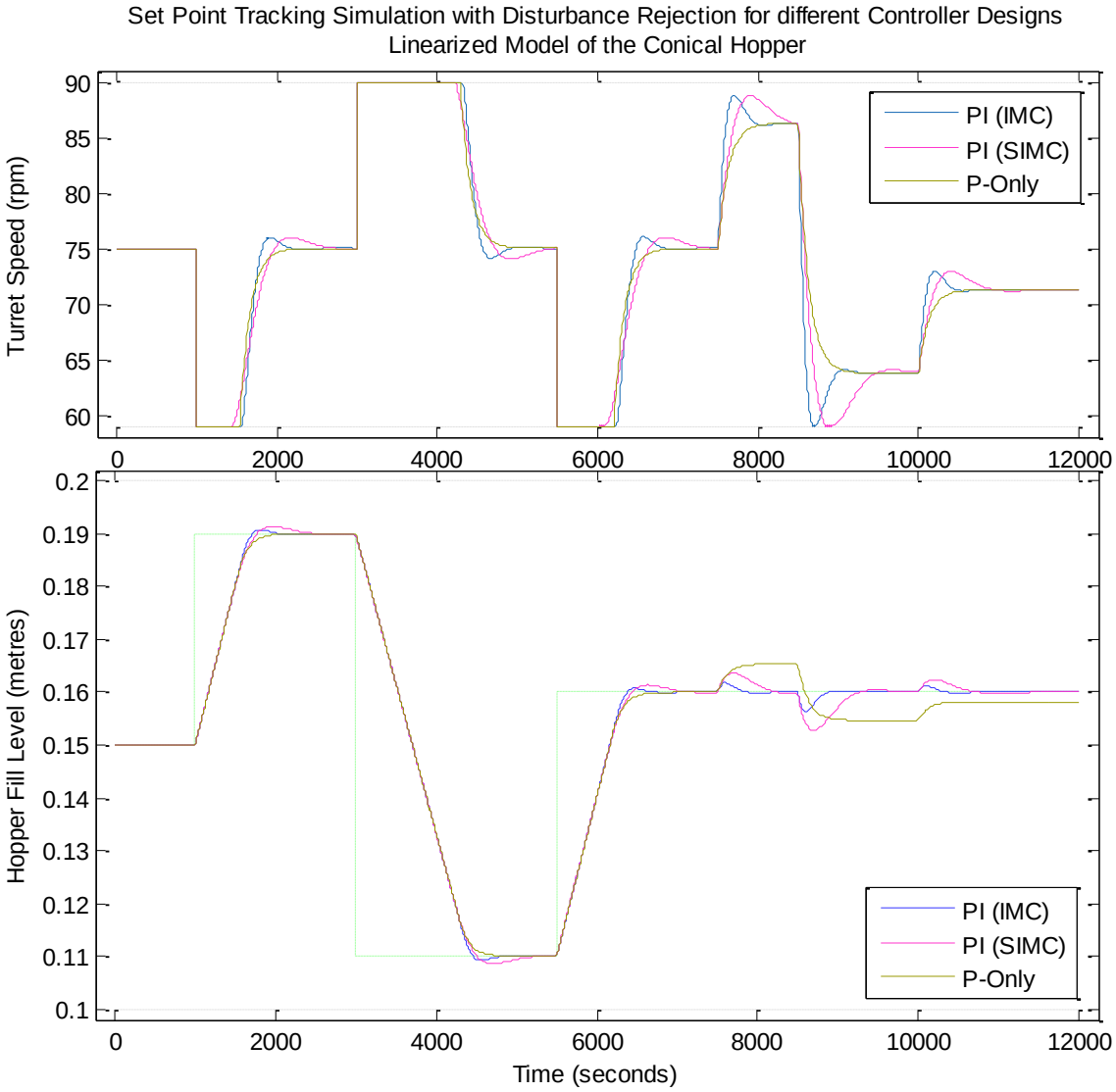

Figure 71: Set-Point Tracking and Disturbance Rejection for different Controller Designs: PI Controller based on IMC Tuning (blue), PI Controller based on SIMC Tuning (pink) and P-Only Controller (dark yellow). Simulation performed using the Linearized Model of the Conical Hopper

VII. VALIDATION AND VERIFICATION OF THE MODEL-BASED CONTROL-LOOP

It is important to keep in mind that a model is nothing else but an imitation of reality, and hence, even though they are never 100% correct, they can become extremely useful if validity is successfully accredited.

In order to demonstrate the validity of the model-based control-loop developed in the previous chapter, the pilot plant of the RCPE was set up in concordance with the Figure 72, developed with Matlab. The cylindrical hopper was selected to carry out the validation, and the ultrasonic sensor was installed in the upper side of the hopper. A process control system was connected to the pilot plant with the main purpose of controlling the hopper fill level (blue area located inside the cylindrical hopper in the Figure 72) at the desired set point (red rectangle beside the hopper). The control system, designed with the values of the IMC tuning method for PI Controllers (see previous Table 20), receives the data from the ultrasonic sensor and manipulates accordingly the turret speed ω_{turret} of the tablet press.

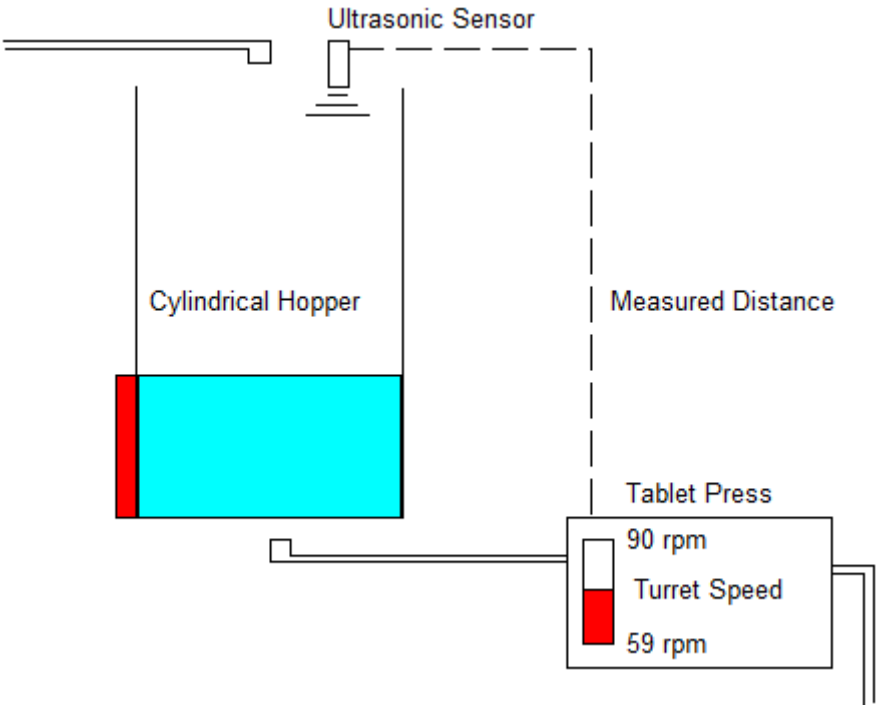

Figure 72: Virtual representation of the RCPE's Pilot Plant by MATLAB

The simulations and the respective validation in the pilot plant were carried out with the following data:

Variable	***Unit***	***Value***
$\boldsymbol{validation/simulation\ time}$	$seconds$	4578
$\bar{\dot{m}}_{in}$	$Kg/_{s}$	0.0022
$\bar{\omega}_{turret}$	rpm	75
$\bar{h}_{hopper}$	m	0.19
n_{die}	$(-)$	8
K_c	rpm/m	-3926.99
τ_I	$seconds$	120
$K_{p,\ cylindrical}$	m	$4.669 \cdot 10^{-6}$
$K_{d,\ cylindrical}$	m/kg	0.1591549431

Table 21: Data for carrying out the simulation in Simulink and its respective validation in the RCPE's Pilot Plant

The simulation in Simulink and the validations in the pilot plant were performed under the same conditions. The Figure 73 summarizes the manual input changes in the hopper fill level set-point and the ones concerning the inlet mass flow rate.

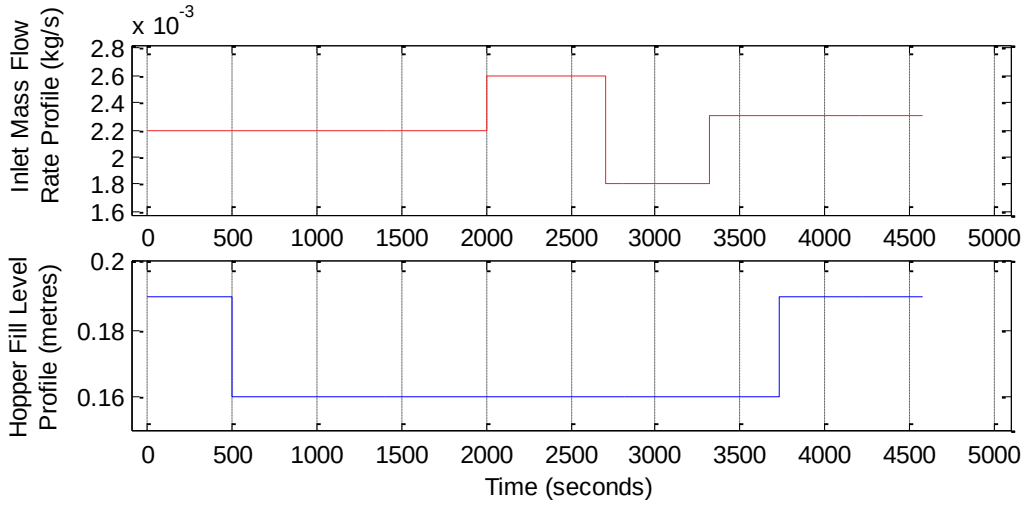

Figure 73: Inlet Mass Flow Rate Profile (upper plot) and Hopper Fill Level Profile (lower plot)

The data obtained from the validation was stored in a specified MAT-file. This file can be read by Simulink as the Figure 74 shows, so that the data obtained from the validations in the pilot plant can be compared with the data coming from the respective simulations. The Figure 74 illustrates within the Simulink diagram two different blocks that import

data from a MAT-file. One of them represents the true data of the validation. The other one though, represents smooth response data from the same validation. The smooth data was performed using a Matlab tool called "*smooth*" and the "*rloess*" method with a span of 10%.

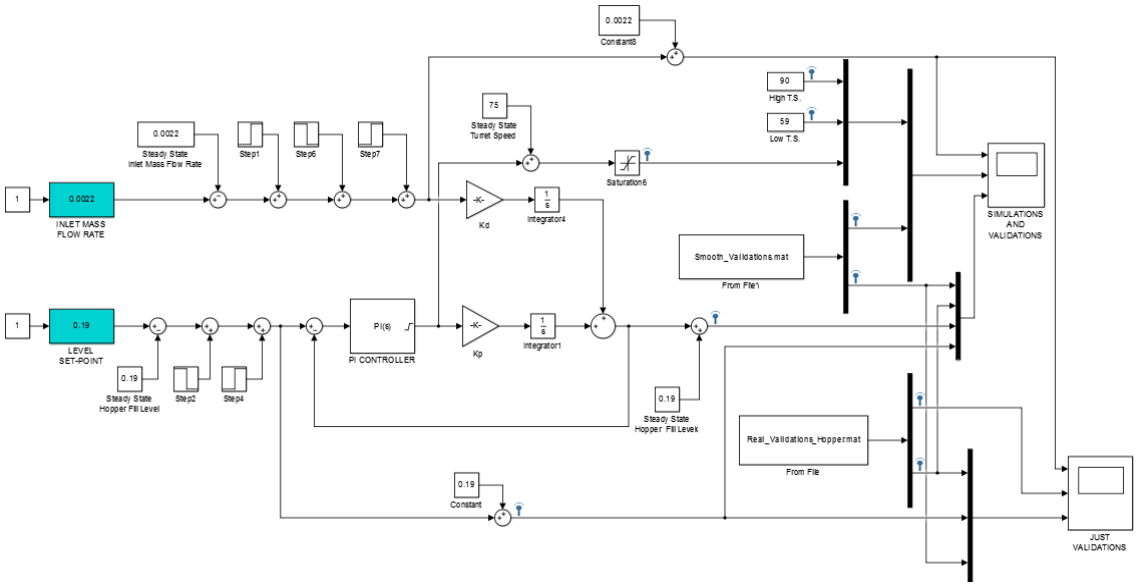

Figure 74: Simulink diagram that plots simultaneously the results from the simulation of the Cylindrical Hopper with PI Controller and the Data obtained from the Validations

The results obtained from running the Figure 74 are illustrated in the Figure 75. The green line in the lower plot represents the set point profile of the hopper fill level that must be followed in the best possible way by the blue line (simulation data) and by the grey line (experimental data). The red line (smooth approximation of the data obtained from the experiments in the pilot plant) was included to enhance the visual difference between the simulation and the validation as well as to remove the noise of the experimental data. Exactly the same is represented in the upper plot of the Figure 75, but with regard to the turret speed.

In the effort to track the set point of the hopper fill level, it is appreciated from the smooth data obtained in the validations (see lower plot of the Figure 75) the higher degree of oscillation once the set point is achieved. This result contrasts with the hardly noticeable oscillation of the respective simulation (see blue line). It is worth mentioning though, that the real controller seems to track the set point faster than the simulated controller. Probably the presence of dust and the aggressiveness of the controller make the difference between the two results.

In the upper plot of the Figure 75 is noticeable the pronounced fluctuation of the turret speed between its saturation range. The most logical explanation to this outcome is the fact that the design of the controller might be too aggressive. As a consequence, as soon as a slightly deviation from the hopper fill level set-point is detected, the controller tends to adjust very fast the turret speed to settle the fill level back to the set point. This would achieve an optimal control performance (see blue lines in the Figure 75 corresponding to the simulation) if the sensor could be able to measure without noise. However, the increasing presence of dust inside the hopper and the generation of uneven surface of the material being measured makes this impossible, and continuous fluctuation on the variables depicted occurs.

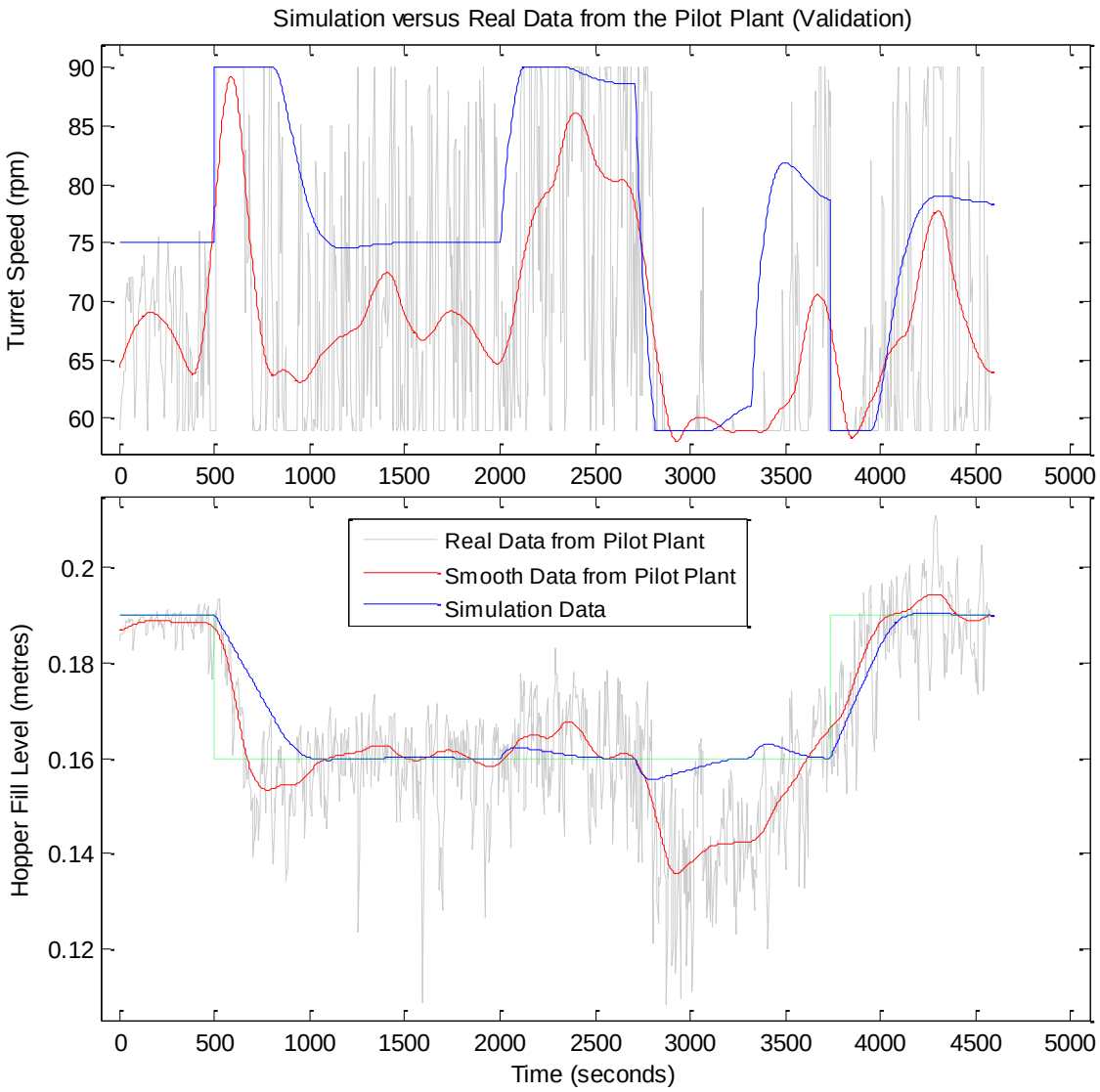

Figure 75: Comparison between the Data obtained from Simulation with Matlab Simulink (blue line) and the Data obtained from Experiments in the Pilot Plant – validations – (grey line). The smooth Data from the validation is represented by a red line. The Set Point Profile of the Hopper Fill Level is represented by a green line

VIII. SUMMARY AND CONCLUSIONS

This thesis comprises a review of the current state of the pharmaceutical industry and the implementation of an automated control system in a continuous direct compaction process. Due to the fact that pharmaceutical industry is currently witnessing its own change towards continuous manufacturing, this work proves that tools such as process understanding, QbD, PAT, engineering sciences or model-based design are the centerpiece for pushing such transformation. However, the current mind-set is hard to be changed and consequently, further research is required.

Bearing this in mind, the heart of this research is the development of an automated control system that keeps the hopper fill level within its own design space. As a first conclusion, ultrasonic technology was selected to carry out this assignment after a comparison with other techniques (guided wave radar, laser, etc.). While uneven surfaces of the bulk solid inside the hopper do not seem to be a problem for the performance of the ultrasonic device, the generation of dust due to the powder movement influences slightly the sound waves, generating some noise in the measurement. As expected, the noise is smaller at the very beginning, and it becomes more pronounced with the time because of the powder motion. Luckily, the amplitude of the noise reaches some stability that gives the measurement validity.

The dynamic behavior of the powder inside the hopper – cylindrical or asymmetrical conical – is first modeled from geometry data and mass balances, and its *non-self-regulating* behavior is simultaneously demonstrated. Secondly, it is implemented into MATLAB/Simulink where a model-based feedback control loop is designed based on IMC and SIMC tuning strategies. Several simulations are run to analyze the performance of the designed P-Only and a PI controller. The IMC tuning strategy for the PI controller turns out to be the preferred design in terms of performance and robustness, since it shows the best ability to reject the unknown disturbances and to track the set-point.

Keeping this in mind, the validation of the developed model is carried out in the RCPE's pilot plant with the cylindrical hopper and the designed PI controller. Process

parameters such as the hopper fill level or the inlet mass flow rate are set firstly to their respective steady state value and several deviations from this state are manually made to study the controller response. Despite the increasing presence of dust inside the hopper or the formation of uneven surfaces with regard to the material being measured, it can be concluded that the design of the controller, despite its aggressive design, is able to reject properly disturbances in the inlet mass flow rate and to track the desired set-point. Besides, the results from the validation match reasonably well with the ones obtained from the simulation, despite some larger oscillation resulting from the process conditions previously described. Consequently, it can be fairly concluded that the mathematical model of the cylindrical hopper and the closed loop controller are successfully validated.

IX. LIST OF FIGURES

X. LIST OF TABLES

XI. ABBREVIATIONS

Abbreviation	*Full Meaning*
ANDA	Abbreviated New Drug Application
API	Active Pharmaceutical Ingredient
CM	Continuous Manufacturing
CMAs	Critical Material Attributes
COGS	Costs of Goods Sold
CPPs	Critical Process Parameters
CAs	Critical Attributes
CQAs	Critical Quality Attributes
CSDD	Centre for the Study of Drug Development
DoE	Design of Experiment
EFPIA	European Federation of Pharmaceutical Industries and Associations
EPRI	The Electric Power Research Institute
EU	European Union
FDA	Food and Drug Administration
FMEA	Failure Mode and Effects Analysis
FTC	Field Time Control
g	Grams
GHz	Gigahertz
GWR	Guided Wave Radar
Hz	Hertz
ICH	International Conference on Harmonization of technical requirements for the registration of pharmaceutical for human use
IMC	Internal Model Control
JPMA	Japan Pharm. Manufacturers Association
kHz	Kilohertz
LC	Level Controller
LT	Level Transmitter
m	Metres
M&S	Model and Simulation
mA	Milliamps
MAs	Material Attributes
MEP	Market Exclusivity Period
mm	Millimetres
MPC	Model Predictable Control

NSTC	National Science and Technology Council
ODE	Ordinary Differential Equation
PAT	Process Analytical Technology
PhRMA	Pharmaceutical Research and Manufacturers of America
PI	Proportional-Integral
PID	Proportional-Integral-Derivative
P-Only	Proportional-Only
PPs	Process Parameters
PSD	Particle Size Distribution
PSE	Process System Enterprise
QbD	Quality by Design
QbT	Quality by testing
QRM	Quality Risk Management
QTPP	Quality Target Product Profile
R&D	Research and Development
RCPE	Research Center Pharmaceutical Development
RM	Risk Management
rpm	Revolutions per minute
RTD	Residence Time Distribution
SIMC	Skogestad Internal Model Control
TDR	Time Domain Reflectometry
TOF	Time of Flight
UK	United Kingdom
USA	United States of America

XII. NOMENCLATURE

Symbol	*Meaning*	*Units*
ff_c	Flowability ratio	-
R	Reflectivity	-
$\mathcal{E}_r$	Relative dielectric permittivity	-
c	Speed of sound	m/s
ρ	Density	kg/m^3
B	Bulk modulus	Pa
T°	Temperature	$^{\circ}K$
V_s	Propagation velocity of the sound	m/s
V_{so}	Propagation velocity of the sound at 0ºC	m/s
Z	Impedance	$Ohm\ (\Omega)$
I_i	Incident radiation intensity	W/m^2
I_r	Reflected radiation intensity	W/m^2
I_t	Absorbed radiation intensity	W/m^2
θ_i	Incidence angle	º
θ_r	Reflection angle	º
θ_t	Absorbing angle	º
$R_{coeff.}$	Reflection coefficient	-
$T_{coeff.}$	Transmission coefficient	-
λ	Wavelength	m
r_1	Radius conical hopper outlet	m
h_2	Height of the section (2) of the conical hopper	m
d_3	Diameter of the section (3) of the conical hopper	m
h_3	Height of the section (3) of the conical hopper	m
A_3	Cross sectional area of the section (3) of the conical hopper	m^2
α	Angle of the section (2) of the conical hopper	º
$A_{cylindrical}$	Cross-sectional area of the cylindrical hopper	m^2
$h_{cylindrical}$	Height of the cylindrical hopper	m
$d_{cylindrical}$	Diameter of the cylindrical hopper	m
$\dot{q}_{in}$	Hopper's inlet volumetric flow rate	m^3/s
$\dot{m}_{in}$	Hopper's inlet mass flow rate (disturbance variable)	kg/s
$\bar{\dot{m}}_{in}$	Hopper's inlet mass flow rate at steady state	kg/s
$\dot{m}'_{in}$	Deviation variable of the hopper's inlet mass flow rate	kg/s
$\dot{q}_{out}$	Hopper's outlet volumetric flow rate	m^3/s
$\dot{m}_{out}$	Hopper's outlet mass flow rate	kg/s
$h\ or\ h_{hopper}$	Hopper fill level (controlled variable)	m
$\bar{h}$	Hopper fill level at steady state	m

h'	Deviation variable of the hopper fill level	m
$h_{set-point}$	Set point of the hopper fill level	m
h_{high}	Upper limit of the hopper's fill level design space	m
h_{low}	Lower limit of the hopper's fill level design space	m
ω_{turret}	Turret speed (manipulated variable)	rpm
$\bar{\omega}_{turret}$	Turret speed at steady state	rpm
ω'_{turret}	Deviation variable of the Turret speed	rpm
ω_{max}	Upper saturation limit of the turret speed	rpm
ω_{min}	Lower saturation limit of the turret speed	rpm
$\dot{m}_{out,tablet\ press}$	Mass flow out of the tablet press	kg/s
n_{Die}	Number of dies in the turret	-
m_{tab}	Mass of a single tablet	kg
t	Time	$seconds$
V	Volume of powder inside the hopper	m^3
$G_p(s)$	Transfer function relating changes in the hopper fill level owing to changes in the turret speed	m
$G_d(s)$	Transfer function relating changes in the hopper fill level owing to changes in the hopper's inlet mass flow rate	m/kg
$K_{p,\ cylindrical}$	Gain of the $G_p(s)$ for the cylindrical hopper	m
$K_{d,\ cylindrical}$	Gain of the $G_d(s)$ for the cylindrical hopper	m/kg
$K_{p,\ conical}$	Gain of the $G_p(s)$ for the conical hopper	m
$K_{d,\ conical}$	Gain of the $G_d(s)$ for the conical hopper	m/kg
K_c	Proportional gain of the controller	rpm/m
K_I	Integral gain of the controller	$rpm/(m \cdot s)$
$\tau_I\ or\ T_i$	Integral time	$seconds$
τ_D	Derivative time	$seconds$
$\tau_c\ or\ T_c$	Closed-Loop time constant	$seconds$
θ	Time delay	$seconds$

XIII. BIBIOGRAPHY

[1] J. Rantanen and J. Khinast, “The Future of Pharmaceutical Manufacturing Sciences,” *J. Pharm. Sci.*, vol. 104, no. 11, pp. 3612–3638, 2015.

[2] M. Sen, R. Singh, and R. Ramachandran, “A Hybrid MPC-PID Control System Design for the Continuous Purification and Processing of Active Pharmaceutical Ingredients,” *Processes*, vol. 2, no. 2, pp. 392–418, 2014.

[3] E. Papadakis, “Modelling and synthesis of pharmaceutical processes: moving from batch to continuous,” Technical University of Denmark, 2016.

[4] S. L. Lee *et al.*, “Modernizing Pharmaceutical Manufacturing: from Batch to Continuous Production,” *J. Pharm. Innov.*, vol. 10, no. 3, pp. 191–199, 2015.

[5] R. Ramachandran, J. Arjunan, A. Chaudhury, and M. G. Ierapetritou, “Model-based control-loop performance of a continuous direct compaction process,” *J. Pharm. Innov.*, vol. 6, no. 4, pp. 249–263, 2011.

[6] L. X. Yu *et al.*, “Understanding pharmaceutical quality by design.,” *AAPS J.*, vol. 16, no. 4, pp. 771–83, 2014.

[7] R. Kamble, S. Sharma, and V. Varghese, “Process analytical technology (PAT) in pharmaceutical development and its application,” *Int. J. Pharm. Sci. Rev. Res.*, vol. 23, no. 2, pp. 212–223, 2013.

[8] R. Singh, M. Ierapetritou, and R. Ramachandran, “An Engineering Study on the Enhanced Control and Operation of Continuous Manufacturing of Pharmaceutical Tablets via Roller Compaction,” *Int. J. Pharm.*, vol. 438, no. 1–2, pp. 307–326, 2012.

[9] F. Hosseinpour and H. Hajihosseini, “Importance of Simulation in Manufacturing,” *World Acad. Sci. Eng. Technol.*, vol. 51, no. 3, pp. 292–295, 2009.

[10] M. C. Martinetz, J. Rehrl, I. Aigner, S. Sacher, and J. Khinast, “A Continuous Operation Concept for a Rotary Tablet Press Using Mass Flow Operating Points,” *Chemie-Ingenieur-Technik*, vol. 89, no. 8, pp. 1–12, 2017.

[11] P. Parikshit Kr, D. Chanchal, and M. Rajani K., “Model based PID controller for integrating process with its real time implementation,” *Proc. Int. Conf. Pervasive Comput. Commun.*, pp. 19–22, 2012.

[12] R. G. Sargent, “Verification and validation of simulation models,” Syracuse University, 2011.

[13] International Trade Administration (ITA), “Pharmaceutical Industry Profile,” *Pharmaceutical Research*, no. July. pp. 1–12, 2010.

[14] T. Opler, B. Garrett, and S. Langer, “Valuation Analysis in Pharmaceutical Licensing and M & A Transactions,” no. January. 2014.

[15] L. Blanc, “The European Pharmaceutical Industry in a Global Economy: what drives EU exports of pharmaceuticals?,” College of Europe, 2014.

[16] EFPIA, “From innovation to outcomes - Annual Report 2015,” Brussels, 2015.

[17] Center for health Policy, “Promoting Continuous Manufacturing in the Pharmaceutical

Sector." Brookings, 2015.

[18] E. S. Langer and R. A. Rader, "Introduction to Continuous Manufacturing : Technology Landscape and Trends." pp. 1–6, 2014.

[19] EFPIA, "The Pharmaceutical Industry in Figures." 2016.

[20] Statistics Explained, "International trade in medicinal and pharmaceutical products - Statistics Explained," 2014. [Online]. Available: http://ec.europa.eu/eurostat/statistics-explained/index.php/International_trade_in_medicinal_and_pharmaceutical_products. [Accessed: 27-Jan-2017].

[21] WHO, "Pharmaceutical Industry: A Strategic Sector for the European Economy," *World Health Organisation*. Brussels, 2014.

[22] PhRMA, "Biopharmaceutical Research Industry Profile." Washington, DC, p. 86, 2016.

[23] E. O'Connell, "Medicines," *Clinical & Experimental Immunology*, 2014. [Online]. Available: https://reellifescience.com/2014/10/15/medicines-by-dr-enda-oconnell/. [Accessed: 12-Jan-2018].

[24] R. Mullin, "Tufts Study Finds Big Rise In Cost Of Drug Development | Chemical & Engineering News," 2014. [Online]. Available: http://cen.acs.org/articles/92/web/2014/11/Tufts-Study-Finds-Big-Rise.html. [Accessed: 27-Jan-2017].

[25] PHRMA, "Biopharmaceutical Research & Development : The Process Behind New Medicines." pp. 1–24, 2015.

[26] A. Hollis, "Me-too drugs: is there a problem," *Submission to the Commission on Intellectual Property Rights, Innovation and Public Health*. pp. 1–8, 2004.

[27] V. Petkantchin, "The advantages of incremental pharmaceutical innovation," *Economic Note*, vol. 1, no. 1. pp. 13–16, 2012.

[28] H. Grabowski, G. Long, and R. Mortimer, "Recent trends in brand-name and generic drug competition.," 2013.

[29] R. Lal, "Patents and Exclusivity," *FDA/CDER SBIA Chronicles*, vol. 505, no. 2. CDER Small Business and Industry Assisance (SBIA), pp. 1–3, 2015.

[30] A. I. Wertheimer and T. M. Santella, "Pharmacoevolution : the advantages of incremental innovation," London, 2005.

[31] S. Globerman and K. M. Lybecker, "The benefits of incremental innovation," no. June. p. 68, 2014.

[32] M. Herper, "Solving The Drug Patent Problem," *Forbes*, 2002. [Online]. Available: https://www.forbes.com/2002/05/02/0502patents.html. [Accessed: 17-Apr-2017].

[33] S. Neuman, "Pharmaceutical industry wastes $50 billion a year due to inefficient manufacturing | The Source | Washington University in St. Louis," 2006. [Online]. Available: https://source.wustl.edu/2006/10/pharmaceutical-industry-wastes-50-billion-a-year-due-to-inefficient-manufacturing/. [Accessed: 26-Jan-2017].

[34] S. Mascia and B. Trout, "Integrated Continuous Manufacturing," 2015. [Online]. Available: http://www.pharmamanufacturing.com/articles/2014/integrated-continuous-manufacturing/?show=all. [Accessed: 27-Jan-2017].

[35] S. Young Rojahn, “The Future of Pharma Is Incredibly Fast,” 2012. [Online]. Available: https://www.technologyreview.com/s/427895/the-future-of-pharma-is-incredibly-fast/. [Accessed: 27-Jan-2017].

[36] Y. Lawrence, “Continuous Manufacturing Has a Strong Impact on Drug Quality | FDA Voice,” 2016. [Online]. Available: http://blogs.fda.gov/fdavoice/index.php/2016/04/continuous-manufacturing-has-a-strong-impact-on-drug-quality/. [Accessed: 27-Jan-2017].

[37] Subcommitte for Advanced Manufacgturing of the National Science and Technology Council, “Advanced Manufacturing: A Snapshot of Priority Technology Areas Across the Federal Government,” *United States Government*, no. April. Washington, DC, pp. 1–63, 2016.

[38] C. Seymour, “Continuous Processing.” Pfizer Inc, pp. 1–26.

[39] K. Plumb, “Continuous Processing in the Pharmaceutical Industry,” *IChemE Adv. Chem. Eng. Worldw.*, no. June, pp. 221–242, 2005.

[40] Pharmaceutical Technology Editors, “Continuous Processing: Moving with or against the Manufacturing Flow,” *PharmTech. Advancing Development and Manufacturing*, 2008. [Online]. Available: http://www.pharmtech.com/continuous-processing-moving-or-against-manufacturing-flow?id=&pageID=1&sk=&date=. [Accessed: 29-Nov-2017].

[41] S. D. Schaber, D. I. Gerogiorgis, R. Ramachandran, J. M. B. Evans, P. I. Barton, and B. L. Trout, “Economic analysis of integrated continuous and batch pharmaceutical manufacturing: A case study,” *Ind. Eng. Chem. Res.*, vol. 50, no. 17, pp. 10083–10092, 2011.

[42] FiercePharma, “Pharma recalls up 54% in Q3 | FiercePharma,” 2011. [Online]. Available: http://www.fiercepharma.com/manufacturing/pharma-recalls-up-54-q3. [Accessed: 28-Jan-2017].

[43] Food and Drug Administration, “Guidance for Industry PAT: A Framework for Innovative Pharmaceutical Development, Manufacuring, and Quality Assurance,” *FDA official document*, no. September. Rockville, MD, p. 16, 2004.

[44] M. Nasr, “Implementation of Quality by Design (QbD) – Current Perspectives on Opportunities and Challenges Topic Introduction and ICH Update.” U.S. Food and Drug Administration, 2011.

[45] U.S. Department oh Health and Human Services, Food and Drug Administration, and Center for Drug Evaluation and Research (CDER), “Advancement of Emerging Technology Applications to Modernize the Pharmaceutical Manufacturing Base,” *FDA Guidance for Industry*. 2015.

[46] ICH Expert Working Group, “ICH Harmonized Tripartite Guideline. Pharmaceutical Development Q8(R2),” vol. 8. 2009.

[47] ICH Expert Working Group, “Quality Risk Management Q9,” no. November. 2005.

[48] ICH Expert Working Group, “Pharmaceutical Quality System Q10,” no. June. 2008.

[49] ICH, “Q8 Q9 Q10 together.” p. 23, 2010.

[50] J. Maguire and D. Peng, “How to Identify Critical Quality Attributes and Critical Process Parameters.” U.S. Food and Drug Administration, Maryland, pp. 1–40, 2015.

[51] S. Stegemann, “The future of pharmaceutical manufacturing in the context of the scientific, social, technological and economic evolution,” Elsevier B.V., Graz, 2015.

[52] Roger Aarenstrup, *Managing Model-Based Design*. Natick, MA: The MathWorks, Inc, 2015.

[53] National Institute of Health, “Computer Modeling and Simulation,” *National Institute of Health*. [Online]. Available: https://www.ors.od.nih.gov/OD/OQM/cms/Pages/default.aspx. [Accessed: 10-Mar-2017].

[54] U.S. Department of Health and Human Services, Food and Drug Administration (FDA), Center for Drug Evaluation and Research (CDER), Center for Biologics Evaluation and Research (CBER), and Center for Veterinary Medicine (CVM), “Guidance for Industry Process Validation: General Principles and Practices,” no. January. p. 22, 2011.

[55] K. Hangos and I. Cameron, *Process Modelling and Model Analysis*. London and San Diego: Academic Press, 2001.

[56] F. Amara, K. Agbossou, A. Cardenas, Y. Dubé, and S. Kelouwani, “Comparison and Simulation of Building Thermal Models for Effective Energy Management,” *Smart Grid Renew. Energy*, no. April, pp. 95–112, 2015.

[57] J. Hauth, “Grey-Box Modelling for Nonlinear Systems,” Technischen Universität Kaiserslautern, 2008.

[58] MathWorks, “Black-Box Modeling - MATLAB & Simulink - MathWorks Deutschland.” [Online]. Available: https://de.mathworks.com/help/ident/ug/black-box-modeling.html. [Accessed: 11-Apr-2017].

[59] M. H. Khalid, P. K. Tuszyński, P. Kazemi, J. Szlek, R. Jachowicz, and A. Mendyk, “Transparent computational intelligence models for pharmaceutical tableting process,” *Complex Adapt. Syst. Model.*, vol. 4, no. 1, p. 7, 2016.

[60] E. Maynard, “Ten Steps to an Effective Bin Design.” American Institute of Chemical Engineers (AIChE), pp. 25–32, 2013.

[61] K. Johanson, “Understanding and solving material caking problems in dry bulk storage vessels,” *Powder Bulk Eng.*, no. November, 2014.

[62] A. J. Rogers, A. Hashemi, and M. G. Ierapetritou, “Modeling of Particulate Processes for the Continuous Manufacture of Solid-Based Pharmaceutical Dosage Forms,” *Processes*, vol. 1, no. 2, p. 61, 2013.

[63] N. P. Nadpara, R. V. Thumar, V. N. Kalola, and P. B. Patel, “Quality by design (QBD): A complete review,” *Int. J. Pharm. Sci. Rev. Res.*, vol. 17, no. 2, pp. 20–28, 2012.

[64] European Medicine Agency, “ICH guideline Q11 on development and manufacture of drug substances (chemical entities and biotechnological/biological entities),” *European Medicine Agency*, no. May. London, p. 27, 2011.

[65] D. J. Cooper, *Control Station Innovative Solutions from the Process Control Professionals*. Connecticut: Control Station, Inc, 2005.

[66] M. Hekmatpanah, “The application of cause and effect diagram in the oil industry in Iran: The case of four liter oil canning process of Sepahan Oil Company,” *African J. Bus. Manag.*, vol. 5, no. 26, pp. 10900–10907, 2011.

[67] “Ultrasonic level measurement,” 2016. [Online]. Available: http://vakratoond.com/instrumentation/ultrasonic-level-measurement/. [Accessed: 25-Sep-2017].

[68] G. Brooker, “Range Measurement Applications,” in *Sensors and Signals*, no. May, Australian Centre for Field Robotics, Ed. University of Sydney, 2006, pp. 171–208.

[69] M. Kuentz and P. Schirg, “Powder flow in an automated uniaxial tester and an annular shear cell: a study of pharmaceutical excipients and analytical data comparison,” *Drug Dev. Ind. Pharm.*, vol. 39, no. 9, pp. 1476–1483, 2013.

[70] D. Schulze, “Flow properties of powders and bulk solids (fundamentals),” Ostfalia University of Applied Sciences, 2006.

[71] D. Zhou and Q. Yihong, “Product and Process Design.,” *J. Valid. Technol.*, pp. 65–77, 2010.

[72] EMERSON Process Management, *The Engineer ’ s Guide to Level Measurement*, 2013th ed. 2013.

[73] SICK Sensor Intelligence, “8 Most Common Level Sensing Methods.” p. 3.

[74] J. Markarian, “Overcoming Obstacles in Process Analytical Technology,” *PharmTech. Advancing Development and Manufacturing*, 2017. [Online]. Available: http://www.pharmtech.com/overcoming-obstacles-process-analytical-technology. [Accessed: 29-Nov-2017].

[75] ARC Advisory Group GmbH & Co KG, “Quality and Efficiency in Pharma Manu-facturing,” Düsseldorf, 2015.

[76] The PAT Team and Manufacturing Science Working Group, “Innovation and Continuous Improvement in Pharmaceutical Manufacturing,” 2004.

[77] E. Mandado Pérez and A. Murillo Roldan, “Sensores y acondicionadores de señal,” E.T.S. deIngenieros de Telecomunicación de Vigo, 2001.

[78] Flow Line Options Inc., “Ultrasonic Transmitters vs . Guided Wave Radar for Level Measurement,” pp. 1–7, 2011.

[79] KOBOLD, “Guided Wave Radar Level Transmitters.” p. 10, 2013.

[80] Flo-Corp level measurement technology, “Ultrasonic Transmitters vs Guided Wave Radar for Level Measurement,” 2011.

[81] M. Migliore, “How Guided Wave Radar Level Measurement Works,” 2015. [Online]. Available: https://www.flowcontrolnetwork.com/how-guided-wave-radar-level-measurement-works/. [Accessed: 26-Dec-2017].

[82] EMERSON, “The Impact of Frequency in Non-Contacting Radar Level Measurement,” Shakopee, USA, 2016.

[83] K. Kaur, “Field Time Control. Based Level Detection for Low Dielectric, Non-conductive Bulk Products,” *AZO Sensors*, 2013. [Online]. Available: https://www.azosensors.com/article.aspx?ArticleID=254. [Accessed: 30-Nov-2017].

[84] M.-C. Amann, T. Bosch, M. Lescure, R. Myllylä, and M. Rioux, “Laser ranging: a critical review of usual techniques for distance measurement,” *Opt. Eng.*, vol. 40, no. 1, p. 10, 2001.

[85] D. Spitzer, “Process Automation Technologies Lasers come to level measurement,” 2006.

[Online]. Available: http://www.controlglobal.com/articles/2006/018/?start=1. [Accessed: 15-Sep-2017].

[86] L. Martin, “Level Measurement Showdown Ultrasonic Vs Radar,” 2013. [Online]. Available: https://www.wateronline.com/doc/level-measurement-showdown-ultrasonic-vs-radar-0001. [Accessed: 23-Sep-2017].

[87] A. E. Onoja and A. M. Oluwadamilola, “Embedded System Based Radio Detection and Ranging (RADAR) System Using Arduino and Ultra-Sonic Sensor,” *Am. J. Nav. Archit. Mar. Eng.*, vol. 2, no. 4, pp. 85–90, 2017.

[88] SICK Sensor Intelligence, “Company Presentation,” *The Linde Group Company Presentation*, no. June. pp. 1–57, 2016.

[89] SICK Sensor Intelligence, “Ultrasonic Sensors, Ultimate Ultrasonic Sensor Solution From SICK.” 2015.

[90] SICK Sensor Intelligence, “UM30-212118.” p. 7, 2017.

[91] PAControl, *Instrumentation & Control Process Control Fundamentals*. 2006.

[92] J. Piriou, B. Elissondo, M. Hertschuh, and R. Ollivier, “Control Strategy as the Keystone of the Product Lifecycle , from Product / Process Understanding to Continuous Process Verification and Improvement,” *Pharm. Eng.*, vol. 32, no. 1, p. 8, 2012.

[93] J. Ulrich and P. Frohberg, “Problems, potentials and future of industrial crystallization,” *Front. Chem. Sci. Eng.*, vol. 7, no. 1, pp. 1–8, 2013.

[94] A. W. Vreman, C. E. van Lare, and M. J. Hounslow, “A basic population balance model for fluid bed spray granulation,” *Chem. Eng. Sci.*, vol. 64, no. 21, pp. 4389–4398, 2009.

[95] K. J. Åström and R. M. Murray, *Feedback systems: an introduction for scientists and engineers*, no. July. California, 2008.

[96] B. Rise and D. Cooper, “Recognizing Integrating (Non-Self Regulating) Process Behavior – Control Guru,” 2015. [Online]. Available: http://controlguru.com/recognizing-integrating-non-self-regulating-process-behavior/. [Accessed: 27-Oct-2017].

[97] B. Rice and D. Cooper, “Analyzing Pumped Tank Dynamics with a FOPDT Integrating Model – Control Guru,” 2015. [Online]. Available: http://controlguru.com/analyzing-pumped-tank-dynamics-with-a-fopdt-integrating-model/. [Accessed: 28-Oct-2017].

[98] F. Aslam and M. Haider, “An Implementation and Comparative Analysis of PID Controller and their Auto tuning method for Three Tank Liquid Level Control,” *Int. J. Comput. Appl.*, vol. 21, no. 8, pp. 42–45, 2011.

[99] O. L. Carrapiço and D. Odloak, “A stable model predictive control for integrating processes,” *Comput. Chem. Eng.*, vol. 29, no. 5, pp. 1089–1099, 2005.

[100] J. Vojtesek, P. Dostal, and M. Maslan, “Modelling and Simulation of Water Tank,” Tomas Bata University in Zlin.

[101] D. E. Seborg, F. E. Thomas, and M. Duncan A, *Process Dynamics and Control*, 2rd Editio. 2004.

[102] D. E. Seborg, T. F. Edgar, D. A. Mellichamp, and F. J. Doyle, *Process Dynamics and Control*, 3rd Editio. 2011.

[103] M. A. Fellani and A. M. Gabaj, “PID controller design for two tanks liquid level control

system using Matlab," *Int. J. Appl. or Innov. Eng. Manag.*, vol. 4, no. 5, pp. 436–442, 2015.

[104] B. Rice and D. Cooper, "Design and Tuning of PID Controllers for Integrating (Non-Self Regulating) Processes," University of Connecticut, 2002.

[105] J. Vojtesek and P. Dostal, "Simulation Analyses of Continuous Stirred Tank Reactor," Tomas Bata university in Zlin, 2009.

[106] T. D. Roopamala and S. K. Katti, "Comments on 'Routh Stability Criterion,'" *Int. J. Comput. Sci. Inf. Secur.*, vol. 7, no. 2, pp. 77–78, 2010.

[107] R. Gordon, "Control Design with MATLAB and Simulink - Video - MATLAB," 2014. [Online]. Available: https://de.mathworks.com/videos/control-design-with-matlab-and-simulink-90419.html. [Accessed: 05-Nov-2017].

[108] F. Haugen, *Basic Dynamics and Control*, no. August. Skien, Norway, 2010.

[109] V. VanDoren, "Fundamentals of lambda tuning | Control Engineering," 2013. [Online]. Available: https://www.controleng.com/single-article/fundamentals-of-lambda-tuning/aaea12b67526bff287b7bed3626df907.html. [Accessed: 30-Oct-2017].

[110] T. Olsen and B. Bialkowski, "Lambda Tuning as a Promising Controller Tuning Method for the Refinery," *AIChE Spring National Meeting*. New Orleans, pp. 1–10, 2002.

[111] M. T. Coughram, "Lambda Tuning — The Universal Method for PID Controllers in Process Control." Emerson Process Management, pp. 1–8, 2006.

[112] J. E. Arbogast, D. J. Cooper, and R. C. Rice, "Graphical Technique for Modeling Integrating (Non-Self-Regulating) Processes without Steady-State Process Data," *Chem. Eng. Commun.*, vol. 194, no. 12, pp. 1566–1578, 2007.

[113] R. Rice and D. J. Cooper, "Improve Control of Liquid Level Loops," *Chemical Engineering Progress*, vol. 104, no. 6. American Institute of Chemical Engineers (AIChE), pp. 54–61, 2008.

[114] T. Olsen and N. Ito, "Implement an effective loop tuning strategy," *Chemical Engineering Progress*, vol. 109, no. 1. American Institute of Chemical Engineers (AIChE), pp. 42–48, 2013.

[115] S. Skogestad and C. Grimholt, "The SIMC Method for Smooth PID Controller Tuning," Norwegian University of Science and Technology (NTNU), 2012.

[116] A. Bodhmage, "Correlation between physical properties and flowability indicators for fine powders," University of Saskatchewan, 2006.

XIV. APPENDIX

A – Data Sheet of the Ultrasonic Sensor UM30-212118

Performance

Working range, limiting range	65 mm ... 350 mm, 600 mm
Resolution	≥ 0.18 mm
Reproducibility	± 0.15 % [1]
Accuracy	± 1 % [1] [2]
Temperature compensation	✓
Response time	64 ms
Switching frequency	12 Hz
Output time	16 ms
Ultrasonic frequency (typical)	400 kHz
Detection area (typical)	See diagrams
Additional function	Set switching mode: Distance to object (DtO) / Window (Wnd) / Object between sensor and background (ObSB), teach-in of switching output, set levels of switching outputs, Invertable switching output, set on delay switching output, teach-in of analog output, scaling of analog outputs, Invertable analog output, automatic selection of analog current or voltage output, temperature compensation, synchronization of up to 10 sensors, multiplexing: no cross talk of up to 10 sensors, set measurement filters: value filter, filter strength, adjustable sensitivity, foreground suppression and detection area, switch-off display, reset to factory default [3]

[1] Referring to current measurement value.
[2] Temperature compensation can be switched off, without temperature compensation: 0.17 % / K.
[3] Functions may vary depending on sensor type.

A – 1. Performance Data Sheet of the Ultrasonic Level Sensor UM30-212118. Extracted from [90]

Interfaces

Analog output	1 x 0 V ... 10 V (≥ 100 kΩ) [1]
Analog output	1 x 4 mA ... 20 mA (≤ 500 Ω) [1] [2] [3]
Resolution analog output	12 bit

Switching output	1 x PNP (200 mA) [4]
Multifunctional input (MF)	1 x MF
Hysteresis	5 mm

[1] Automatic selection of analog current or voltage output dependent on load.
[2] For 4 mA ... 20 mA and V_S ≤ 20 V max. load ≤ 100 Ω.
[3] Subsequent smoothing of the analog output, depending on the application, may increase the response time by up to 200 %.
[4] PNP: HIGH = V_S - (< 2 V) / LOW = 0 V.

A – 2. Interface Data Sheet of the Ultrasonic Level Sensor UM30-212118. Extracted from [90]

Mechanics/electronics

Supply voltage V_s	DC 9 V ... 30 V [1]
Power consumption	≤ 2.4 W [2]
Initialization time	< 300 ms
Design	Cylindrical
Housing material	Nickel-plated brass, PBT Display: TPU Ultrasonic transducer: polyurethane foam, glass epoxy resin
Connection type	Male connector, M12, 5-pin
Indication	LED display, 2 x LED
Weight	150 g
Sending axis	Straight
Enclosure rating	IP67
Protection class	III

[1] 15 V ... 30 V when using the analog voltage output.
[2] Without load.

A – 3. Mechanistic/electronic Data Sheet of the Ultrasonic Level Sensor UM30-212118. Extracted from [90]